THE EFFECTS OF AN ALPINE FAULT EARTHQUAKE ON THE TARAMAKAU RIVER, SOUTH ISLAND, NEW ZEALAND

A thesis submitted in partial fulfilment of the

requirements for the Degree

of Master of Science

at the University of Canterbury

by Mattilda Sheridan

University of Canterbury

2014

"The face of [the river], in time, became a wonderful book…which told its mind to me without reserve, delivering its most cherished secrets as clearly as if it uttered them with a voice…In truth, the passenger who could not read this book saw nothing but all manner of pretty pictures in it, painted by the sun and shaded by the clouds, whereas to the trained eye these were not pictures at all, but the grimmest and most dead-earnest of reading matter"

-Mark Twain, Life on the Mississippi p. 118

Contents

List of Figures

List of Tables

Acknowledgments

I would like to thank my supervisor Tim Davies, for providing insightful perspective, constructive criticism and for supporting my ideas. Also thank you to my associate supervisor Chris Gomez, for monitoring my progress and being my go to river expert. Thank you to Tom Robinson, for always willing to help and show me the ropes when it came to anything Alpine Fault related. A huge thank you must go to Maree Hemmingsen for reviewing my work and assisting with the construction of my thesis. In addition, special thanks to Jarg Pettinga, Pat Roberts and Janet Warburton in the Department of Geological Sciences for their miscellaneous help. I received funding from the Mason Trust and the EQC (New Zealand Earthquake Commission) fund which was great assistance and very much appreciated, so thank you for that. I would also like to thank ECan (Environment Canterbury) for their assistance in funding towards my project.

To the Geological Sciences Department at the University of Canterbury, thank you for welcoming me into the department and assisting me over the last two years, I could not have completed my thesis without the help and support provided by the fantastic Geological Science staff and students at the University of Canterbury.

Special thanks must go to Justin Harris and Nick Key for helping design and construct the physical model employed in my studies, while we had a few hiccups along the way I was always confident that the design could be modified without delay, your input into the physical modelling was invaluable and will not be forgotten.

Lastly to my parents and sisters, for your continual support and encouragement (albeit long distance). Most importantly I have to thank you, Mum and Dad for your constant reassurance and financial support providing me with the freedom and time to complete my work relatively stress free. I greatly appreciate the help you have given me throughout my degrees and I hope I haven't made you bankrupt.

Abstract

An Alpine Fault Earthquake has the potential to cause significant disruption across the Southern Alps of the South Island New Zealand. In particular, South Island river systems may be chronically disturbed by the addition of large volumes of sediment sourced from coseismic landsliding. The Taramakau River is no exception to this; located north of Otira, in the South Island of New Zealand, it is exposed to natural hazards resulting from an earthquake on the Alpine Fault, the trace of which crosses the river within the study reach. The effects of an Alpine Fault Earthquake (AFE) have been extensively studied, however, little attention has been paid to the effects of such an event on the Taramakau River as addressed herein. Three research methods were utilised to better understand the implications of an Alpine Fault Earthquake on the Taramakau River: (1) hydraulic and landslide data analyses, (2) aerial photograph interpretation and (3) micro-scale modelling. Data provided by the National Institute of Water and Atmospheric Research were reworked, establishing relationships between hydraulic parameters for the Taramakau River. Estimates of landslide volume were compared with data from the Poerua landslide dam, a historic New Zealand natural event, to indicate how landslide sediment may be reworked through the Taramakau valley. Aerial photographs were compared with current satellite images of the area, highlighting trends of avulsion and areas at risk of flooding. Micro-scale model experiments indicated how a braided fluvial system may respond to dextral strike-slip and thrust displacement and an increase in sediment load from coseismic landslides. An Alpine Fault Earthquake will generate a maximum credible volume of approximately 3.0×10^8 m^3 of landslide material in the Taramakau catchment. Approximately 15% of this volume will be deposited on the Taramakau study area floodplain within nine years of the next Alpine Fault Earthquake. This amounts to 4.4×10^7 m^3 of sediment input, causing an average of 0.5 m of aggradation across the river floodplains within the study area. An average aggradation of 0.5 m will likely increase the stream height of a one-in-100 year flood with a flow rate of 3200 m^3/s from seven metres to 7.5 m overtopping the road and rail bridges that cross the Taramakau River within the study area – if they have survived the earthquake. Since 1943 the Taramakau River has shifted 500 m away from State Highway 73 near Inchbonnie, moving 430 m closer to the road and rail. Paleo channels recognised across the land surrounding Inchbonnie between the Taramakau River and Lake Brunner may be reoccupied after an earthquake on the Alpine Fault. Micro-scale modelling showed that the dominant response to dextral strike-slip and increased 'landslide' sediment addition was up- and downstream aggradation separated by a localised zone of degradation over the fault trace. Following an Alpine Fault Earthquake the Taramakau River will be disturbed by the initial surface rupture along the fault trace, closely followed by coseismic landsliding. Landslide material will migrate down the Taramakau valley and onto the floodplain. Aggradation will raise the elevation of the river bed promoting channel avulsion with consequent flooding and sediment deposition particularly on low

lying farmland near Inchbonnie. To manage the damage of these hazards, systematically raising the low lying sections of road and rail may be implemented, strengthening (or pre-planning the replacement of) the bridges is recommended and actively involving the community in critical decision making should minimise the risks of AFE induced fluvial hazards. The response of the Taramakau River relative to an Alpine Fault Earthquake might be worse, or less severe or significantly different in some way, to that assumed herein.

Chapter 1 – Introduction

1.1 Project Background

New Zealand is a country prone to natural hazards due to the tectonic motion of the Australian plate with the Pacific plate meeting at the Alpine Fault (Berryman et al., 2012; Langridge et al., 2010; Yetton, 2000). Natural hazards induced by an Alpine Fault Earthquake (AFE) have the potential to cause extensive damage and disruption to alpine townships and major infrastructure and transportation links that cross the Southern Alps. Consequences of an AFE include intense shaking, local uplift, debris flows, landslides, rockfalls and rock avalanches. The focus of this study is on changes to the fluvial regime of the Taramakau River resulting from such effects.

The Taramakau River is a major alpine fluvial system, located in the northwest of the South Island in New Zealand (Figure 1.1). This river runs adjacent to State Highway 73 from Aickens to Kumara. The Taramakau River is crossed by the Alpine Fault near Inchbonnie, and runs parallel to the Hope Fault east of this. The study area for this project is the reach of the river that runs alongside State Highway 73 from Aickens to where the Taipo River meets the Taramakau River seven kilometres downstream of Inchbonnie.

Despite the known high annual probability of an AFE (1 - 2%; Rhoades & Van Dissen, 2003) minimal hazard assessment and mitigation measures regarding fluvial implications have been conducted to date. Very little is understood about the short- and long-term impacts that an AFE will have on the behaviour of the Taramakau River. This is an issue that requires attention as it may have major consequences for critical transportation links and land management within the studied area.

The purpose of this research has been based around a problem statement mentioned by McSaveney (1982), "*the generally high level of river beds at present may enhance the probability of damage should additional large quantities of sediment be added to the channel networks in the future*" (McSaveney, 1982. p. 77). This statement refers to the alpine rivers in the South Island of New Zealand, and is the starting point for the research conducted in this thesis.

Figure 1.1 Location of the Taramakau River in the Southern Alps of New Zealand. White box identifies study area. Base map sourced from Google Earth 2014.

1.2 Project Objectives

The aim of this research is to investigate the effects that an AFE will have on the Taramakau River. This study will consider natural hazard processes such as aggradation, avulsion and flooding which are commonly associated with both large scale earthquakes and with rainstorms. The major objectives of this study are to;

- Address the effects of earthquake-induced landslides on alpine rivers and the threats that these processes pose to major transportation routes
- Analyse hydraulic parameters of the Taramakau River under current flow conditions
- Search for evidence of past channel aggradation and avulsion within the study reach of the Taramakau River
- Model the response of a braided river to a dextral strike-slip and vertical displacement as well as to large sediment inputs
- Assess the long term hazards that earthquake-related fluvial processes pose to infrastructure and land, suggesting strategies for managing the consequent risks

Extensive information exists about the natural hazards and susceptibility of the region to such events, however, this currently fails to address fluvial effects on the land and infrastructure in the Taramakau valley. More information is critical to better understand the implications, and thus potentially reduce the impacts, of an AFE. This study will assist hazard planners, transportation agencies and land management organisations to make better informed decisions regarding hazard mitigation measures relevant to the fluvial regime of the Taramakau.

1.3 Study Area

This thesis focusses on the Taramakau River along State Highway 73 from Aickens through to where the Taipo River meets the Taramakau (Figure 1.2a). KiwiRail's Midland rail line follows this stretch of highway, before crossing the Taramakau River parallel to the Stanley Goosemen road bridge near Jacksons. The Alpine Fault crosses the Taramakau at Inchbonnie (Figure 1.2b).

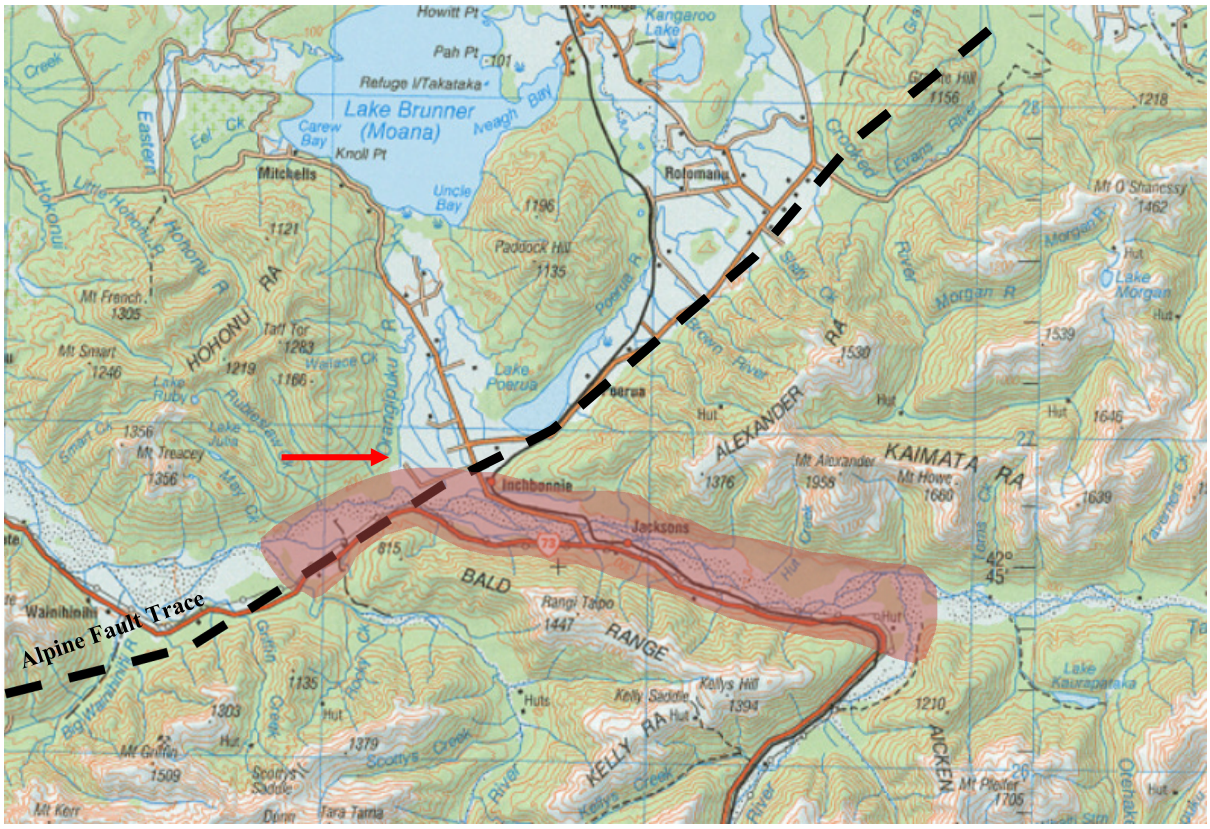

Figure 1.2a Extent of the study area (red zone) from Aickens to the Taipo River confluence with the Taramakau River along State Highway 73. Red arrow indicates view in Figure 1.2b. Base map sourced from Topo Map.

Figure 1.2b Trace of the Alpine Fault, obliquely cutting across the Taramakau River. White arrow indicates direction of flow. View looking east. Source Nathan et al (2002).

1.3.1 Topography, Vegetation and Land Use

The study area is predominantly alpine, encompassing the western Southern Alps between the main divide and the Alpine Fault. The Taramakau River has a wide flood plain and is not as closely confined by steep alpine mountains as are the Otira and Bealey Rivers to the southeast. The river bed elevation at the eastern border of the study reach is at 284 m asl and at the western end of the study reach it is at approximately 120 m asl. The Taramakau catchment is bounded to the south by the Bald Range, with a maximum elevation at Rangi Taipo of 1459 m (Figure 1.2a). Between Aickens and Inchbonnie, the Taramakau is bounded to the north by the Kaimata Range, with the highest peak Mt Alexander at 1958 m. From Inchbonnie to the confluence of the Taipo River with the Taramakau, the river is bounded to the northwest by the Hohonu Range with a maximum elevation of 1283 m. Surrounding Inchbonnie the Taramakau is bounded by low lying land in the north (~140 m asl) that extends towards Lake Brunner and Lake Poerua (Figure 1.2a).

The land immediately adjacent to the Taramakau River is river flats which are privately owned and grazed while the valley sides and ridge tops are managed by the Department of Conservation (DoC) (Smith, 2004). The higher land is predominantly covered by native forest. The vegetation varies with altitude and rainfall across the Southern Alps. Based on studies by McSaveney (1982) the vegetation on the lower flanks of the Bealey and Otira valley consists almost exclusively of mountain beech (*Nothofagus solandri var. cliffortioides*) which grades upwards into subalpine scrub, similarly to the Taramakau valley. As altitude increases so too does the harshness of the climate resulting in more resilient alpine grasslands and herbfields, up to elevations of about 1770 m. Above this elevation is predominantly bare rock. The lower elevations of the Taramakau catchment consist of gravel or grassed/shrubby river beds. Riparian vegetation is seen on floodplains and channel bars that have become inactive. More substantial scrubby vegetation and gorse grow on parts of the Taramakau River that have been inactive for a longer time.

1.3.2 Climate

The West Coast of the South Island, New Zealand is subject to substantial rainfall induced by moist westerly airstreams from the Tasman Sea coming into contact with the steep north western range front of the Southern Alps, which deflects warm moist westerly winds upwards (Nathan, Rattenbury, & Suggate, 2002). There are generally more frequent westerly airstreams during summer and fewer in winter resulting in higher orographic rainfall, peaking west of the main divide, in the spring and summer months (Hessell, 1982; Robertson, 1963).

The steep precipitation gradient across the Southern Alps exerts a strong influence on fluvial geomorphology (McSaveney, 1982). High rainfall poses a threat to the study area, frequently bringing down debris from hillside streams onto the State Highway. High rainfall also causes flooding which has the ability to rapidly undercut fallen scree, resulting in the collapse of the scree (McSaveney, 1982). Rainfall has historically produced the most significant geomorphic changes across the landscape. The storm which resulted in the greatest recent geomorphic change as well as structural damage to infrastructure in the Southern Alps occurred on the 26 - 27 December 1957, with a total of 334 mm of rainfall recorded within 24 hours at Arthurs Pass Store rain gauge (McSaveney, 1982).

Documentation of temperatures and rainfall is sparse for the study area, thus a lot of the information for this thesis has been inferred from nearby records in Otira, Kumara, Inchbonnie and Arthurs Pass. The annual average precipitation for the Taramakau catchment has been recorded as 4847 mm (Figure 1.3a) (Hicks et al., 2011, NIWA). High intensity storms can cause extreme flooding events (West Coast Regional Council, 2010). Deep snow rarely accumulates in the valley bottom. The average annual temperature for the Taramakau valley is between 6° and 10°C (Figure 1.3b).

McSaveney (1982) suggests that the levels of river beds fluctuate about an equilibrium profile, with the upper and lower limits determined by the frequency of storms with high intensity rainfall and sediment inputs. Rainfall and seismically induced hazards are intrinsically intertwined. As New Zealand has no well-defined wet season it is likely that a major rainstorm will occur soon after an Alpine Fault Earthquake (Robinson & Davies, 2013). A rainstorm and high river flow following a major earthquake will have the ability to mobilise large volumes of landslide detritus generating hazards of river aggradation, avulsion and flooding in the Taramakau.

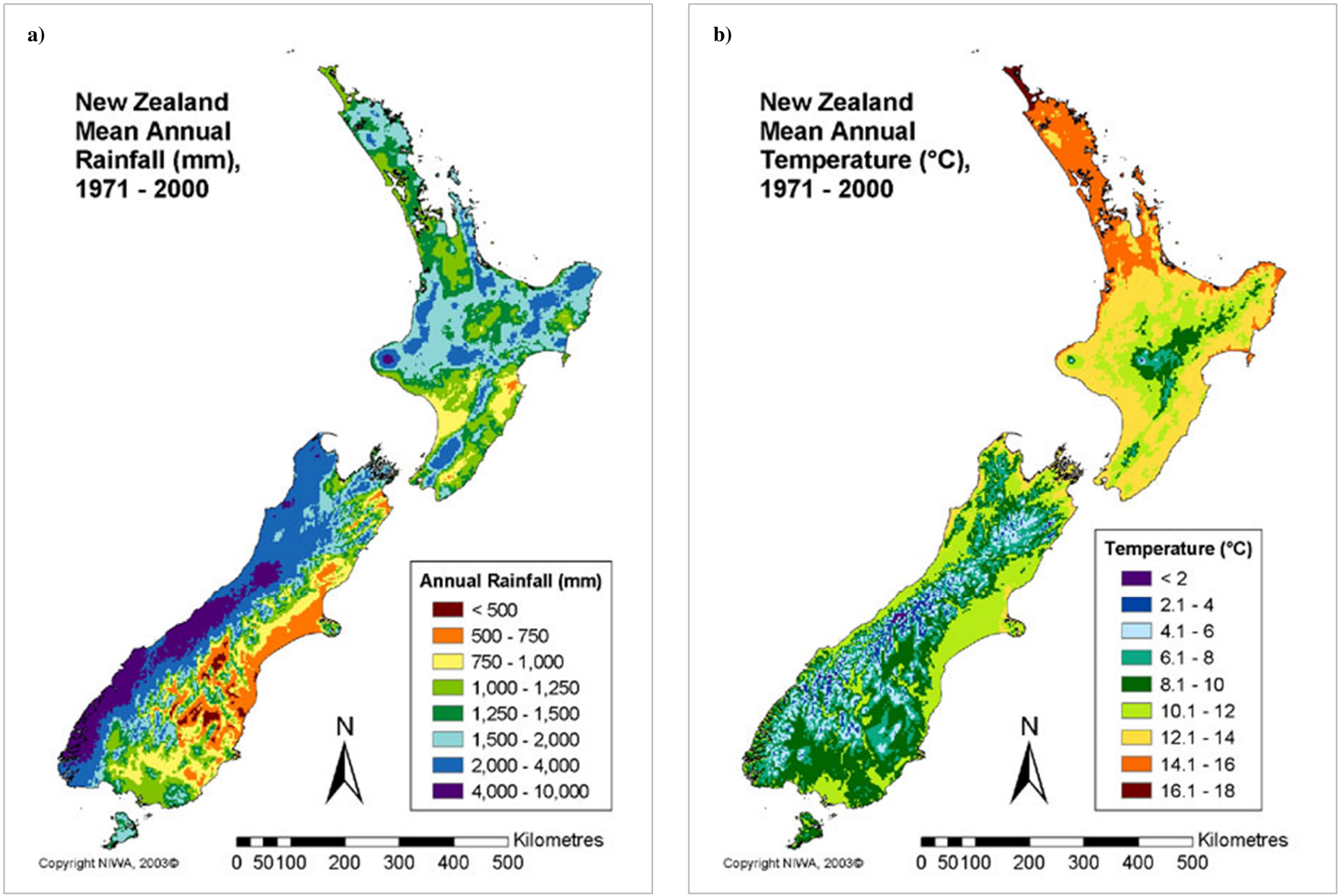

Figure 1.3 Climate patterns for New Zealand a) Mean annual rainfall b) Mean annual temperature from 1971-2000. Sourced from National Institute of Water and Atmospheric Reseach, 2003.

1.4 Geology

The geology of the area consists of rocks that have been folded, faulted and uplifted producing complex metamorphic patterns and textures that are associated with dynamic metamorphic processes. These processes have made the main lithologies very susceptible to weathering and erosion resulting in frequent rock slides and landslides across the alpine terrain. Most of the geological interpretations in this thesis have been based on studies conducted by Nathan et al (2002) and the 1:250 000 geological map of the Greymouth area (QMap) (Figure 1.4a).

1.4.1 Lithology/Stratigraphy

Southeast of the Alpine Fault lies a major geological sequence that extends across the Southern Alps to the east coast and is termed the Torlesse Supergroup. This consists of large sedimentary sequences of late Carboniferous to early Cretaceous greywacke units sourced from Triassic submarine fans. Part of the Torlesse Supergroup is the Rakaia terrain that outcrops east of the Alpine Fault in the study area. This terrain consists of quartzofeldspathic sandstone interbedded with alternating sandstones and mudstone along with thick bedded mudstone, red and green mudstone and conglomerate, with bedding that trends roughly north to northeast (Nathan et al., 2002).

The Rakaia terrain shows increasing metamorphic grade towards the Alpine Fault producing the Alpine Schist which is further subdivided into separate metamorphic zones. These zones are recognised as semi schist and schist textural zones (IIA, IIB, III, and IV) also referred to as the Haast Schist Group (Nathan et al., 2002). The schist belt is approximately 10 - 12 km wide truncated in the northwest by the Alpine Fault (Cave, 1987).

Based on the geological map of the Greymouth area (1:250 000: Nathan et al., 2002), from Aickens to Inchbonnie, the Taramakau is bounded either side by Torlesse composite terrain, progressing through the different mineralogical, textural and metamorphic zones of the Rakaia terrain (Figure 1.4b). Furthest east of the Alpine Fault within the study area, the Taramakau is bound by a sub unit of the Rakaia terrain (Tt) that has been metamorphosed to semi schist and schist (Haast Schist zones IIA to IV). Moving westward from the bands of semischist and schist towards to Alpine Fault, rare bands of greenschist (Ttg) is found.

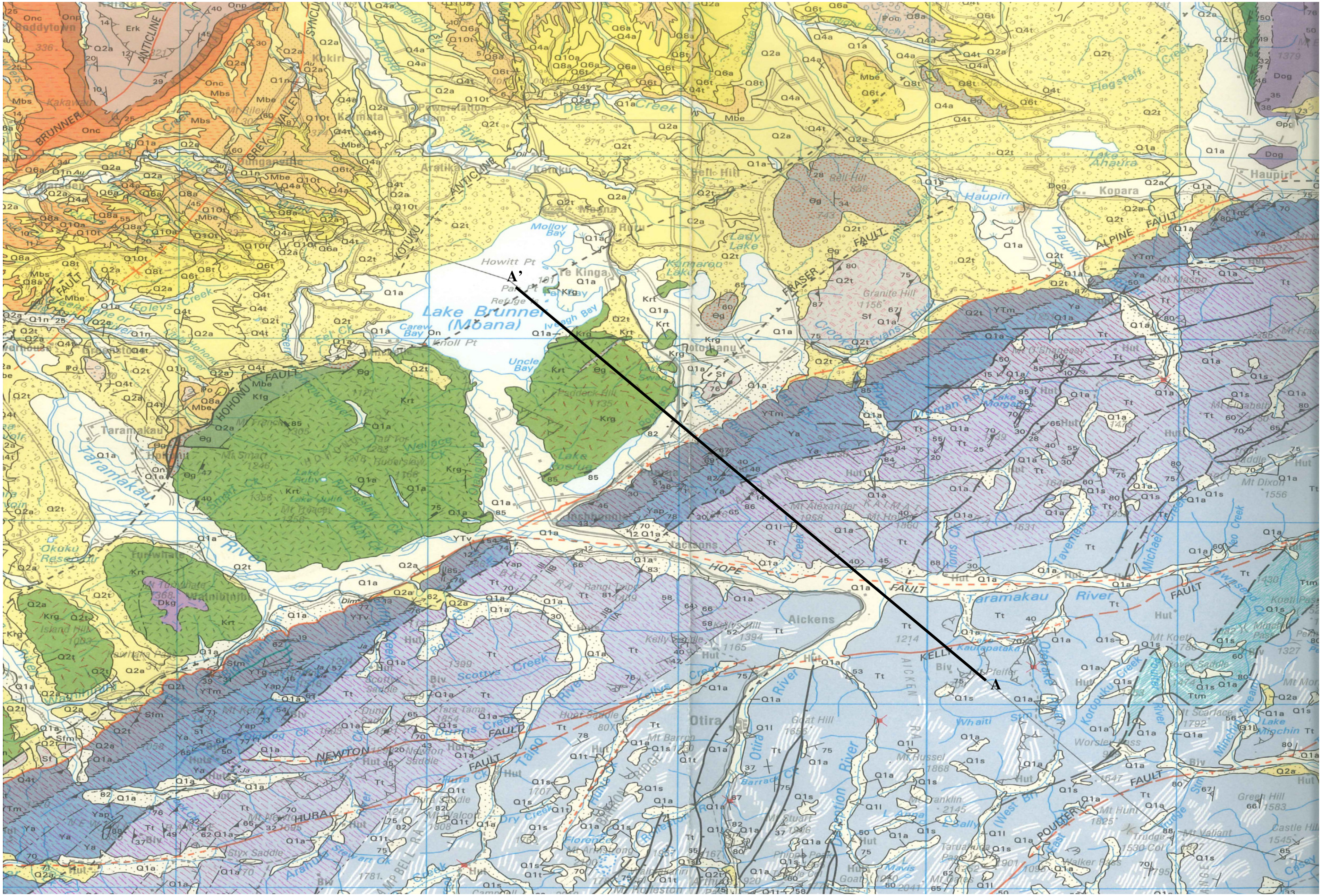

Figure 1.4a Geological Map of the study area, legend attached in Figure 1.4b. Source Nathan et al (2002).

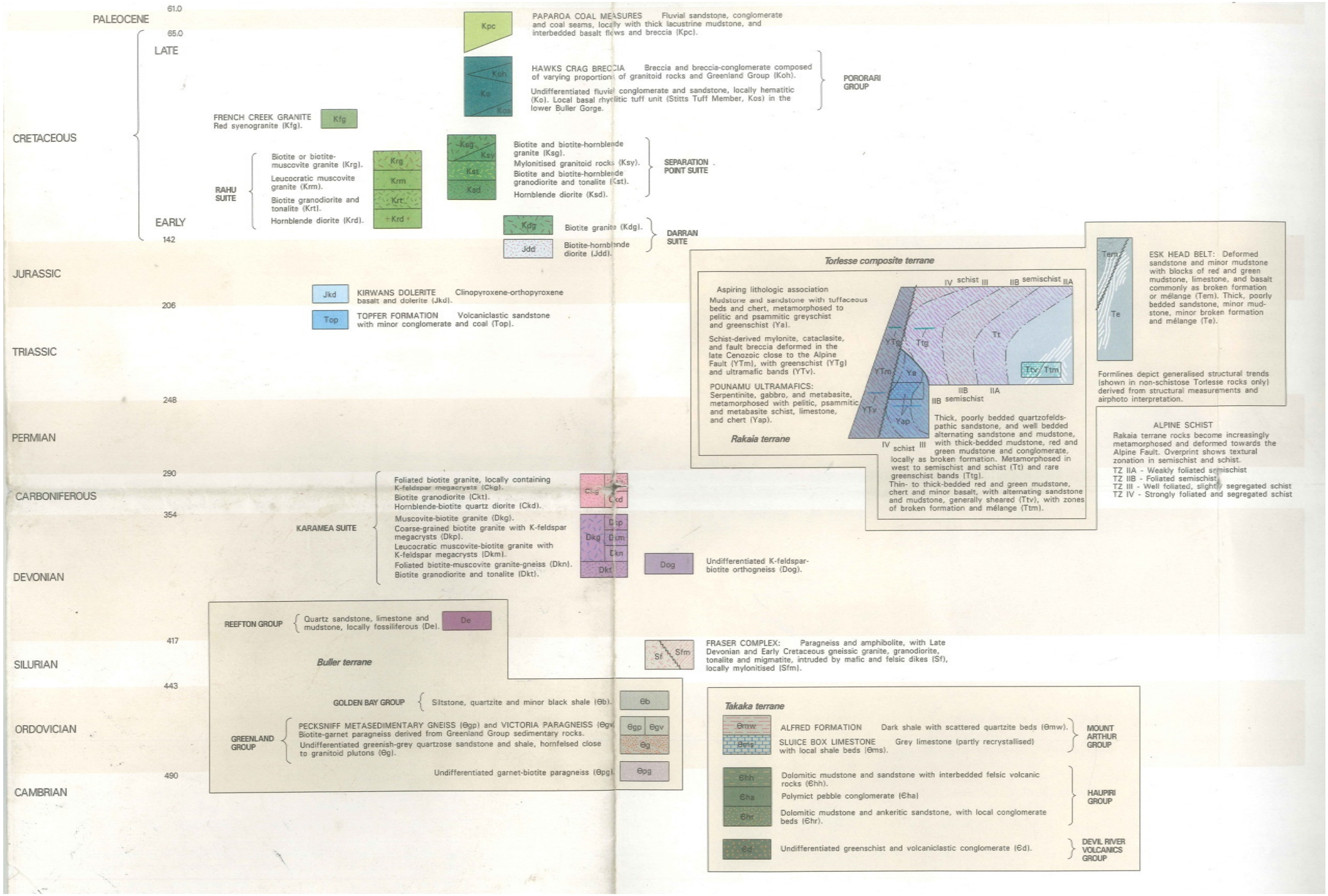

Figure 1.4b Pre Quaternary stratigraphy associated with the geological map of the study area. Torlesse Composite Terrane and Rahu Suite are found in the study area. Source Nathan et al (2002).

West of the greenschist, outcrops of the Pounamu Ultramafics occur, characterised as a zone of serpentine, gabbro and metabasite metamorphosed with pelitic, psammitic and metabasite schist, limestone and chert (Yap). Moving further west towards Inchbonnie, directly adjacent to the Alpine Fault sits schist-derived mylonite, cataclasite and fault breccia that has been deformed in the late Cenozoic due to the close proximity to the Alpine Fault (YTm) with bands of ultramafics (YTv) (Nathan et al., 2002).

From Inchbonnie to where the Taipo River meets the Taramakau, the river is bounded to the north by younger geological units of the Hohonu Range. The Torlesse composite terrain is Late Carboniferous to Early Cretaceous in age, while the geological units that lie directly northwest of the Alpine Fault are Cretaceous with evidence of postglacial deposits. The Hohonu Range consists of the Cretaceous Rahu suite, a biotite, granodiorite and tonalite unit (Krt). This suite contains postglacial Quaternary deposits including river gravels and sands, fan deposits and swamp deposits (Figure 1.4b).

The older rocks of the Southern Alps have been covered by a thick sequence of younger Cenozoic sediments, deposited in the Tertiary and Quaternary. Those deposited in the Eocene to Pliocene consist of fluvial sandstone, mudstone and conglomerate. Younger Quaternary units are glacial debris deposits. Most of the alluvial and fluvioglacial deposits in the study area consist of well rounded boulders composed of Rakaia greywacke and minor schist in a sandy matrix (Nathan et al., 2002).

1.4.2 Structural Features and Active Tectonics

The study area includes two significant fault lines; (1) the Alpine Fault and (2) the Hope Fault (Figure 1.5).

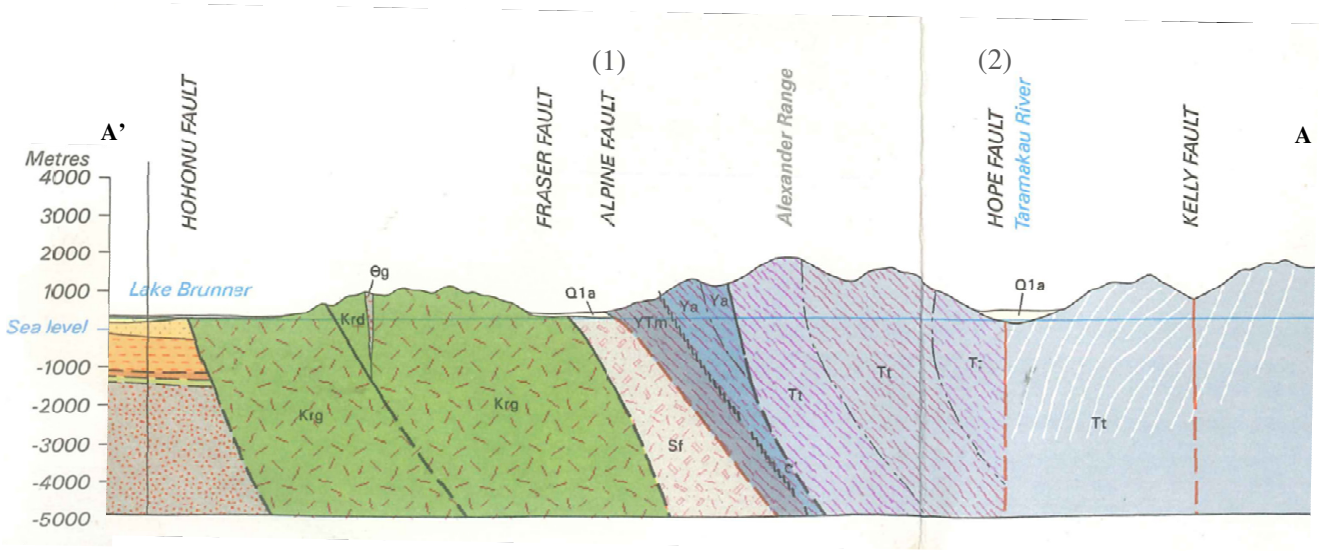

Figure 1.5 Geological cross section of the study area from A'-A highlighted in Figure 1.4a. Major faults in the study area include the Alpine Fault and the Hope Fault. Source Nathan et al (2002).

The Alpine Fault marks the dextral strike-slip boundary between the Australian (to the northwest) and Pacific (to the southeast) Plates, accommodating large amounts of strain in the central part of the South Island, trending approximately 050^{o} (Nathan et al., 2002). The fault has a 600 km long onshore surface expression (Robinson & Davies, 2013). This plate boundary developed during the Cenozoic and approximately 480 km of strike-slip movement has accumulated along the contact, measured by offset geological terrains (Cave, 1987; Nathan et al., 2002). Uplift associated with this active boundary has led to the development of mountains since the Pliocene.

The Alpine Fault obliquely crosses the Taramakau River within the study area demarking abrupt changes in lithology (Nathan et al., 2002; Robinson & Davies, 2013). It separates the study area in two; from mountainous pre Cretaceous Torlesse Supergroup and Rakaia terrain in the southeast to Cretaceous, metasedimentary and plutonic rocks in the northwest (Nathan et al., 2002). Late Cenozoic movement along this plate boundary has led to the juxtaposition of these two different geological provinces.

Berryman (as cited in Berryman et al., 2012) suggests that there is strong evidence that there was an Alpine Fault rupture in 1620AD which caused significant aggradation in alpine rivers of up to several metres in Westland. There is now evidence that this may not have been an Alpine Fault Earthquake (De Pascale, Quigley, & Davies, 2014). The most recent documented rupture of an Alpine Fault Earthquake was in 1717 AD (Davies & Korup, 2007; Wells, Yetton, Duncan, & Stewart, 1999; Yetton, 2000). Hancox, McSaveney, Manville, and Davies (2005) and Yetton (2000) suggest that there is a high probability that another earthquake of similar magnitude will occur along this fault line within the next 50 years. Nathan et al (2002) consider that the probability of a major rupture on the Alpine Fault is up to 20% over the next 20 years. Relative plate motion measured at Inchbonnie has been recorded as 39.5 ± 3 mm a^{-1}, with uplift rates up to or exceeding 5 mm a^{-1} (Rhodes & Van Dissen, 2003). An estimate of Alpine Fault rupture is 8 m lateral and 1 - 2 m of vertical displacement (Berryman et al., 2012; Robinson & Davies, 2013).

The second major fault line, the Hope Fault (Figure 1.5) runs along the Taramakau River, and extends approximately 190 km from Inchbonnie to Kaikoura (Freund, 1971). There is no visible surface trace of the Hope Fault anywhere on the river bed of the Taramakau (Cave, 1987). It is one of four major oblique dextral strike-slip faults (the Wairau, Awatere, Clarence and Hope), constituting the Marlborough Fault System (Robinson & Davies, 2013). The

Hope Fault joins the Alpine Fault at an oblique angle indicated by the straightness of the Taramakau valley and offset metamorphic isograds on either side of the river (Figure 1.2b) (Nathan et al., 2002).

The Alpine and Hope Faults have the potential to initiate substantial natural hazards. Both are strike-slip type (Chamberlain, 1996). The transfer of stress and motion from the Alpine Fault to the Hope fault is currently poorly understood, however, it has been noted that the slip rate of the Alpine Fault reduces north of where the Hope Faults meets the Alpine Fault at Inchbonnie (Norris & Cooper, 2001). Both faults are capable of producing high magnitude earthquakes and when the Alpine Fault ruptures it is possible that the Hope Fault may rupture simultaneously or within a few years – perhaps with a major aftershock; however, further research is required to test this suggestion.

1.4.3 Geomorphology

West of Arthurs Pass the rivers are steep, boulder-strewn and rough. The landscape has been shaped by Cenozoic uplift coupled with Quaternary glaciation, postglacial mass-wasting, fluvial incision and aggradation processes. The Taramakau valley drains formerly glaciated alpine catchments. The most recent glaciation was the Otiran from 12,000 to 74,000 years ago (Nathan et al., 2002). The former Taramakau glacier during this time branched into three different lobes, namely, the Taramakau, Orangipuku and Poerua, each denoted by moraine troughs extending towards Kumara, Orangipuku River and Lake Poerua respectively (Langridge et al, 2010). The Taramakau, later filled with alluvium during the Holocene following the retreat of the valley glacier. The Taramakau valley along with other alpine valleys has been substantially modified by fluvial erosion since deglaciation (McSaveney, 1982).

1.5 Thesis Structure

The research conducted for this thesis has been predominantly desktop based with physical modelling and field verification. The flow diagram below outlines the structure of this thesis.

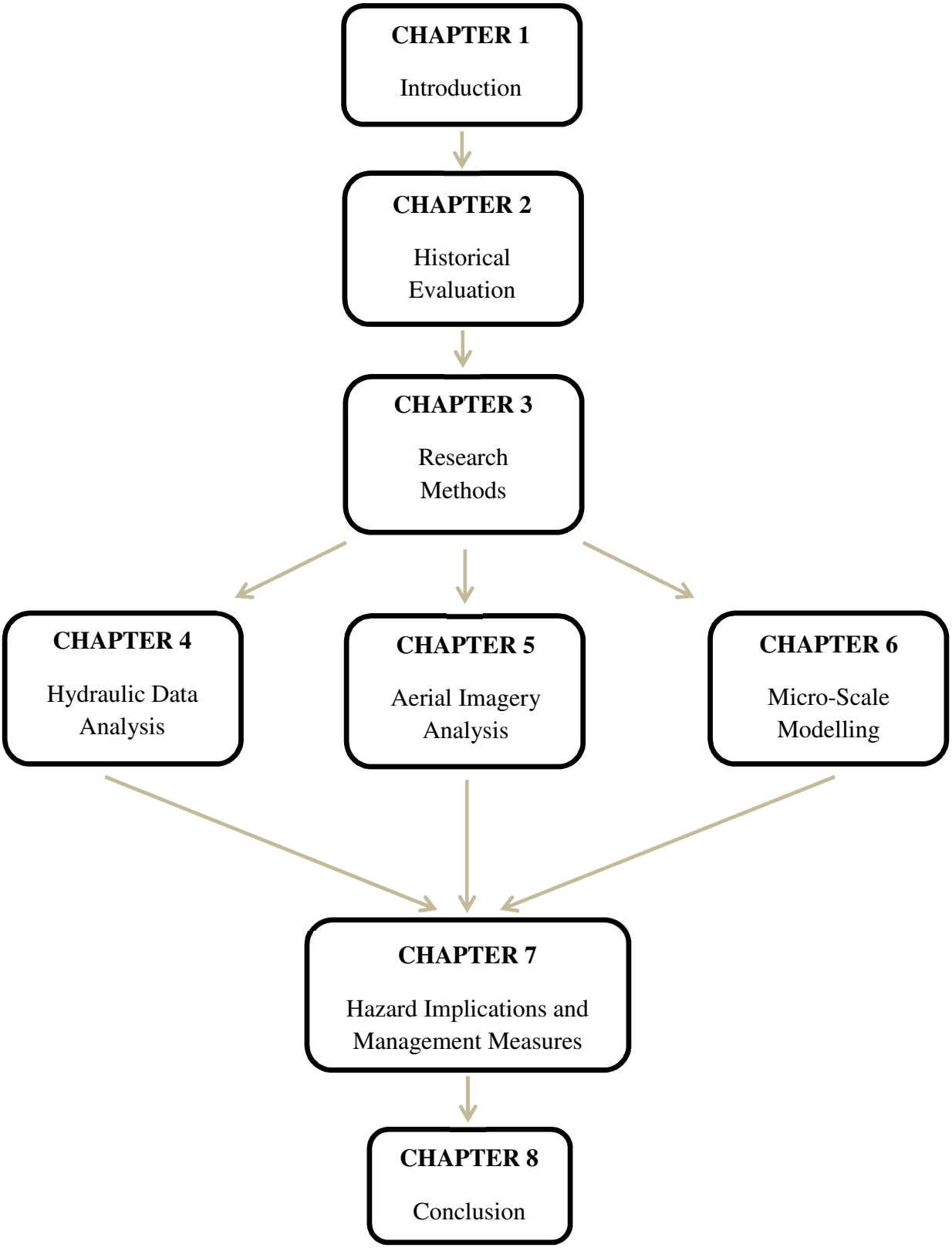

Chapter 2 focuses on a historical evaluation of the area and documented changes to mountainous fluvial networks. Chapter 2 includes information on past mass movements and consequent hazards that have impacted major fluvial systems in New Zealand as well as international case studies. General terminology is also discussed, touching on the definitions of aggradation, avulsion and landslides.

Chapter 3 outlines the research methods used in this thesis, including hydraulic data analysis, aerial imagery studies and physical modelling.

Chapter 4 presents the results found from a hydraulic analysis of data sourced from the National Institute of Water and Atmospheric Research (NIWA). Landslide volume calculations are also carried out to estimate how much sediment will be added to the Taramakau following a major earthquake, and how it will be redistributed throughout the river system.

Chapter 5 examines how the Taramakau River has changed over recent time, through an aerial imagery analysis. Aerial photographs dating back to 1943 were compared with current satellite images.

Chapter 6 presents the micro-scale modelling results, describing three different experiments modelling varying AFE scenarios.

Chapter 7 discusses the results presented in the previous three chapters, assembling the findings of each. The effects of an AFE on the Taramakau River and adjacent transportation networks are addressed. Management measures are also mentioned.

Chapter 8 summarises the objectives and achievements of the work presented.

Chapter 2 – Historical Evaluation

2.1 Introduction

Chapter 2 analyses previous work relative to coseismic landslides and fluvial systems, defines the processes and hazards expected to occur following an AFE and addresses particular examples of such hazards that have occurred in New Zealand and across the world. Extensive work has been undertaken by Korup (2002; 2004 a, b, c; 2005a, b, c; 2006) Korup, McSaveney, and Davies (2004), Korup, Strom, and Weidinger (2006), Davies and McSaveney (2006), Davies and Korup (2007), Davies, Manville, Kunz, and Donadini (2007), Davies and McSaveney (2011), Davies, Campbell, Hall, and Gomez (2013), McSaveney (1982), Keefer (1984; 1994; 1999), Robinson and Davies (2013) and Robinson (2014) on the implications of landslides on alpine rivers in the Southern Alps of New Zealand as well as addressing the relationship between earthquakes and landsliding. Currently, little specific attention has been paid to the Taramakau catchment and the fluvial changes that will result from an AFE. Aggradation, channel avulsion, landslides and (possibly) landslide damming are expected to occur following an AFE and may impact the fluvial regime of the Taramakau River. New Zealand examples of aggradation and avulsion have occurred in Gaunt Creek, Boulder Creek and Poerua valley. Similar events have occurred internationally, following the 2008 Wenchuan earthquake in China and the 1999 earthquake in Taiwan. Both the New Zealand and international examples are potential analogues of how the New Zealand landscape, including the Taramakau River, may respond to the next AFE.

2.2 Previous Work

Korup et al (2004) employed aerial photographic interpretation in order to identify impacts of landslides on fluvial geomorphology, scanning for channel avulsions, blockage and occlusion in New Zealand. Landslides were identified from scars in the vegetation cover as well as changes in the dense vegetation of the Southern Alps. To support Korup et al's (2004) study, Digital Elevation Maps (DEM) were produced, mapping the interface between landslides and river channels through GIS. Surveys of the landscape were taken through Electronic Distance Meters (EDM). Other field analyses involved sediment sampling and dendrogeomorphic techniques, dating fan aggradation. Korup (2005) identified relationships between landslides and fluvial regimes as well as geomorphic interaction between slope instability and river channels. The results of that study imply that landslides have a direct control on the channel

and valley floor landforms and that the sedimentary input of such events initiate and strongly influence changes in fluvial morphology.

Davies and Korup (2007) searched for past aggradation surfaces through the trenching of alluvial fans on the West Coast of New Zealand. They found that aggradation has occurred along many of the West Coast river alluvial fans since the last two Alpine Fault Earthquakes in 1620 and 1717 AD. Large woody debris remnant terraces were identified by Yetton (2000) in West Coast South Island Rivers, providing evidence of catastrophic post-earthquake aggradation sourced from coseismic landslides. Wells and Goff (2007) dated dune ridges relative to past Alpine Fault Earthquakes.

McSaveney (1982) recorded recent geomorphic changes of the Bealey and Otira valleys over a span of 39 years and the Mingha and Deception valleys over span of 34 years in Arthurs Pass National Park. Paterson (1996) discussed the vulnerability of the State Highway 73 through Bealey to Otira valley, indicating that periodic rockfalls, rock slides, debris flows and rock avalanches, as well as snow avalanching, aggradation and scour will cause significant damage and potential closure of this major transportation link in the future.

Significant research on earthquake-induced landslides has been undertaken by Keefer. Keefer (1999) quantified the amount of sediment deposited by earthquake triggered landslides by analysing world wide data, modelling sediment inputs from such events. He found that with increasing earthquake magnitude, the volume of landslide material also increased. Earthquakes with magnitudes of 6.0, 7.0 and 8.0 are likely to trigger landslides with approximate total volumes of 1.6 million, 45 million and 1.3 billion m^3 respectively (Figure 2.1) (Keefer, 1999). The sediment produced is remobilised and transported downstream contributing to river aggradation and avulsion. A major conclusion of Keefer's (1999) work was that earthquakes with a magnitude of 8.0 or above have the potential to move more than 1 billion m^3 of landslide material. The expected magnitude of an AFE is greater than or equal to $M_w = 8.0$, therefore more than 1 billion m^3 of sediment could be distributed through the alpine river catchments of the South Island New Zealand.

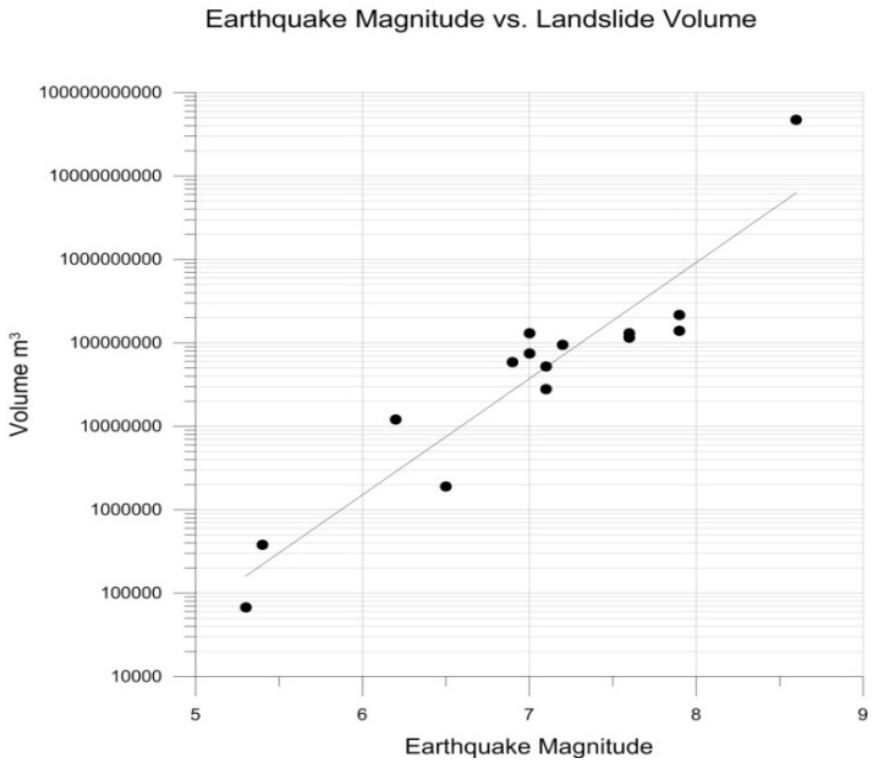

Figure 2.1 Keefer's (1999) data representing the relationship between earthquake magnitude and landslide volume. Modified from Keefer (1994).

Robinson and Davies (2013) confirm that landsliding resulting from an AFE affects an approximate area of >30, 000 km^2 containing a total volume of landslide material of >1 billion m^3. The narrow gorges of the Southern Alps are susceptible to being affected by these events, inducing blockage and inundation of transportation links, particularly those that lie close to the Alpine Fault trace. Robinson and Davies (2013) also note that up to 1000 secondary debris flows would be triggered in the mobilised sediment during the next intensive rainfall period.

It was recognised by Keefer (1994) that the smallest earthquake magnitude capable of producing landslides was $M_w = 4$, very few landslides are produced by earthquakes with a magnitude $M_w < 5$ and thousands and tens of thousands can be triggered by earthquakes exceeding magnitudes $M_w = 7.5$ (Keefer, 1994). Voight and Pariseau (as cited in Yetton, 2000) studied trigger mechanisms for global rockfalls and landslides; they discovered that when a trigger is known it is more often than not associated with an earthquake compared to a heavy rainfall event. This conclusion is interesting given the high frequency of heavy rainfall seasons (monsoon) across the globe versus the comparably low frequency of high magnitude earthquakes. It also challenges Keefer's (1994) finding that very few landslides are produced by lower magnitude ($M_w < 5$) earthquakes.

2.3 Processes and Hazards

2.3.1 Aggradation

Whitehouse and McSaveney (1992) state that aggradation occurs when "*gravel is deposited in stream channels where channel slope decreases or where channel width increases*" (Whitehouse & McSaveney, 1992. p. 2). Dundas (2008) has defined aggradation as "*a temporary process and signifies the river is out of equilibrium*" (Dundas, 2008. p. 137). These definitions touch on the basic concept of aggradation; it is a complex process that involves the gradual or in some instances rapid increase in river channel elevation due to an increase in sediment input or decrease in sediment transport and thus sediment deposition. This process is not always temporary and the fluvial systems do not always fully recover, particularly in the active and dynamic landscapes of New Zealand. According to Dundas (2008) potential triggers of aggradation include;

- High magnitude earthquakes, inducing landslides that deliver large amounts of sediment to fluvial systems
- Slope failures
- Bank undercutting

2.3.2 Avulsion

Jones and Schumm (2009) define avulsion as the relocation of river channels across the floodplain resulting from changes in channel slope. Channel avulsion is often a secondary process in aggrading channels; it is defined as a natural process where flow is diverted from an existing established channel to a new (or old) course on the adjacent floodplain (Slingerland & Smith, 2004). This process of switching channels is one that occurs frequently with minor implications in constantly moving braided channels, in which case the 'new' channels may be re-occupations of older ones; however, avulsions can take on multiple forms depending on the morphology and type of the river as well as the triggering event (Korup, 2004c).

Aggradation and avulsion can be synchronous, avulsion will occur if aggradation continues and aggradation will occur in newly avulsed channels if the sediment load is sufficiently high. An increase in sediment load increases the probability of these natural processes occurring and can be sourced from landslides and landslide dam failures.

2.3.3 Landslides and Landslide Dams

Korup (2005c) implies that landslides have two major effects on fluvial geomorphology, (1) they contribute significant supplies of sediment into the downstream river system, and (2) they can fully or partially impede river channels in the form of semi-permanent landslide dams. Both of these processes have the potential to affect the Taramakau River following an AFE.

Landslides

Landslides involve the mass movement of rock, earth, debris and vegetation downslope. They are a potentially disastrous natural hazard often triggered by earthquakes and heavy rainfall. Keefer (1999) classifies landslides into eight different types (Figure 2.2);

- Falls
- Disrupted slides
- Avalanches

} Disrupted Landslides

- Slumps
- Block slides
- Slow flows

} Coherent Landslides

- Lateral spreads
- Rapid flows

} Lateral Spreads and Flows

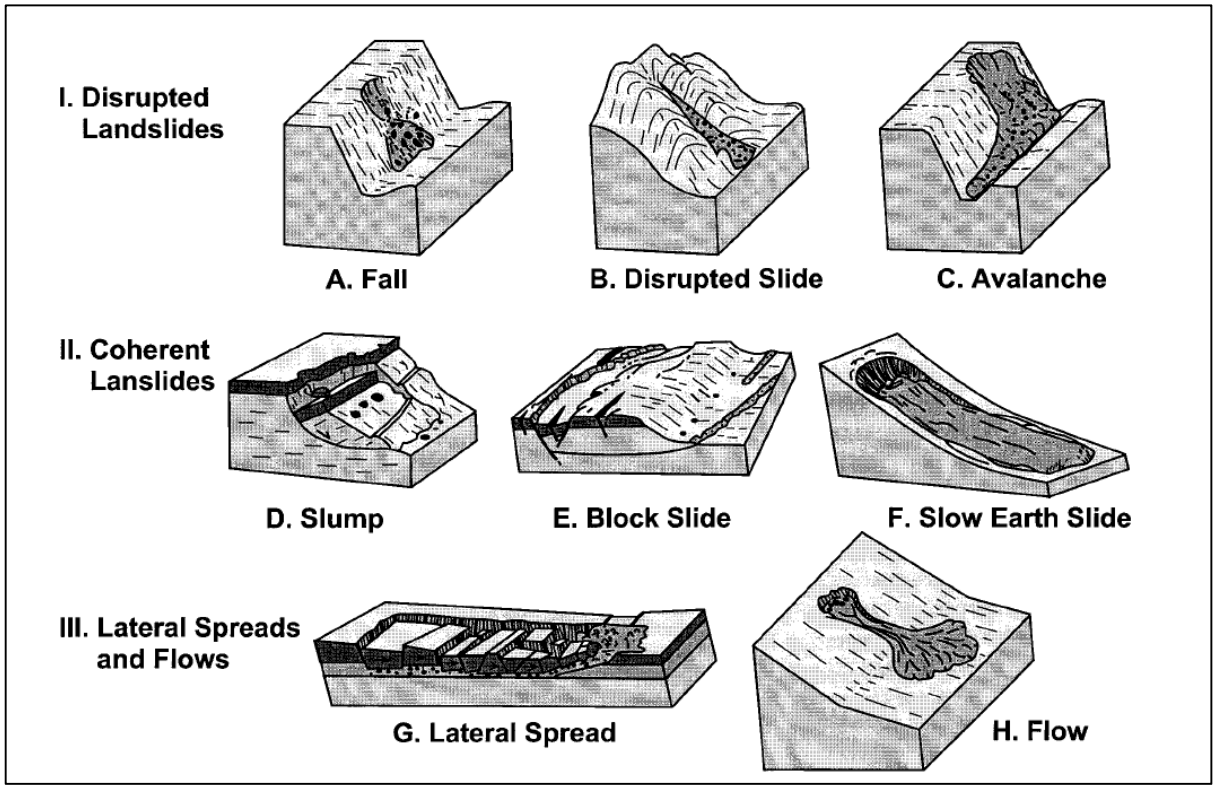

Figure 2.2 Keefer's (1999) classification of landslide types

Falls, disrupted slides and avalanches are sub-categories of a main group classed as disrupted landslides. These mass movements are capable of transporting debris long distances and often originate on steep slopes and move at high velocities. Slumps, block slides and slow flows are sub categories of coherent landslides as they remain fairly intact during movement. Slumps and block slides occur in earthquakes. Slow flows are induced by partly saturated cohesive earth materials, taking much longer to move than slumps and block slides. Lateral spreads and rapid flows take the form of very fluid-like movements that take place only in earth and debris materials.

Landslide deposits are often poorly consolidated making them susceptible to further erosion and remobilisation during intense or prolonged rainfall and/or continued seismic tremors (Harp & Jibson, 1996; Keefer, 1999). Reworking of the loose disaggregated material by surface run off, debris and river flows further contributes to major aggradation downstream (Keefer, 1999).

Landslide Dams

Landslide dams are natural phenomena that result from landslides falling into fluvial systems blocking the flow of water. Two important processes that trigger large scale landslide dams are excessive rainfall and seismic activity, understandably the same triggering processes that cause landslides (Costa & Schuster, 1988). It is likely that a number of landslide dams will form in the steep gorges of the Southern Alps following the next AFE, causing significant damage upon failure.

Landslide dam failures cause downstream river aggradation that deposits sediment and debris across river flats and agricultural land, inducing channel aggradation, avulsion and thus flooding. Upstream of the dam, prior to failure, flooding and subsequent sediment deposition can occur, resulting in aggradation and some avulsion. Hewitt (1998) expresses the effect that landslide dam failures have on river systems;

> *"Where multiple landslide barriers occur, whose occurrence is more or less independent and irregular in space and time, an entire river system may be chronically disturbed."*
>
> (Hewitt, 1998. p. 1)

2.4 New Zealand Case Histories

Three past catastrophic New Zealand examples of aggradation and avulsion triggered by aseismic (i.e not earthquake-generated) mass movements include (1) the Gaunt Creek Slip into the Waitangitaona River, Westland; (2) Boulder Creek debris slumps into the Moeraki

River, Westland and (3) the Mt. Adams rock avalanche into the Poerua River, Westland. These examples provide important insights into the potential impacts of coseismic landsliding on the Taramakau River and are used as proxies to understand the hazards of aggradation and avulsion following increases in sediment input.

Gaunt Creek

Substantial debris input into Gaunt Creek in Westland has been recorded since 1918. In 1967 a minor flood coupled with an increase in sediment input from a debris slip triggered a major avulsion of the Waitangitaona River. The avulsion resulted in the development of a braided fan complex which threatened swamp and farmland subsequently burying 3.7 km^2 of it (Figure 2.3) (Korup, 2004c). The braided fan complex shifted flow of the Waitangitaona River into Lake Wahapo across previously untouched farmland. Consistent and progressive landsliding at this site has contributed a significant increase in sediment supply to the Waitangitaona catchment.

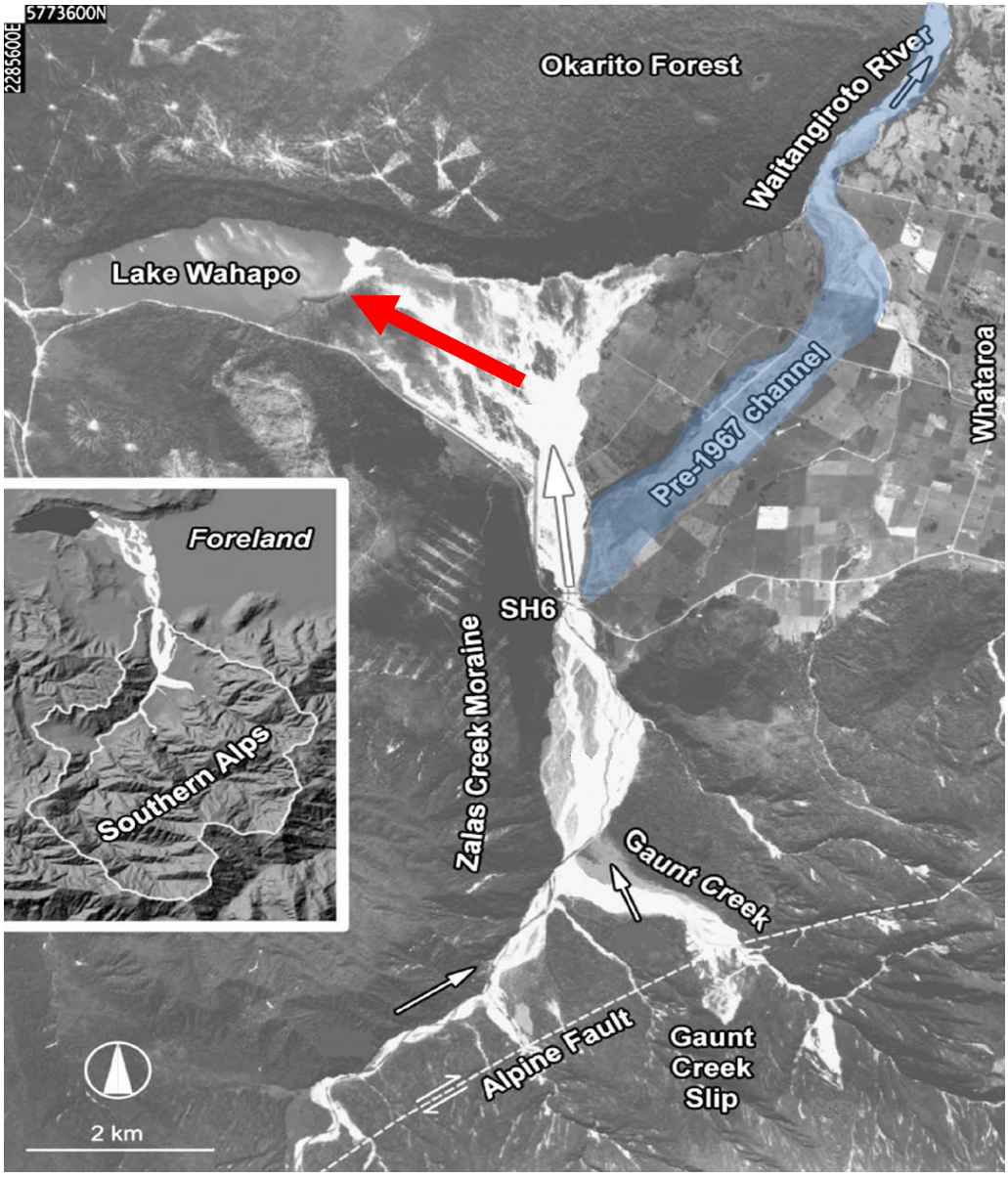

Figure 2.3 Gaunt Creek channel avulsion of the Waitangitaona River. Arrows highlight the direction of flow. Red arrow indicates direction of new channel flow toward Lake Wahapo. The pre 1967 channel is highlighted in blue. Inset image identifies catchment boundary in Southern Alps. Modified from Korup (2004c).

Boulder Creek

Similar to the Waitangitaona River avulsion was a significant channel avulsion seen in Boulder Creek, on the West Coast of the South Island New Zealand. This avulsion was triggered by episodic tributary sedimentary input from Boulder Creek debris flows into the Moeraki catchment. Aggradation occurred over a total area of 0.28 km^2. Schumm (as cited in Korup, 2004c) found that the input of landslide debris can result in river metamorphosis, increasing the active channel area downstream fourfold, consequently resulting in in-channel aggradation which may promote over bank deposition, channel avulsion and further flooding. Schumm's (as cited in Korup, 2004c) conclusion summarises part of the effects seen by the Boulder Creek channel avulsion.

Poerua Valley

The Mt. Adams rock avalanche is well documented (Hancox et al., 2005) and a significant New Zealand example of the hazards that surround landslide dam break failure and subsequent aggradation. It occurred in 1999 on the Poerua River. This event is one of a series of recent large scale New Zealand landslides, and has caused considerable changes in fluvial geomorphology, dominated by channel avulsion. A dam resulted from an aseismic rock avalanche that fell into the Poerua valley on the 6th October 1999. Overtopping of the dam soon commenced resulting in an outburst flood through the Poerua valley moving as a sediment-laden wave through the valley. Significant amounts of fine sediment were deposited as the wave reached the alluvial fan, but more important were the millions of cubic metres of dam material that were deposited on the fan during subsequent high river flows. Major channel avulsion occurred reactivating an abandoned channel of the Poerua River, 16 months after the dam had failed (Figure 2.4). The avulsion resulted in destruction of farmland and assets. The dam break flood tore up vegetation depositing it as large woody debris resulting in knick points and the production of micro-cascades (Korup, 2004c).

Figure 2.4 Poerua channel avulsion induced by gravel aggradation. The former channel shifted east towards the McKenzie farm, reactivating a previous channel of the Poerua River. Source Hancox et al (2005)

A previous, much smaller landslide occurred at this site in 1997. Hancox et al (2005) suggests that the Mt. Adams collapse was likely caused by a combination of processes including ongoing weathering, the weakening of the steep mountain slopes associated with fluvial erosion, and the previous occurrence of a landslide on the lower slopes which could have ultimately contributed to the instability of the upper slopes.

The Poerua dam itself lasted less than a week, however, overtopping was inevitable with the next high rainfall event, causing dam failure by channel erosion. Costa and Schuster (1988) state that landslide dams worldwide often fail within the first year of formation, however on the West Coast of New Zealand it is rare for a landslide dam to survive long periods of time due to the combined effects of high rainfall and an active landscape, commonly failing within days; nevertheless the Young River landslide dam of 2008, similar in size to the Poerua dam, remains intact to this day (Davies pers comm, 2014). The Poerua dam overtopped the day following its formation on the 7th October 1999 and subsequently failed on the 12th October 1999. Two years later, the course of the Poerua River had shifted approximately 800 metres east from the previous active channel (Figure 2.5). This channel avulsion was a result of gravel deposition in the main channel. The new channel overwhelmed previously untouched farmland. Another two years and the channel had avulsed back towards the centre of the valley. The unpredictable switching back and forth of the river channel continues to threaten and restrict the use of surrounding farmland (Hancox et al., 2005).

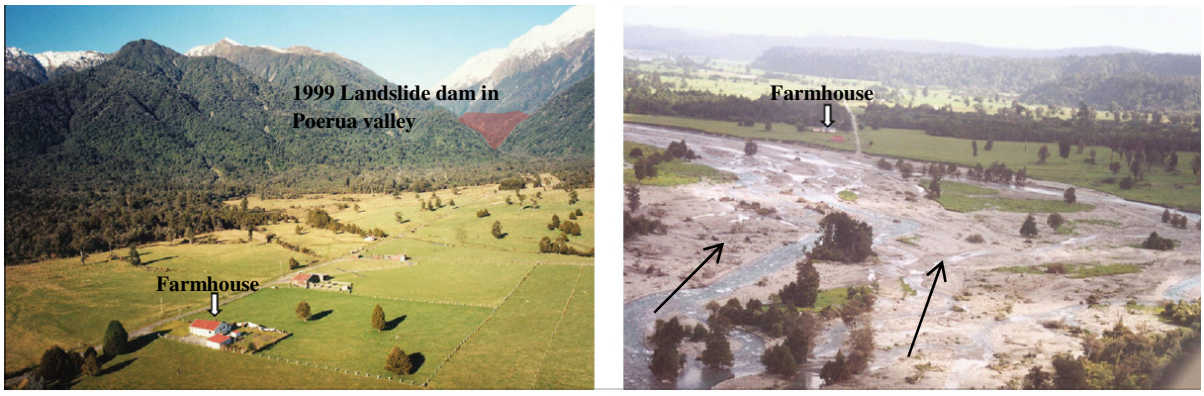

Figure 2.5 Poerua Valley before and after the Mt Adams rock avalanche. Left image is from 1987; right image is from 2002 and is a view downstream of Poerua valley three years after the dam break failure. Black arrows indicate the direction of flow. Source Davies and McSaveney (2011)

Davies, McSaveney, and Doscher (2005) found that within six years of the failure, 1.5 x 10^6 m^3 of sediment had been deposited on downstream farmland. Davies et al (2005) calculated

that the increase in sediment load was equivalent to 500 years' worth of regular sediment input within just six years. The magnitude of this value caused by an aseismic landslide suggests a high magnitude ($M_w = 8.0$) event such as an AFE will cause extensive damage and channel aggradation.

The impacts observed at the Poerua River fan are expected to continue for several decades emphasizing the longevity of fluvial hazards such as aggradation and avulsion. When the system becomes exhausted of landslide-derived sediment, aggradation will slow and degradation will become more prominent. Nelson (2012) found that aggradation on the fan head ceased and degradation became apparent in 2005, six years after the event. This major natural disaster can be used as a generic analogue indicating what is likely to happen to the Taramakau River in the event of an AFE.

Continual, episodic debris pulses from landslides in Westland, South Island (eg. Gaunt and Boulder Creeks), have caused extensive damage to State Highway bridges and roads through aggradation on fans which has promoted lateral channel instability resulting in an increase in flood frequency (Korup, 2004c). The next AFE is predicted to occur within the next 50 years (Hancox et al., 2005). A rupture will result in the formation of multiple landslide dams and the subsequent hazards that follow such an event. It is emphasized by Hancox et al (2005) that the information gained from studies conducted on the Poerua event has provided an insight into the potential risks associated with large coseismic landslides reflected in fluvial geomorphology.

2.5 International Cases

The 2008 Wenchuan earthquake in China and the 1999 Chi Chi earthquake in Taiwan were destructive natural disasters taking numerous lives, destroying infrastructure and severely modifying the surrounding landscapes. These two events are discussed below due to the similarities in earthquake magnitude to that which has been estimated for the next AFE. Data from these earthquakes are subsequently used to calculate landslide volume estimates for the Taramakau catchment (see Chapter 4).

Wenchuan Earthquake

On the 12th of May 2008 the Longmenshan thrust belt ruptured producing a $M_w = 8.0$ earthquake felt across the Chinese counties of Wenchuan, Beichuan, and Qingchuan (Cheng, He, Chen, & Tao, 2010; Dai et al., 2011; Tang et al., 2011; Wang, Cui, & Wang, 2009). The Wenchuan earthquake was a direct result of the rupture of, the Beichuan and Pengguan faults,

centrally located on the Longmenshan thrust belt, beneath the eastern margin of the Tibetan Plateau in Sichuan (Dai et al., 2011; Xu et al., 2009). This earthquake triggered more than 60,000 landslides, producing a total volume of 5 - 15 billion m^3 of debris (Dai et al., 2011; Huang & Li, 2014). The landslides varied in size and have been classed into different types corresponding to those ranked by Keefer (1999) (Figure 2.2). Disrupted landslides, including falls, slides and avalanches, contributed to the significant volume of sediment produced from this earthquake. The sediment was subject to remobilization during periods of heavy rainfall. During August of 2010 a rainstorm triggered 21 catastrophic debris flows causing widespread damage (Figure 2.6) (Tang et al., 2011). These debris flows directly blocked rivers producing debris dams which later failed inducing river aggradation, avulsion and downstream flooding. The similarities in hillslope gradient, lithology and rupture characteristics make the Wenchuan earthquake a significant analogue to an AFE.

Figure 2.6 Before and after the Wenchuan Earthquake. A) depositional fan with construction site (before), B) debris flow covering the fan, burying the road and impeding on the river (after). Source Tang et al (2011).

Chi Chi Earthquake

The Chi Chi earthquake (M_w = 7.6) in 1999 triggered approximately 20,000 landslides, the largest of which produced a total volume of 120 million m^3 of landslide material (Chen, Lin, & Hung, 2004). A further 30,000 landslides were initiated a year after the earthquake by Typhoon Toraji. From these landslides more than 100 landslide dams and subsequent lakes formed (Yanties, Tucker, Mueller, & Chen, 2010).

The sediment from the multitude of landslides entered drainage networks overwhelming the fluvial systems and halting erosional processes. Yanites et al (2010) found that gauges in the Peking River revealed that six years after the earthquake, a total of 3.4 m of aggradation had occurred in the main channel of this river resulting in the burial of bridge piers (Figure 2.7).

Figure 2.7 Bridge piers that have almost completely been engulfed by Chi Chi earthquake derived sediment. Source Yanites et al (2010).

The production of river knickpoints caused by local uplift during the rupture resulted in rapid local down cutting that generated a knick-point which retreated upstream (Figure 2.8). An increase in sediment load in rivers farther away from the surface rupture, however, resulted in river aggradation and avulsion from landsliding. The relative proximity of the Taiwanese rivers to the fault controlled the magnitude, type and longevity of geomorphic change that occurred within the river systems. This finding is one that must be considered relevant to the

Taramakau River, which is obliquely cut by the trace of the Alpine Fault as well as being close to the source of landsliding.

Figure 2.8 Production of large river knickpoints from the surface rupture of the Chi Chi earthquake 1999. Clear damage to infrastructure and approximately five metres of vertical displacement to the river bed. *Pifeng Bridge,* n.d photograph, viewed 2 July 2014, < http://www.geologie.geowissenschaften.uni-muenchen.de/archiv/taiwan_/index.html>

Both the Wenchuan and Chi Chi earthquakes provide useful insights into the effects that an AFE will have on the surrounding landscape and the changes and potential hazards that will impact the Taramakau River system.

2.6 Summary

New Zealand has a history of catastrophic natural hazards, many of which originate from seismic activity. Relative to this study, three prime examples of river aggradation and avulsion have been discussed; Gaunt Creek, Boulder Creek and the Mt. Adams rock avalanche into the Poerua River. These Westland examples are critical in understanding the relationship between landslides and the impacts on fluvial systems. While each of these events was aseismic, the processes of aggradation, avulsion and flooding (but not necessarily their magnitudes) are likely to be similar following an AFE. The 2008 Wenchuan earthquake and 1999 Chi Chi earthquake are international analogues of how the New Zealand landscape may respond to the next AFE. These high magnitude earthquakes produced voluminous landsliding resulting in river aggradation, avulsion and flooding. The next major AFE may be expected to have similar effects translating through the alpine drainage network including the Taramakau River.

Chapter 3 – Research Methods

3.1 Introduction

The research methods used in this thesis follow similar approaches used in previous fluvial hazard assessments (Korup et al., 2004; Ouchi, 1983, 2004; Schumm, Dumont, & Holbrook, 2000). The aim of Chapter 3 is to describe the research methods employed in this thesis providing background information on each procedure. Dedicated chapters detail each individual research method and the subsequent results.

Three different research methods have been employed to model and better understand the implications of an AFE on the Taramakau River; these are (i) a hydraulic data analysis (see section 3.2), (ii) aerial imagery (see section 3.3) and (iii) micro-scale modelling (see section 3.4), all of which were carried out in parallel throughout the project. A hydraulic data analysis was the first step in understanding the current fluvial regime of the Taramakau River under "normal" conditions and how it may behave after large sediment inputs from landslides. Hydraulic data for the Taramakau River were sourced from the Sustainable Water Allocation team at the National Institute of Water and Atmospheric Research (NIWA). Landslide volume values were provided by algorithms developed and utilised by Robinson (2014). Aerial photographic interpretations were carried out through satellite imagery and stereoscopic interpretation. Google Earth played a role in visually inspecting the studied site from above recognising significant geomorphic structures. Results from the data analysis and aerial imagery ultimately controlled the design of the micro-scale model. Micro-scale modelling was employed to identify the direct physical implications that uplift and lateral displacement on the Alpine Fault may have on the course of the river. Increases in sediment supply were modelled, representing coseismic landsliding. All of the research methods combined to develop a greater understanding of the Taramakau River currently and how it may behave during and after an AFE.

3.2 Hydraulic Data Analysis

To understand the current fluvial dynamics of the Taramakau River, a basic data analysis was conducted. The data were sourced from the Sustainable Water Allocation team at NIWA, and included information on;

- Daily mean flows
- Sediment concentration (further used to calculate suspended sediment load and mean annual sediment load)
- Hydraulic data (mean water flow velocity, mean and maximum depth, wetted area, hydraulic radius)
- Precipitation readings (Inchbonnie) sourced from NIWA CliFlo database

The data span approximately 44 years from December 1970 to February 2014, a useful window into the behaviour of the Taramakau River under normal flow conditions.

The hydraulic readings have been measured at one specific site in the river (Figure 3.1). The data from this one site have been used as representative values for the entire Taramakau River, assuming that the river behaves similarly throughout the whole system. It must be considered however that as the gauging station is located approximately 30 km downstream of the study area, hydraulic parameters will vary progressively downstream as tributaries join the Taramakau River. To account for this, hydraulic parameters from the Taipo River, the major tributary to the Taramakau, have been subtracted from the Taramakau data, representing more accurate hydraulic parameters for the study area. Empirical and regression models have been developed to estimate the hydraulic properties throughout fluvial systems, scaling the values to best represent different domains of the catchment. The methods underpinning such models are beyond the scope of this thesis however more information can be found in Hicks et al (2011) and at NIWA. Nevertheless the data sourced from this one site minus Taipo River readings will be used in this thesis to represent the hydraulic parameters of the Taramakau River within the study area.

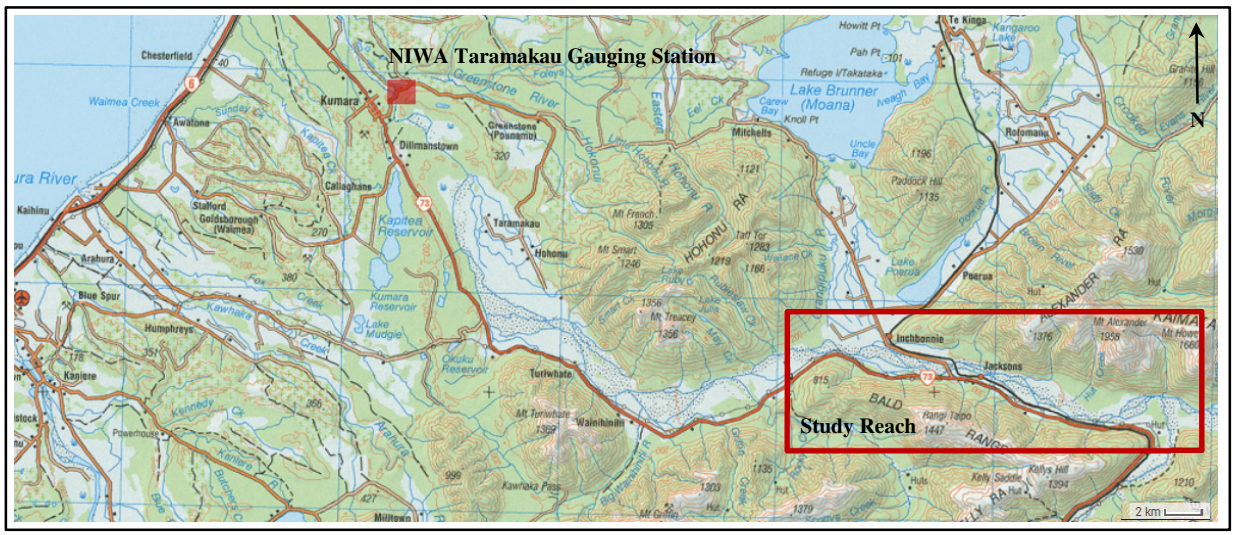

Figure 3.1 NIWA Gauging Site 91104 Taramakau at Greenstone Bridge relative to study reach. Base map sourced from Topo Map.

The sediment load of any river consists of both suspended sediment load and bed load. Suspended sediment load is the amount of sediment transported through the river in suspension (usually fine sands, silts and clays). Bed load sediment consists of material that moves downstream along the bed of the river (sand and gravel). Suspended sediment load was calculated through the NIWA river discharge and sediment concentration values. This amounted to the volume of suspended sediment that the Taramakau River could carry over a year under normal conditions. For the data calculations in this thesis, it was assumed that the total sediment load consists of 50% suspended sediment and another 50% of bedload sediment (Davies and McSaveney, 2006). It is likely, however, that this ratio will vary progressively downstream. Typically braided rivers, identified by bed load channel patterns, develop into a meandering river further downstream, characterised by suspended sediment load and meandering channel patterns. Schumm (as cited in Schumm et al., 2000) suggests that total bedload decreases downstream as suspended sediment load increases in fluvial systems. Nevertheless for this thesis a ratio of 50% suspended sediment and 50% bed load sediment has been used in the braided study reach.

Landslide volumes following an AFE for the Taramakau catchment were provided by Robinson (2014). Robinson (2014) produced landslide volumes with the aid of methods conducted by Brunetti, Guzzetti, and Rossi (2009) that assess the likelihood of landslides through probability distribution functions (Brunetti et al., 2009; Robinson, 2014). Landslide volume estimates were also based on information and measurements gathered from similar magnitude earthquakes in Wenchuan, Chi Chi and Northridge, deriving comparable numbers

of landslides and consequent volumes. This thesis acknowledges that the landslide volumes employed for further calculations here, are based on data provided by one study. It is the aim of this thesis to build on the research conducted by Robinson (2014). Knowing an estimate of landslide volume potentially produced in the Taramakau catchment from an AFE, it was then calculated how the river might respond to this sediment addition, estimating the likely scale of river aggradation. To estimate how the landslide sediment would be distributed through the catchment, comparative studies were done with the Mt Adams 1999 rock avalanche, discussed in Chapter 2. Quantitative analysis of Poerua sediment input, sediment discharge and aggradation values have been conducted by Korup et al (2004), Hancox et al (2005), Davies and McSaveney (2007) , Nelson (2012) and the West Coast Regional Council (WCRC, 2002). Comparisons were made between the landslide volumes of Poerua and those estimated by Robinson (2014) to produce apparent values of sediment input, sediment discharge and aggradation following AFE landslides in the Taramakau catchment. Combining these calculated values with the reworked NIWA data, it was possible to estimate how the additional sediment may be reworked and remobilised through the system. To determine aggradation values the floodplain area had to be calculated. This was done through standard GIS based cut and fill algorithms. These calculations were done to understand the amount of aggradation that may result from an AFE, leading to an understanding of the potential risk of avulsion and flooding within the study reach.

3.3 Aerial Imagery

It is essential that historical knowledge of past events is established as this is integral to anticipating future events. A key method in establishing this is through aerial imagery and geomorphology studies. Aerial photographs were collected from the University of Canterbury's Geological Sciences Department and date back to 1943. When used in conjunction with present satellite images sourced from Land Information New Zealand (LINZ) significant shifts in Taramakau River channels were recognised.

The aerial photographs were interpreted through stereoscopic analysis, from which observations were made and the differences in channel morphology were identified relative to the present day location of the river. Recognising past shifts in the Taramakau River channels assists in understanding how the river may avulse after an AFE.

3.4 Micro-Scale Modelling

Micro-scale models were employed to reproduce fluvial regimes at a small scale. Micro-scale models have been extensively employed throughout the recent literature. The micro-scale modelling for this thesis was conducted on a stream board (Figure 3.2). The spatial and temporal parameters of this model were not accurately scaled to the Taramakau River, however, understanding qualitatively how a braided fluvial system may respond to fault displacement and large sediment inputs was established. The advantages of this model were that the experiments were conducted in a controlled environment and were constantly monitored through photography.

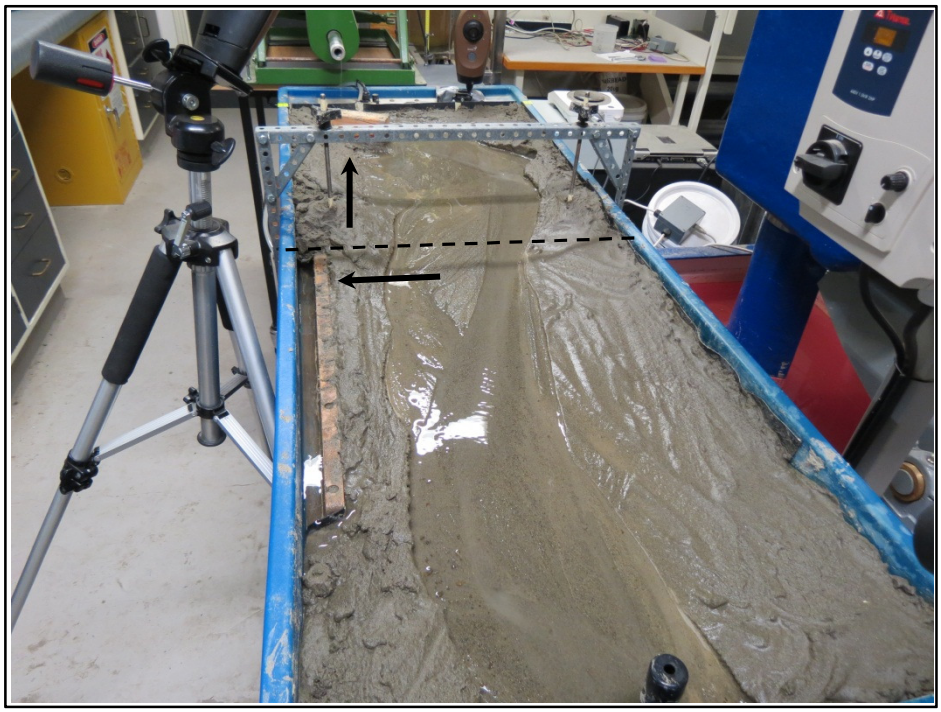

Figure 3.2 Stream board set up used during the experiments.

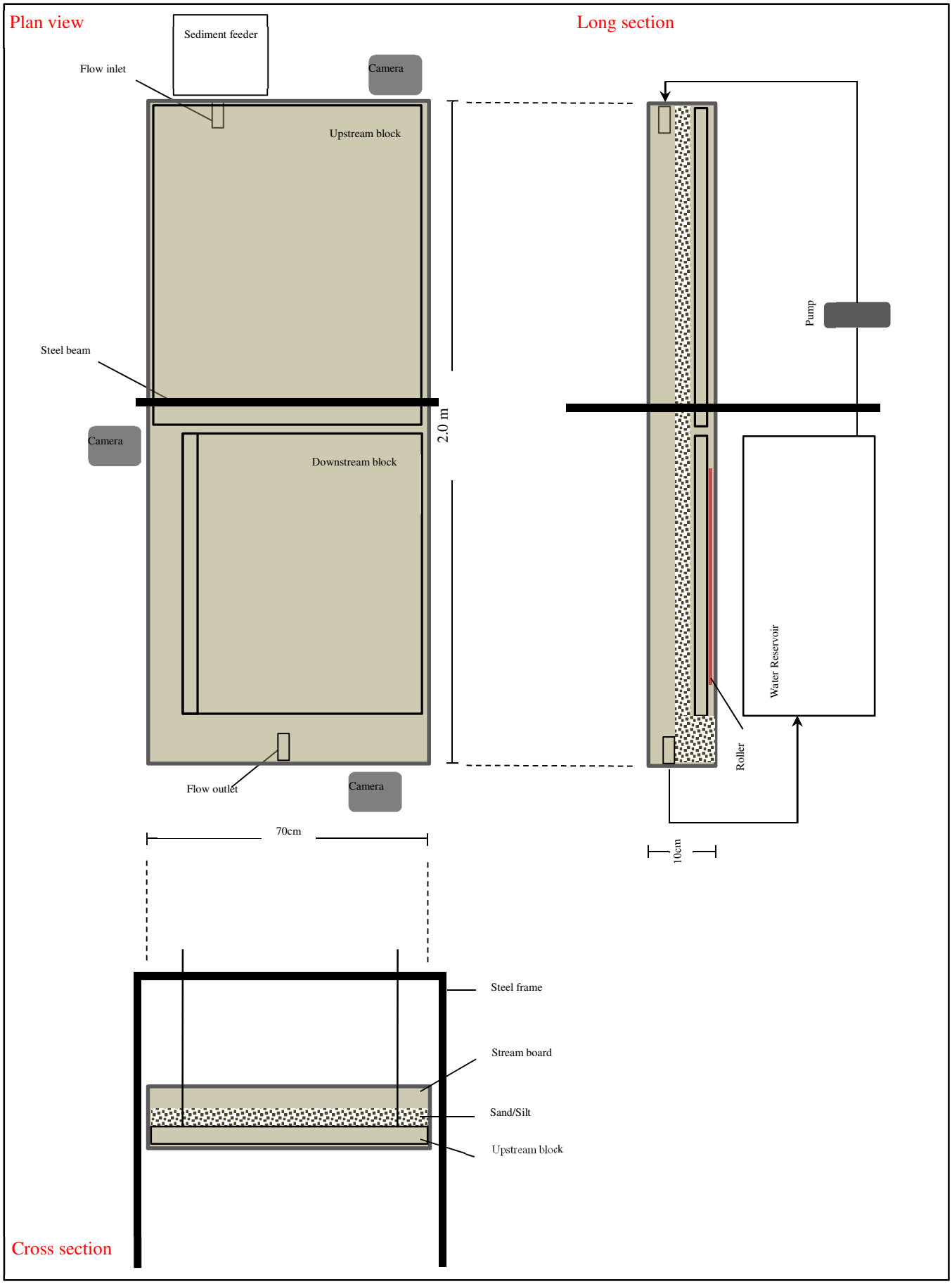

Figure 3.3 Stream board layout and dimensions.

The experiments were performed at the University of Canterbury. Throughout the modelling, observations were recorded manually, and photos were taken every five minutes to monitor changes while the stream board was unattended. The stream board has a width of 70 cm, length of two metres and depth of 10 cm (Figure 3.3). Sitting inside the stream board are two blocks of ply-wood divided in the middle marking the trace of the modelled strike-slip fault. The upstream block is attached to a frame enabling vertical displacement. The downstream block is narrower than the upstream block and has a plank of wood attached to one end enabling the block to be pulled dextrally along rollers, representing strike-slip movement (Figure 3.3). The wooden planks have rubber seals between them and with the boundaries of the stream board to prevent leakage during flow. The stream board was tilted downstream to produce a river bed slope of 0.5 degrees, which promoted sufficient channel flow.

Three main experiments were run, observing how the system responded to dextral strike-slip and vertical displacement followed by an increase in sediment load.

I. Complete instant rupture and complete instant sediment addition
II. Complete instant rupture, with delayed incremental sediment additions
III. Incremental rupture, with instant incremental sediment additions

Each experiment began with the development of the channel. The wooden blocks were covered by 25 mm depth of 750 µm sieved sediment, and water flowed out of one nozzle at a rate of approximately 0.4 L/min. This flow rate was chosen as it was sufficient to produce braided channels across the stream board. Sediment was continually added to the system at a rate of 0.05 g/s through a rotating sediment feeder at the upstream end. This rate was chosen as it was fast enough for the sediment to be transported downstream as bed load and at the same time did not overload the system with sediment blocking the flow of water upstream. Three cameras were set to record images at five minute intervals to monitor the development of channels. Once the system was well established and clear braids had developed a dextral strike-slip fault rupture with vertical displacement was modelled in Experiments I and II. During the rupture phase, the cameras were set to five second intervals to closely monitor changes. The rupture phase first involved the vertical component of displacement by winding the upstream block vertically by approximately 25 mm. This was immediately followed by the lateral shift of the downstream block simply by pulling it to the true right of the river. In Experiment I, 100 g of additional sediment was supplied to the system immediately after the rupture based on experimental practice, representing an increase in sediment load from

modelled upstream landsliding. Thirty minutes after displacement in Experiment II, 25 g of additional sediment was supplied to the stream board modelling delayed and episodic delivery of landslide material. A further three additions of sediment were added over the next hour and a half, at 30 minute intervals. After 15 minutes of the time lapse cameras being set at five second intervals since displacement in Experiment II, the cameras intervals were increased to five minutes as the river began to slowly adjust to the change and did not have to be as closely monitored. The cameras then recorded the changes to the fluvial system after the dextral strike-slip movement and abrupt increase in sediment load over the following five hours. Experiment III varied in that the displacement was incremental and 'landslide' sediment was added to the system with each individual phase of displacement. Four evenly spaced phases of displacement were modelled representing aftershocks that may follow an AFE. Equal amounts of sediment were added with each displacement event as it is likely that with each aftershock, landslide material will be remobilised through the fluvial system. Each of the three experiments took approximately 2 - 3 days from start to finish depending on any modifications that had to be made during the experiments.

3.5 Summary

From the data analysis, the distribution of AFE landslide material through the Taramakau catchment and associated aggradation values were estimated. Conclusions from the data analysis and from the aerial imagery analysis assisted in the construction of the micro-scale model. The model experiments replicated dextral strike-slip displacement perpendicular to the flow of a braided river system, representing the Taramakau River as well as modelling increased sediment loads representing landslide material addition. Qualitative and quantitative results from these methods contribute to a hazard assessment of the area regarding channel aggradation, avulsion and flooding, as outlined in the following chapters.

Chapter 4 – Data Analysis

4.1 Introduction

Chapter 4 presents the findings of a hydraulic data analysis for the Taramakau River. New Zealand Rivers are monitored by the National Institute of Water and Atmospheric Research (NIWA). The Taramakau River has hydraulic readings that date back to 1970, the majority of which are from 1979 to 2014, a 44 year time period. Landslide volume data for the Taramakau catchment provided by Robinson (2014) are an approximation based on three major historic earthquakes that generated significant landsliding; Wenchuan, Chi Chi and Northridge (Dai et al., 2011; Harp & Jibson, 1996; Tang., 2011, Wang, Chigira, & Furuya, 2003; Xu., 2009).

The data analysis involved (1) graphing the NIWA data and identifying relationships between different parameters, (2) calculating maximum aggradation levels from estimated landslide volumes, (3) analysing data from the Mt Adams rock avalanche in 1999 and comparing landslide volume percentages to what may be deposited in the Taramakau catchment distributed through the study area, and (4) calculating a one-in-100 year flood based on the NIWA flow rate data. From these four steps an estimate on the magnitude of an AFE and associated landsliding in the Taramakau catchment was derived, indicating the likely scale of river aggradation and highlighting the potential damage to critical transportation links.

4.2 Taramakau River NIWA Data

Discharge in the Taramakau River varies considerably throughout the year (Figure 4.1). Discharge closely follows the average precipitation trend for the study area (Figure 4.1), so a positive correlation exists between monthly average discharge and monthly average precipitation for the study area. Higher discharge readings are associated with the months from October to December with average values ranging between 145 m^3/s to 150 m^3/s. This increase in discharge corresponds to the spring snow melt as well as an increase in average precipitation during this time. The average annual discharge for the Taramakau River is approximately 115 m^3/s and the average annual precipitation for the study area is 427 mm.

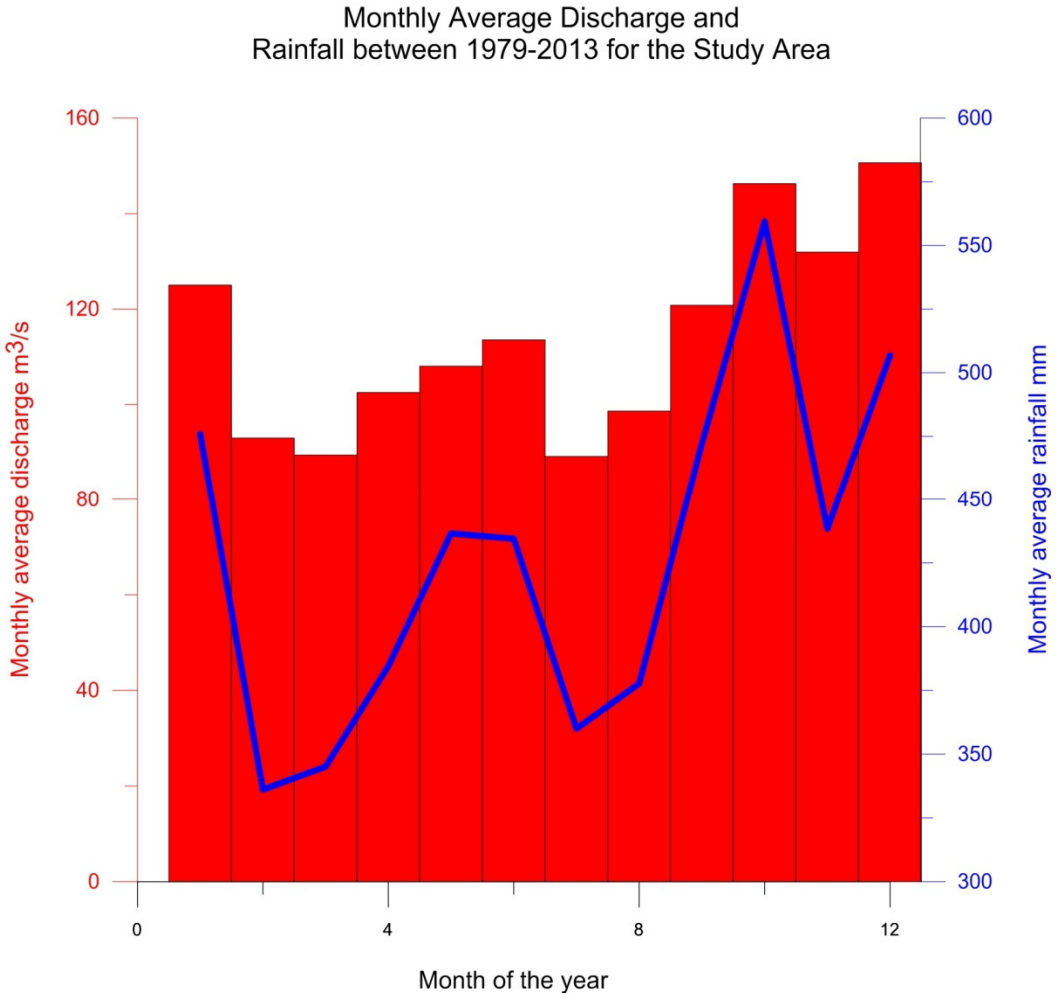

Figure 4.1 Average monthly discharge and precipitation values collated for each year from 1979-2013. Data sourced from NIWA (M. Hicks, pers comm, 2014).

Crucial to this study is the movement of sediment through the fluvial network described by the relationship between sediment load and discharge. To calculate the sediment load, values of sediment concentration are needed. Unfortunately the data supplied from NIWA contain a

significant number of empty sediment concentration values, limiting the sample size available. Of the recorded dates 286 out of 321 readings have no sediment concentration values. This left 35 usable data sets that were used for further analysis from 1970 to 1995 (Figure 4.2). This thesis acknowledges that this data set is reduced and that relationships between sediment concentration and other variables have been built on occasional measurements for the Taramakau River.

Suspended sediment load was calculated by multiplying the gauged flow by sediment concentration. The calculated average suspended sediment load for the Taramakau is 382 kg/s. Bedload measurements were not provided by NIWA, however, it was assumed that bedload would contribute 50% of the total sediment load (Davies & McSaveney, 2006); the average total sediment load for the Taramakau River has been calculated as 9.64 x 10^6 m^3/yr. using an average schist bulk density of 2500 kg/m^3 (Table 1).

Table 1 Average hydraulic parameters for the Taramakau River. Values reworked from raw NIWA data provided by M. Hicks, personal communication, March 27, 2014.

Average Precipitation mm	Average Discharge m^3/s	Average Suspended Sediment load kg/s	Average Total Sediment load m^3/yr
427	115	382	9.6 x 10^6 m^3

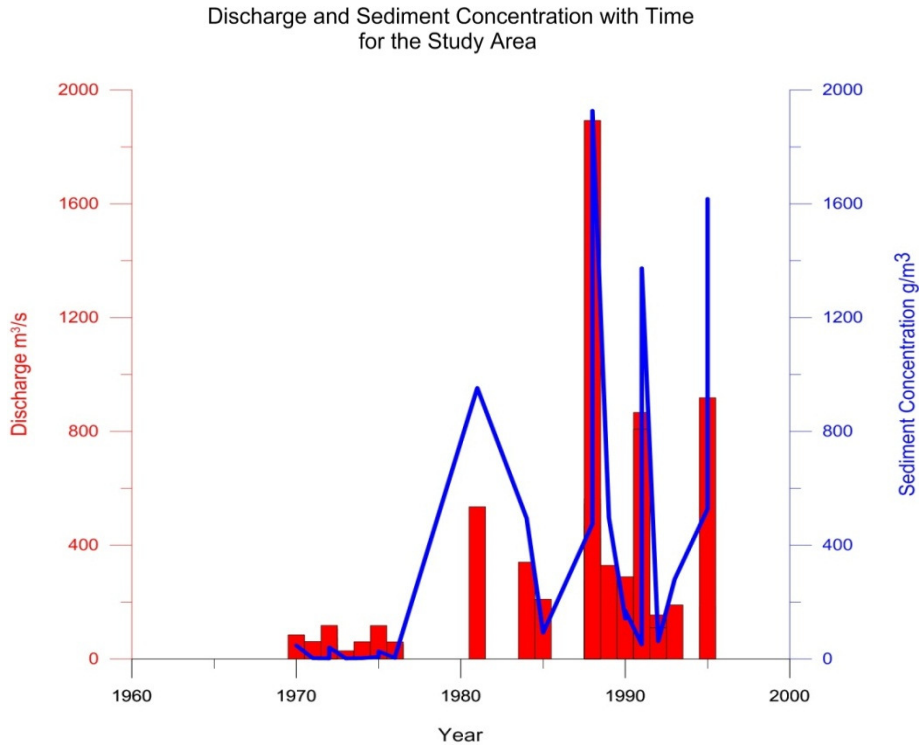

Figure 4.2 Average Discharge and sediment concentration for a reduced data set from 1970-1995. Data sourced from NIWA (M. Hicks, pers comm, 2014).

A distinct relationship is evident when plotting sediment concentration against average discharge (Figure 4.2 & 4.3). Both suspended sediment concentration and load increase with increasing discharge. All three of these variables mirror each other for the period of 1970 - 1995 (Figure 4.4). As suspended sediment load and sediment concentration both increase with increasing discharge it is calculated that the total sediment load also increases with increasing discharge (Figure 4.5). As discharge increases the river is capable of carrying an increased total sediment load (suspended sediment and bedload sediment), as indicated by the trend in Figure 4.5.

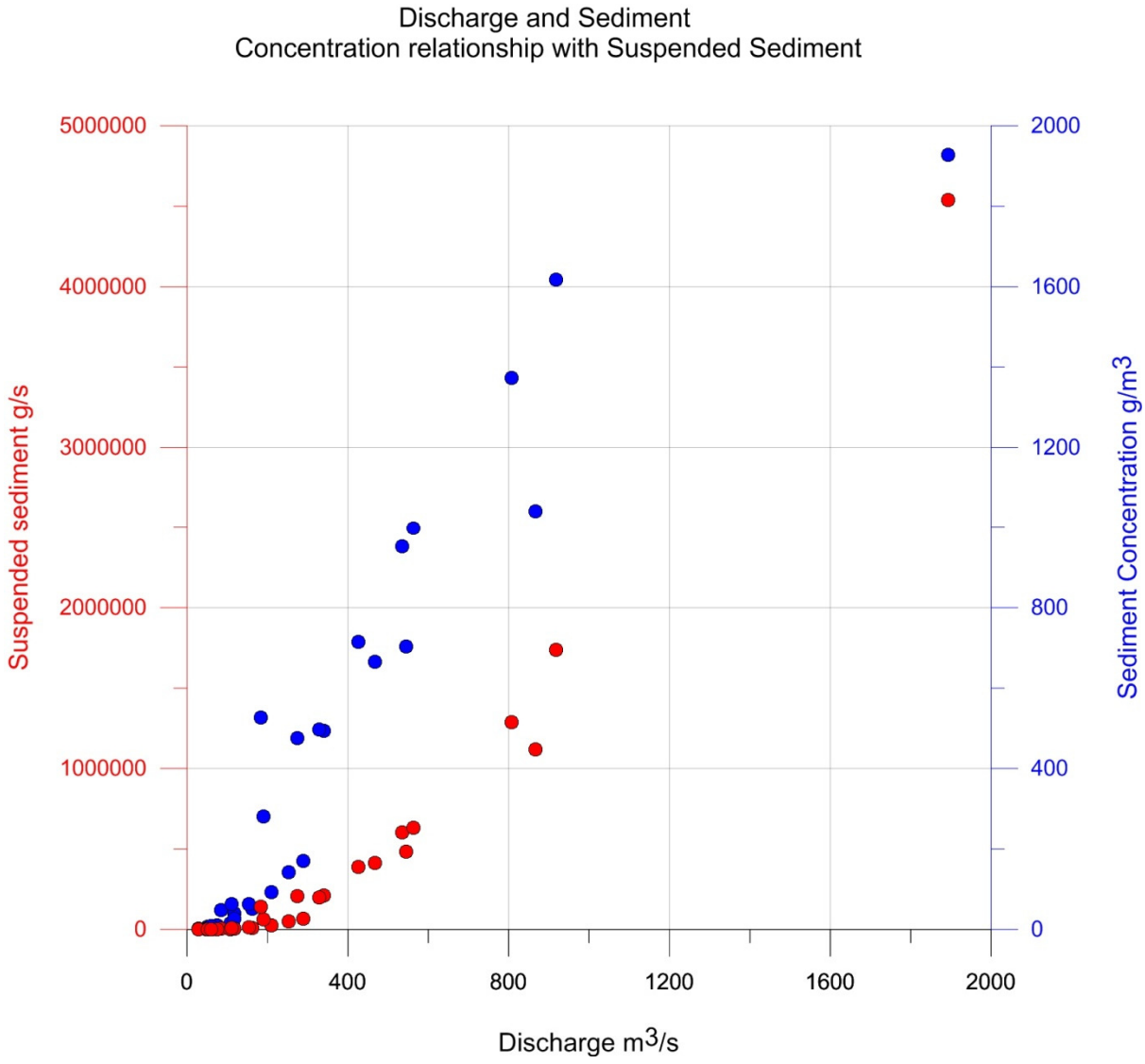

Figure 4.3 Relationship between suspended sediment and sediment concentration with average discharge for the Taramakau River. Data sourced from NIWA (M. Hicks, pers comm, 2014).

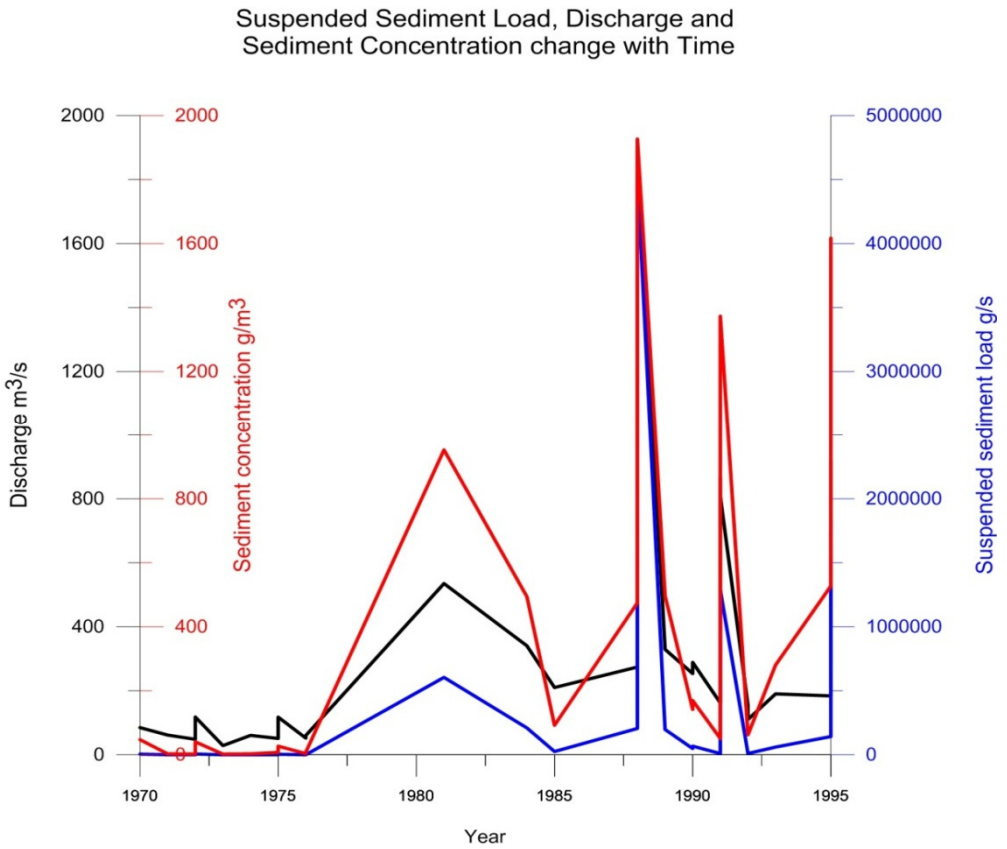

Figure 4.4 Relationship between average discharge, sediment concentration and suspended sediment load between 1970 and 1995 for the Taramakau River. Data sourced from NIWA (M. Hicks, pers comm, 2014).

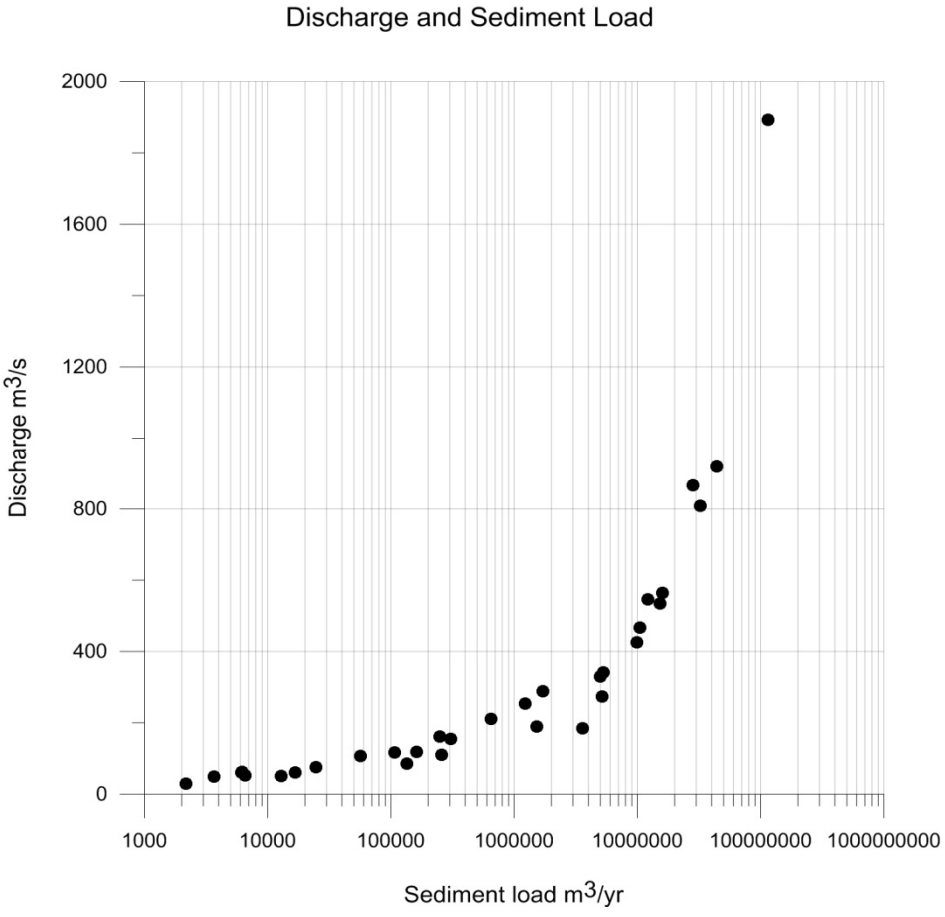

Figure 4.5 Increasing relationship between average sediment load and average discharge for the Taramakau River. Data sourced from NIWA (M. Hicks, pers comm, 2014).

All of the hydraulic data including velocity, depth, width and other variables will not be presented here as they are not relevant to the focus of this study, however, they are attached in Appendix One.

4.3 Landslide Volume Data

The landslide volume data provided by calculations conducted by Robinson (2014) represent estimated volumes of sediment deposited by landslides immediately following an AFE and are in units of m^3. The average minimum and maximum credible volumes of landslide material deposited in the Taramakau catchment are estimated as; 6.8×10^7 m^3 and 3.0×10^8 m^3 respectively. The average total sediment load for the Taramakau River is 9.6×10^6 m^3. Immediately, it is seen that the amount of instantaneous sediment sourced from coseismic landsliding in the Taramakau catchment could potentially be 1 - 2 orders or magnitude greater than that annually transported by the Taramakau River.

Aggradation values were obtained by dividing landslide volumes by the floodplain area (8.4×10^7 m^2). The flood plain area was estimated through GIS cut and fill algorithms. The calculated values below represent the absolute maximum levels of aggradation associated with an AFE in the study area. These calculations infer that all landslide material will be deposited in the channel and on the floodplain of the Taramakau study area, when in fact a large amount of the landslide derived material is likely to remain in the lower gorges of the Taramakau valley, upstream of the study area;

-A minimum landslide volume will result in an upper aggradation value of 0.81 m.

-A maximum credible landslide volume will result in an upper aggradation value of 3.6 m.

Based on studies conducted on the Mt Adams rock avalanche in 1999 by Korup et al (2004) and Nelson (2012) small percentages of landslide material were reworked through the system and delivered to the alluvial fan (Table 2). Almost half of the Poerua landslide material (at the time) was deposited in the lower gorges of Poerua valley, upstream of the alluvial fan, and was not reworked through the system (Table 3). Similar sediment movement may occur in the Taramakau valley following an AFE, which would result in lower values of aggradation than those seen above.

4.4 Comparison with Poerua

The Mt Adams aseismic rock avalanche of 1999 has been used as a proxy for estimating the likely scale and duration of river aggradation induced by a minimum and maximum credible AFE. Chapter 2 describes the events of 1999 in the Poerua valley; a large 10 – 15 x 10^6 m^3 rock avalanche fell from Mt Adams into the Poerua gorge, blocking the river and producing a 100 m high landslide dam (Davies & Korup, 2007; Hancox et al., 2005; Korup et al., 2004; Nelson, 2012). Research has been conducted on this event, concentrating on the changes in sediment flux downstream of the landslide dam. Korup et al (2004) and Nelson (2012) measured the changes in sediment elevations along the alluvial fan and lower gorge of the Poerua River; their results are presented in Tables 2 and 3. Sediment volume changes on the alluvial fan were measured three years after the event by Korup et al (2004) and a further six years later by Nelson (2012) through cross section analysis. Data from Poerua have been reworked in this thesis and compared to Robinson's (2014) AFE landslide volume estimates for the Taramakau catchment. This was done to calculate how much of the estimated total AFE landslide material may be reworked through the Taramakau catchment to the fluvial system contributing to river aggradation.

Table 2 Average sediment loads recorded on Poerua alluvial fan (modified from Korup et al., 2004 and Nelson, 2012).

Alluvial Fan	Years	Contributing Catchment km^2	Sediment Input m^3	% Sediment Input from Landslide Total ($12x10^6m^3$)	Apparent Sediment Discharge $m^3/yr.$	Reference
May 99- Nov 99	0.5	59	932,800	7.7	1,865,600	Korup et al. 2004, Nelson 2012
Nov 99- Jun 00	0.6	59	342,700	2.8	587,500	Korup et al. 2004, Nelson 2012
Jun 00- Dec 00	0.5	59	165,500	1.4	330,900	Korup et al. 2004, Nelson 2012
Dec 00- Feb 02	1.2	59	163,400	1.4	140,100	Korup et al. 2004, Nelson 2012
Feb 02- Aug 03	1.5	59	52,700	0.44	35,200	Nelson 2012
Aug 03- Jul 05	1.9	59	116,600	0.97	60,800	Nelson 2012
Jul 05- May 08	2.8	59	-279,000	-0.02	-98,500	Nelson 2012
May 99- May 08	**9**	**59**	**1,494,700**	**14.69**	**2,921,600**	**Korup et al. 2004, Nelson 2012**

Table 3 Sediment volume recorded in the lower gorge of Poerua valley. From Korup et al (2004).

Lower Gorge	Years	Catchment km^2	Sediment Input m^3	% Sediment Input from LS Total ($12x10^6m^3$)	Apparent Sediment Discharge $m^3/yr.$	Reference
Oct 99- Jan 02	2.3	51	5, 683, 400	47.4	2, 525, 900	Korup et al. 2004

A Poerua landslide volume of 12 x 10^6 m^3 was used to calculate the percentage of sediment input that was delivered to the alluvial fan. From May 1999 to November 1999 (Table 2) preliminary evidence of sediment input from the landslide dam break was identified (Korup et al., 2004). The first addition of sediment accounted for 7.7% of the total Poerua landslide material that had been deposited on the alluvial fan. The calculated percentages corresponding to the sediment input found on the alluvial fan, progressively decreased with time (Table 2). Nelson (2012) showed that after approximately six years (2005), aggradation on the fan head ended and incision began (Table 2). The trend shows episodic aggradation on the valley floor and fan head, trending towards degradation phases. Since the event in 1999, a total of seven separate sediment measurements have been made showing overall declining sediment discharge with time (Figure 4.6).

Applying Poerua percentages to the calculated minimum and maximum landslide volumes for the Taramakau catchment (6.8 x 10^7 m^3 and 3.0 x 10^8 m^3), apparent sediment volumes that may be reworked through the fluvial network and deposited in the Taramakau study area are calculated and are presented in Tables 4 and 5.

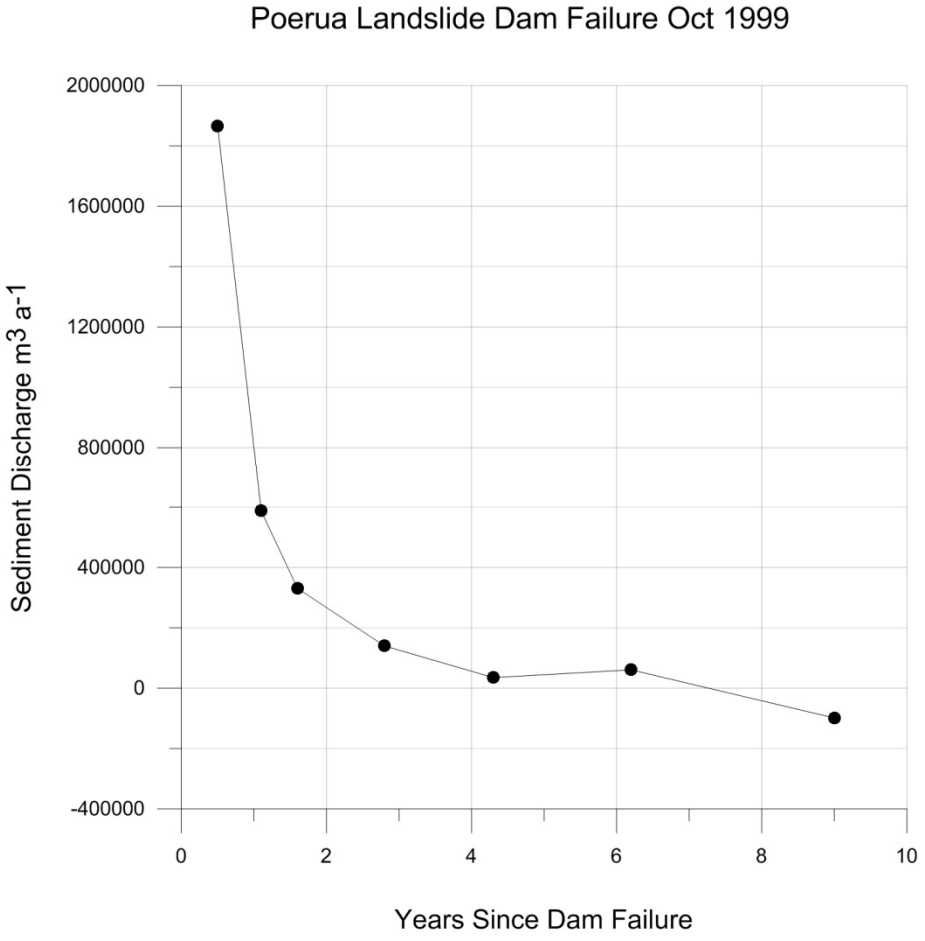

Figure 4.6 Decreasing sediment discharge on the Poerua fan head with time after the initial rock avalanche. Data from Korup et al (2004), Nelson (2012).

Table 4 Minimum AFE Sediment input on the Taramakau alluvial fan. Sediment input is calculated as a percentage of the average minimum landslide volume (6.8×10^7 m^3)

Taramakau Channel	Years	Contributing Channel Area m^2	% Sediment Input from Landslide Total (6.8×10^7 m^3)	Sediment Input m^3	Aggradation m	Cumulative Aggradation m
Time Period 1	0.5	84390019	7.7	5,236,000	0.06	0.06
Time Period 2	0.6	84390019	2.8	1,904,000	0.02	0.08
Time Period 3	0.5	84390019	1.4	952,000	0.01	0.09
Time Period 4	1.2	84390019	1.4	952,000	0.01	0.1
Time Period 5	1.5	84390019	0.44	299,200	0.004	0.104
Time Period 6	1.9	84390019	0.97	659,600	0.008	0.112
Time Period 7	2.8	84390019	-0.02	-13,600	-0.0002	0.1118
Total	9	84390019	14.69	9,989,200	0.11	0.11

Table 5 Maximum AFE Sediment input on the Taramakau alluvial fan. Sediment input is calculated as a percentage of the average maximum landslide volume (3.0×10^8 m^3)

Taramakau Channel	Years	Contributing Floodplain Area m^2	% Sediment Input from Landslide Total (3.0×10^8 m^3)	Sediment Input m^3	Aggradation m	Cumulative Aggradation m
Time Period 1	0.5	84390019	7.7	23,100,000	0.28	0.28
Time Period 2	0.6	84390019	2.8	8,400,000	0.10	0.38
Time Period 3	0.5	84390019	1.4	4,200,000	0.05	0.43
Time Period 4	1.2	84390019	1.4	4,200,000	0.05	0.47
Time Period 5	1.5	84390019	0.44	1,320,000	0.02	0.49
Time Period 6	1.9	84390019	0.97	2,910,000	0.03	0.52
Time Period 7	2.8	84390019	-0.02	-60,000	-0.0007	0.52
Total	9	84390019	14.69	44,070,000	0.52	0.52

Tables 4 and 5 apply the same time periods as those presented in Table 2 by Korup et al (2004) and Nelson (2012), relative to the timing of sediment movement through the Poerua valley. The floodplain area within the Taramakau study area is 8.4×10^7 m^2. This value was calculated from cut and fill algorithms using QMap data in GIS. The percentages of sediment

input from the total landslide volumes relate to those calculated from the Poerua sediment input values (Table 2). Each percentage was used to calculate the estimated volume of sediment that may be delivered to the Taramakau alluvial fan from the total produced landslide volume values. Aggradation values were established by dividing the calculated volume of sediment input by the calculated receiving floodplain area, providing an estimate of aggradation in metres.

The amount of sediment that is likely to propagate through the Taramakau catchment to the fan head in the six months after the AFE may account for approximately 7.7% of the total landslide volume. Focusing on the maximum credible landslide volume (3.0 x 10^8 m^3), 7.7% amounts to 23.0 x 10^6 m^3 of sediment. This may cause approximately 30 cm of aggradation if the depositional surface is horizontal. The amount of aggradation progressively decreases with time due to decreasing sediment input. With each phase, however, the amount of aggradation cumulates and progressively increases with time, resulting in an increasingly elevated river bed (Figure 4.7). Applying a similar time scale as Poerua to the events following an AFE, approximately nine years after a maximum landslide volume, a total of 4.4 x 10^7 m^3 of sediment will be deposited on the fan head resulting in an average of about half a metre of aggradation deposited across the floodplains of the study area (Table 5).

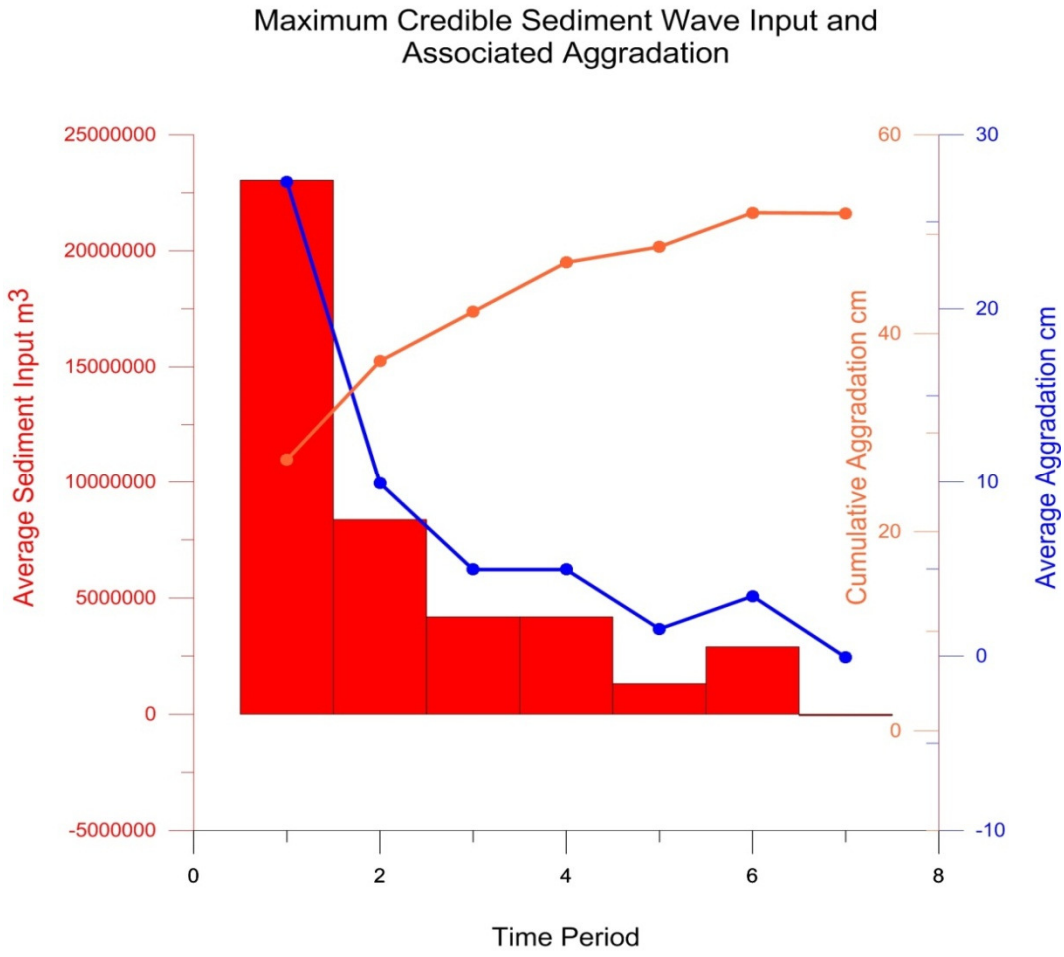

Figure 4.7 Periodic high magnitude aggradation tied to different sediment inputs from landsliding in the Taramakau catchment. Cumulative aggradation is also shown

4.5 Impacts

Immediate impacts of the 50 cm aggradation may not instantly be recognised. The raised river bed, however, will enhance the effects of a major flood. A one-in-100 year flood has a 1% chance of occurring within any given year. Recurrence intervals have been calculated from NIWA recorded daily flow rates. Maximum yearly flows from an expanded NIWA data set dating 1979 – 2013 were ranked in order to calculate the discharge of a one-in-100 year flood in the Taramakau River (Appendix Two). Graphing recurrence intervals against discharge, the flow rate of a one-in-100 year flood was identified to have a maximum discharge of about 3200 m^3/s (Figure 4.8).

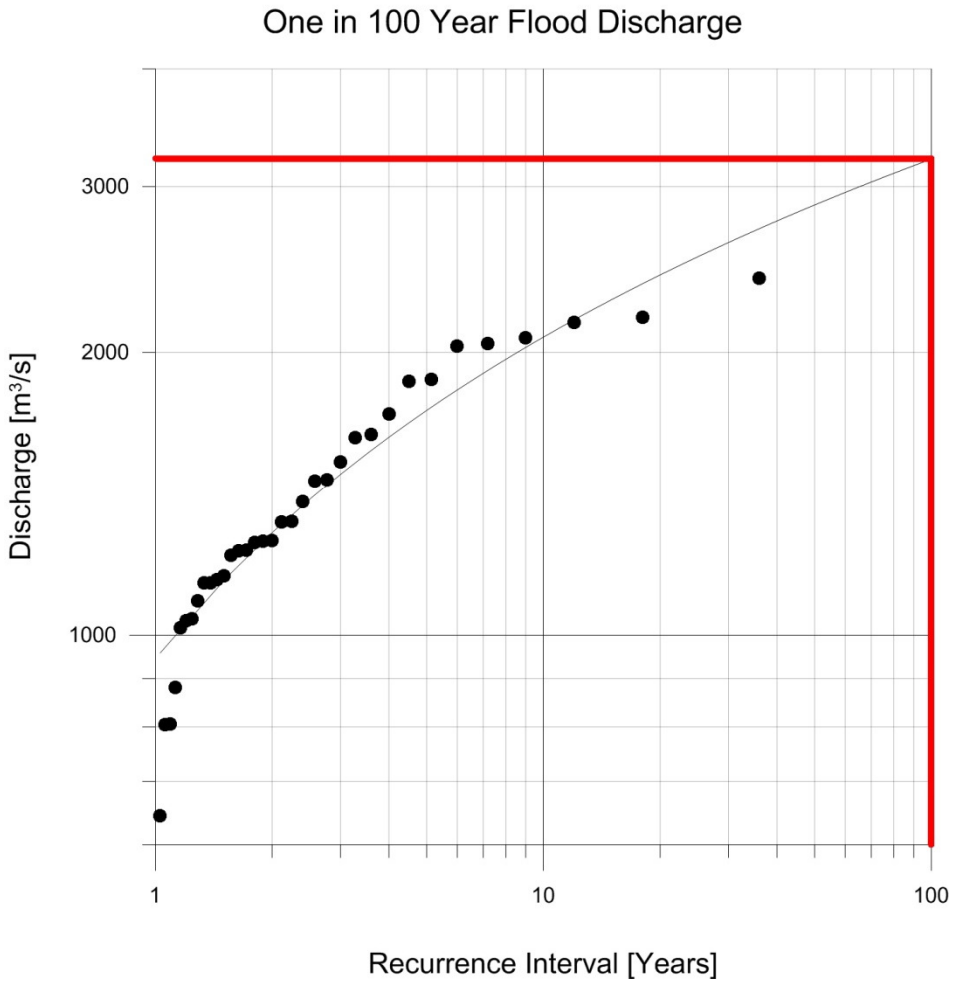

Figure 4.8 Discharge values associated with flooding frequency. A one-in-100 year flood corresponds to a discharge value of 3200 m^3/s.

The NIWA Taramakau River gauge has recorded water elevations (relative to the datum level at the gauging station) with general discharge values, the data has been reworked by NIWA into rating tables and used in this thesis to calculate the average stream height for certain flow rates (Appendix Two). The average water elevation for certain flow rates were graphed (Figure 4.9). An increase in flow from a low value to the calculated one-in-100 year flood flow rate of 3200 m^3/s corresponds to an increase of average water surface-elevation of approximately seven metres. The top of the Stanley Gooseman Bridge and the Midland Railway Bridge which cross the Taramakau River within the study area, sit seven metres above the current bed level of the Taramakau River. In the event of a one-in-100 year flood, the addition of half a metre of landslide derived sediment (Table 5) will increase the height of the water surface elevation to approximately 7.5 m, affecting both the road and rail bridges. The implications of this are discussed further in Chapter 7.

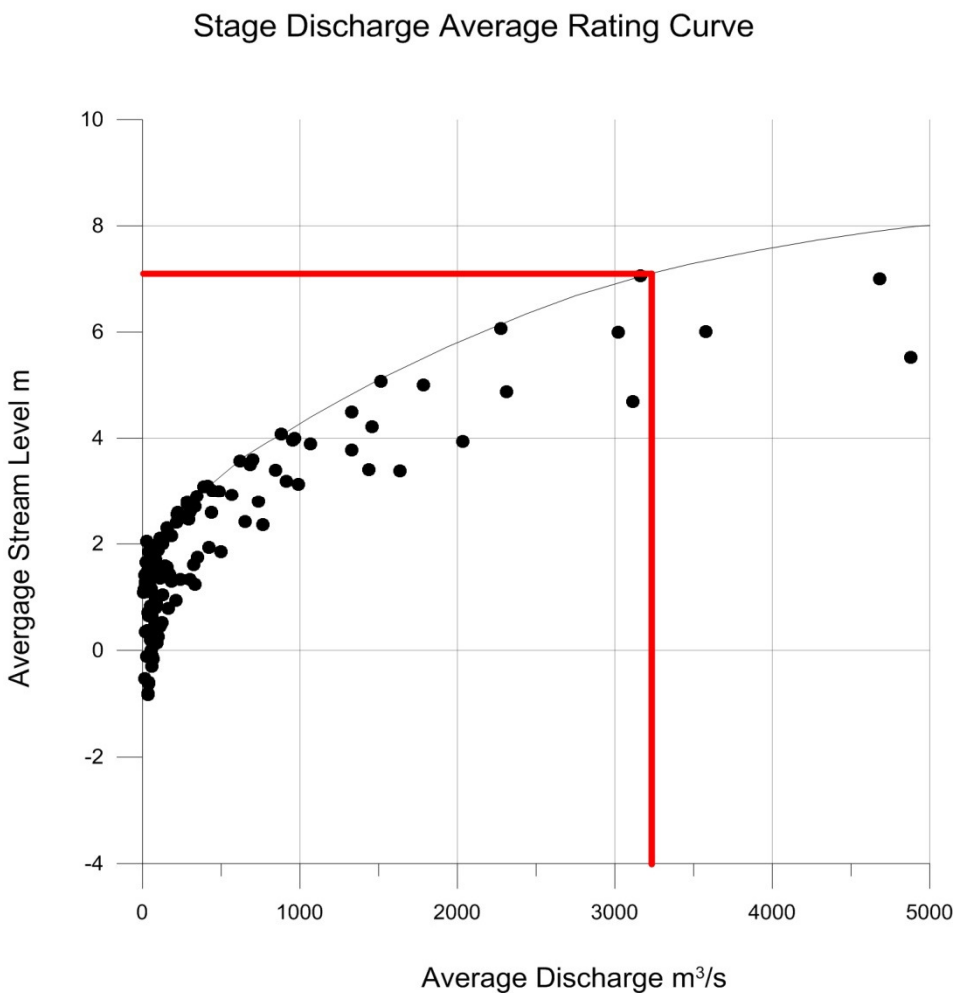

Figure 4.9 Stage rating curve, highlighting Taramakau River water elevation during a one-in-100 year flood.

4.6 Summary

The three main variables that assist in a broad understanding of this river system are water discharge, suspended sediment concentration and total sediment load, all of which are intrinsically related and follow the same trend since recordings began in the Taramakau River in 1970.

Maximum aggradation levels for minimum and maximum credible AFE landslide volumes are 0.81 m and 3.6 m respectively. However, it cannot be assumed that all of the AFE derived sediment will be deposited on the floodplain of the Taramakau River in the study area. Similarly to Poerua, smaller percentages of landslide material may be reworked through the system. Approximately 15% of the total Taramakau catchment AFE landslide volume may be deposited on the floodplain within nine years of the event, inducing an average amount of 0.5 m of aggradation within the study area. The percentages of landslide sediment input from Poerua show delivery of sediment through the system progressively decreasing over time, as it propagates through the fluvial network.

A one-in-100 year flood has a flow rate of about 3200 m^3/s. This flow rate corresponds to a water elevation height of seven metres, based on stream rating data provided by NIWA. The addition of half a metre of sediment from maximum credible AFE landsliding may enhance the impacts of a one-in-100 year flood, increasing the water elevation height to 7.5 m, affecting both bridges that cross the Taramakau River within the study reach.

Chapter 5 - Aerial Imagery

5.1 Introduction

Chapter 5 presents the findings of aerial photographic interpretation. Aerial photograph analysis is a useful way to identify channel avulsions across active fluvial envelopes. Braided rivers are characterised by continual channel movement across the river bed. The Taramakau River bed is not fully occupied by channel flow (Figure 5.1); as with all braided rivers, the river beds are relatively wide containing networks of presently unoccupied channels. It is likely that many of these unoccupied channels will be reactivated by landslide-driven aggradation and avulsion following the next AFE. A series of aerial photographs has been collected and analysed using a stereoscope. The photographs date from 1943 and are held in the University of Canterbury's Geological Sciences Department collection. The aerial photographs cover the study area from Aickens to where the Taipo River meets the Taramakau.

Figure 5.1 Air photo of the Taramakau River near Jacksons. View looking west towards Hokitika. Photo taken in January 2013, approximately average flow rates (115 m^3/s). Channel flow does not occupy the entire river bed. *Taramakau Rail Bridge,* (2013) photograph viewed 1 August 2014, <http://www.recwings.com/newsletters/2013/mar13/index.html>

5.2 Aerial Photographs

The University of Canterbury's aerial photograph collection for the study area includes photographs from aerial survey 262 (1943), flight line 827; survey 1063 (1959), flight line 2741 and survey 1063 (1960), flight lines 2744 and 2743. The historic aerial photographs were compared with current (2014) aerial photographs sourced from Landsat Satellite Imagery New Zealand (LINZ) to identify shifts in the river channels, highlighting undercut and unstable river banks which may collapse in the wake of the next AFE.

One of the most significant channel movements observed in the Taramakau has occurred along the stretch of the river south of Inchbonnie, close to State Highway 73 (Figure 5.2). Two sets of aerial photographs from this site were analysed. The aerial photographs in Figure 5.3 and Figure 5.4 show that since 1943, the Taramakau River has moved in a northward direction towards Inchbonnie. Figure 5.3a and b show that the Taramakau has avulsed away from State Highway 73 in the south by almost 500 m in some sections since 1943. Figure 5.4 a and b show that in 2014 Taramakau channels flow approximately 430 m closer to the Lake Brunner Road and the Midland Railway, than they did in 1943. Should the Taramakau continue to avulse north, the Lake Brunner Road and Midland Railway could become threatened by bank erosion and undercutting, which may result in the collapse of these structures and the potential temporary closure of these cross-island road and rail transportation routes.

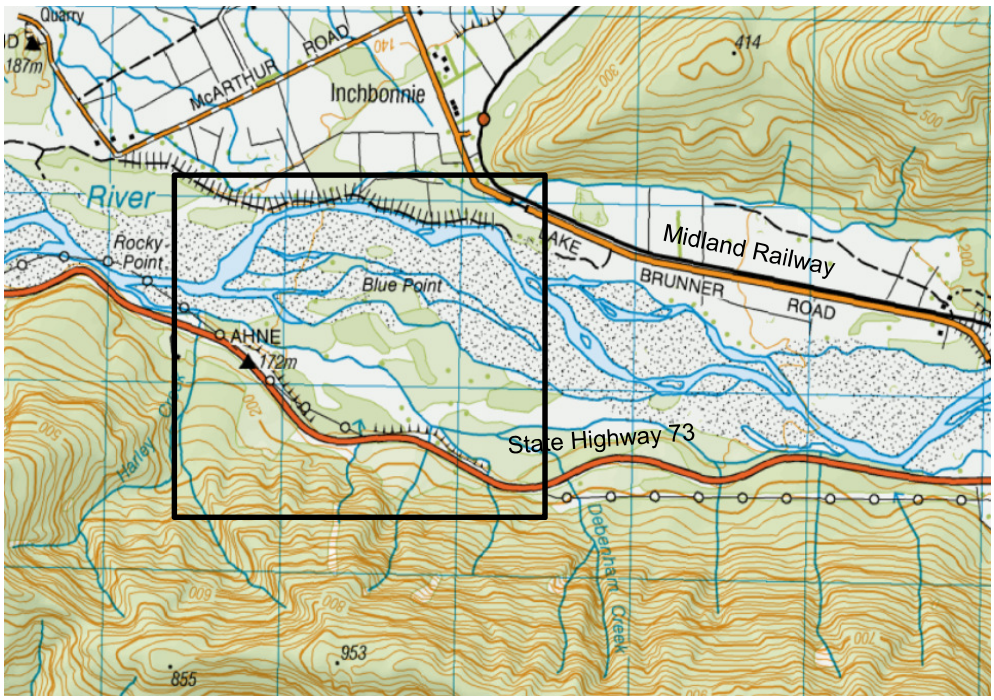

Figure 5.2 Location of aerial photographs in Figure 5.3 and Figure 5.4, survey 262, flight line 827 south of Inchbonnie. Base map sourced from Topo Map.

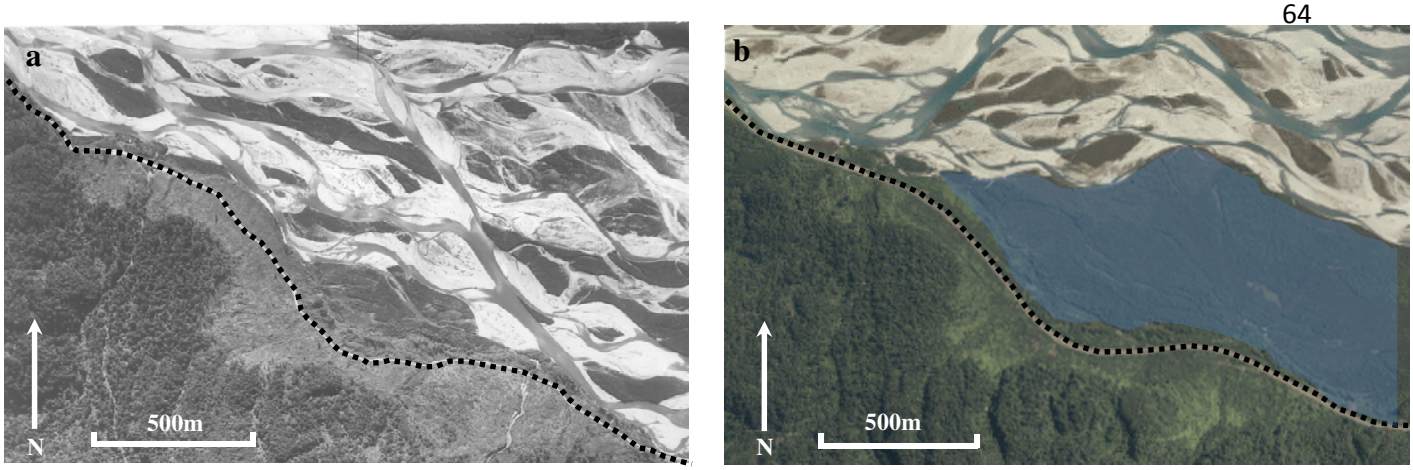

Figure 5.3 a) 1943 aerial photograph of the Taramakau River south of Inchbonnie, flight line 827/53, b) 2014 LINZ image of the same stretch of river seen in a). Highlighted area represents previous extent of the active channels in 1943.

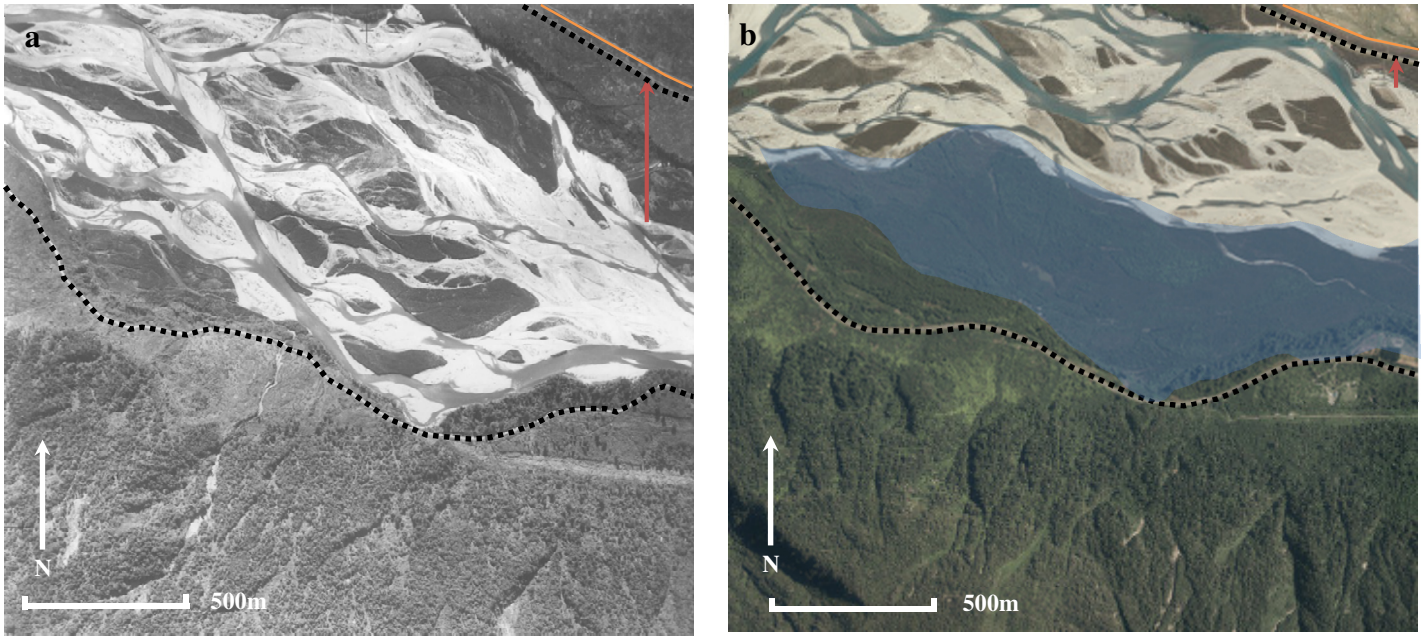

Figure 5.4 a) 1943 aerial photograph of the Taramakau River south of Inchbonnie, flight line 827/54 b) 2014 LINZ image of the same are seen in a). Highlighted area represents previous extent of the active channels in 1943.

Legend

Road **Rail** **Channel avulsion** **1943 Channels**

Towards Jacksons, the Taramakau River channels have also moved northward across the channel bed since 1960 (Figure 5.5). The 1960 aerial photographs for this stretch of the river were compared with current (2014) LINZ photos (Figure 5.6a, b). The current channel bed occupies the approximate same space as it did in 1960, however, some of the 2014 active channels have moved to the north by approximately 360 m, incising into alluvial fans on the true right of the river (Figure 5.6 a, b). This continual incision may lead to bank erosion and consequent collapse.

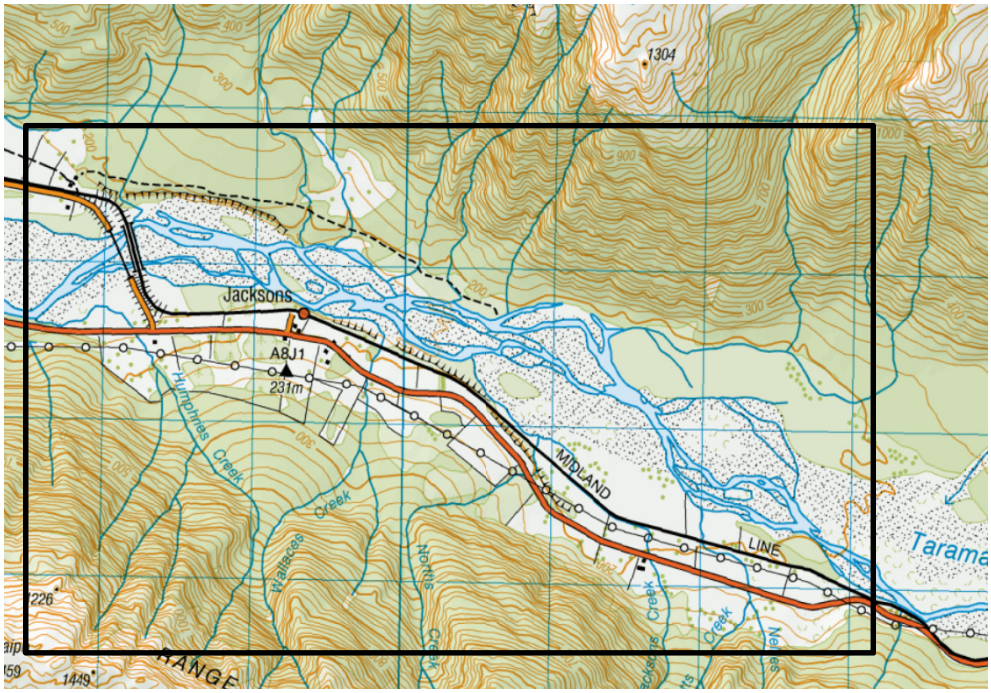

Figure 5.5 Location of aerial photographs presented in Figure 5.6a and b. Survey 1063, flight line 2743. Base map sourced from Topo Map

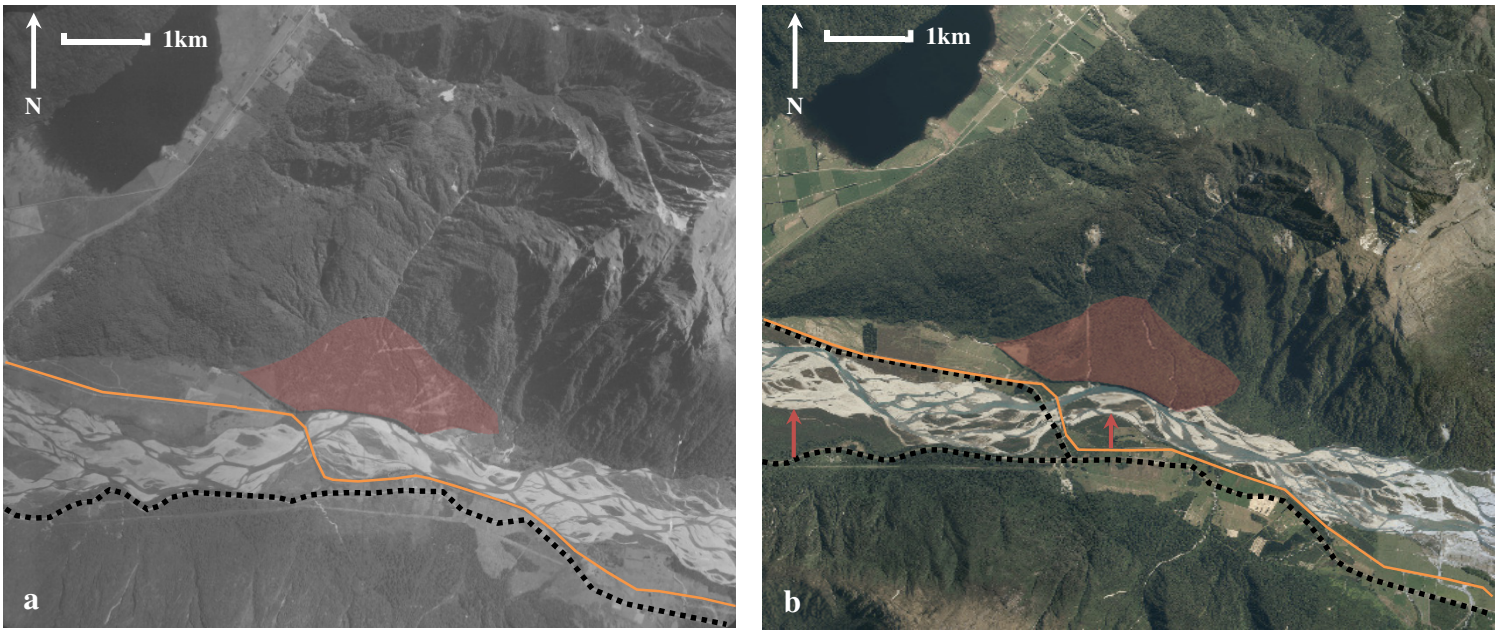

Figure 5.6 a) 1960 aerial photograph of the Taramakau River near Jacksons, flight number 2743/1 b) 2014 LINZ image of the same stretch of river seen in a). Large alluvial fan is highlighted and displayed in Figure 5.7.

Legend

Road **Rail** **Channel avulsion** **Alluvial Fan**

The Taramakau River has been trimming the toe of a large alluvial fan on the true right of the river, east of the Stanley Goosemen and Midland Railway Bridges, since at least 1960 (Figure 5.6a, b), and continues to do so. The resulting bank is an approximately 30 m high vertical wall covered in vegetation (Figure 5.7). In the event of an AFE, the collapse of the vertical face may contribute a large amount of sediment directly to the Taramakau River. Assuming that the face may retreat by approximately five metres during an AFE, around 150, 000 m^3/km of sediment could be added to the Taramakau River at this location. The addition of sediment directly into the river from the collapse of the face could induce immediate channel avulsion which could increase the threat of flooding within the study area.

Figure 5.7 Incised alluvial fan true right bank of the river, looking upstream, east of the Stanley Gooseman Bridge and Midland Railway Bridge. White arrow indicates direction of flow.

Some of the most recognisable channel shifts seen in the study area are at the confluence of the Taramakau River with the Taipo River, a major tributary at the western border of the study area (Figure 5.8). Aerial photographs of this area were taken in 1943 and 1959. These have been compared with current (2014) LINZ images. These comparisons clearly show three channel movements laterally across the floodplain (Figure 5.9a, b, c). Figure 5.9a shows that the Taipo River flowed into the Taramakau in a northwest direction in 1943. In 1959 the Taipo River flowed into the Taramakau River in a more westerly direction (Figure 5.9b) and in 2014 the Taipo River flows into the Taramakau River in a more northerly direction (Figure 5.9c). This continual shifting of river channels is common in braided fluvial systems, and the farmland surrounding the Taipo River junction is vulnerable to flooding during periods of high flow and increased sediment load, such as potentially induced from an AFE.

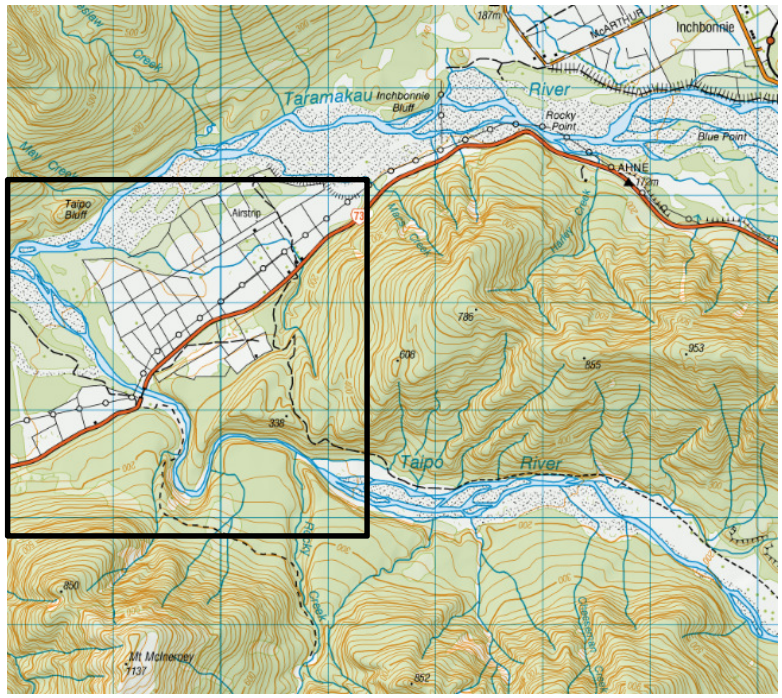

Figure 5.8 Location of aerial images seen in Figure 5.9a, b and c. Survey 262 flight line 827 and survey 1063 flight line 2741. Base map sourced from Topo Map.

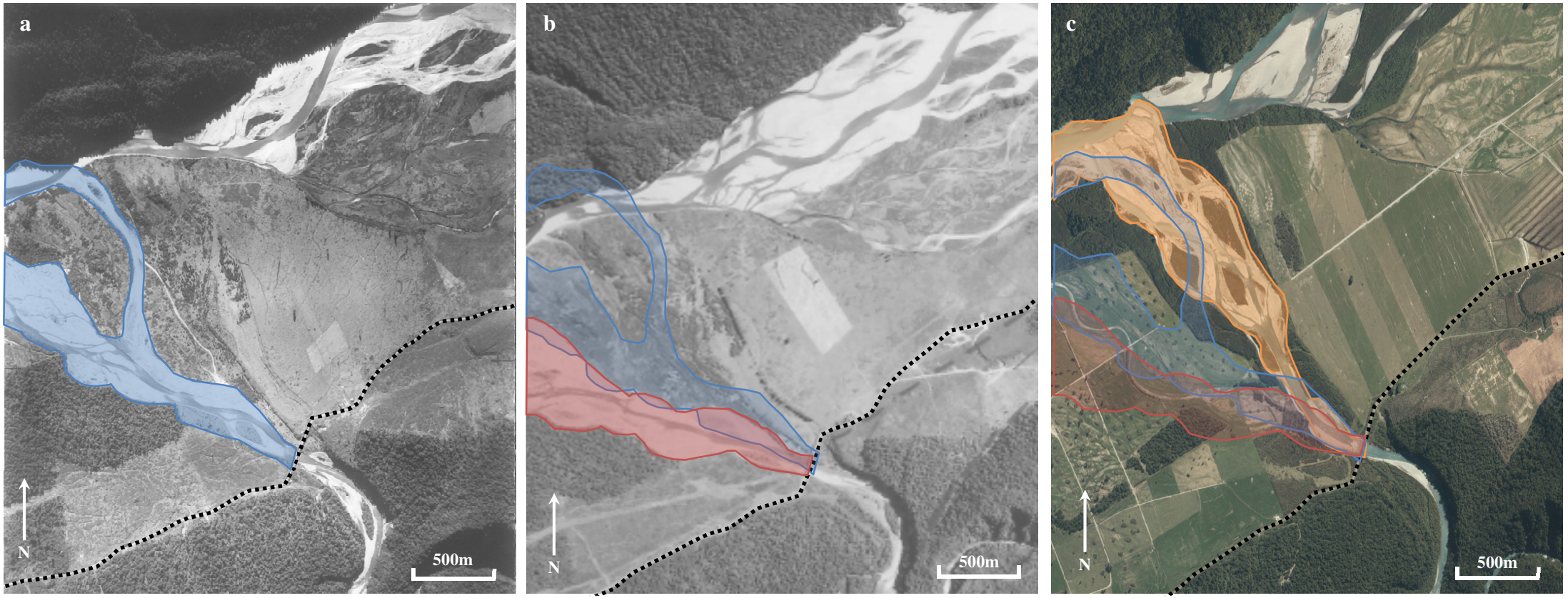

Figure 5.9 Time lapse aerial photographs for the Taipo River fan head. Channel avulsions are highlighted. Blue channel indicates the 1943 channel, red channel indicates the 1959 channel and the orange channel highlights the current course of the Taipo River. Dotted line represents State Highway 73 in all three photographs. Paleo channels are also recognised north east of this junction across farmland. A) flight path 827/47 taken in 1943 Taipo river joining the Taramakau in a north west direction b) flight path 2741/2 taken in 1959, Taipo River flowing into the Taramakau in a west north west direction c) 2014 LINZ image, Taipo River flowing into the Taramakau in a north north west direction.

Of considerable concern is the hydraulic connection between the Orangipuku River and the Taramakau River (Figure 5.10). The Orangipuku River flows into Lake Brunner north of the study area. If Taramakau flow were to enter the Orangipuku River, the volume of water entering Lake Brunner would increase. An increased inflow into Lake Brunner would increase water flows in the Arnold River that flows out of Lake Brunner subsequently entering and inducing flooding in the Grey valley, further north of the study area. The possibility of hydraulic connection between the two rivers was recognised in the 1940's by the West Coast Regional Council. Prior to the 1940's the Orangipuku River ran parallel to the Taramakau River, flowing as close as five metres to the true right of the Taramakau River banks (WCRC, 2010).

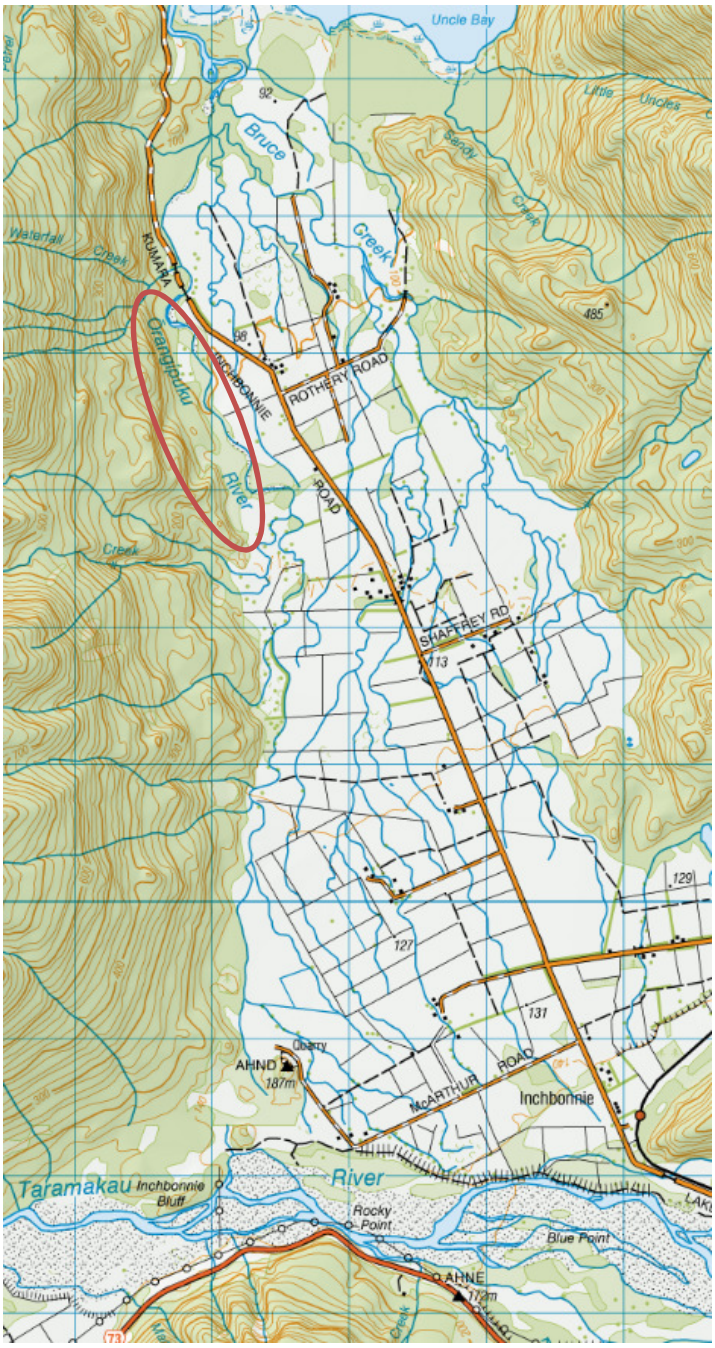

Figure 5.10 Orangipuku River (circled) in the north and Taramakau River in the south. The Orangipuku River flowed parallel to the Taramakau prior to the 1940's. Lake Brunner lies north of the Orangipuku River. Base map sourced from Topo Map.

To address hydraulic connection between the Taramakau and Orangipuku River, a stopbank was constructed along the true right of the Taramakau River. In 1959 an engineering report suggested the construction of a 2.5 km stopbank strengthening the existing 1.2 km stopbank. This proposal was approved and construction commenced in August 1959 (WCRC, 2010). Since completion of the stopbank the risk of hydraulic connection between the Taramakau and the Orangipuku River has decreased, evidenced by the shrinkage of the Orangipuku River (Figure 5.11a, b). Figure 5.11a is an aerial photograph taken in February of 1959, at this time the Orangipuku River flowed approximately 100 m north of the Taramakau River. The stopbank on the true right of the Taramakau River was strengthened six months after this photograph was taken. Figure 5.11b shows the current (2014) course of the Taramakau River and the Orangipuku River. From the LINZ photograph, the Orangipuku River has moved north and no longer flows parallel to the Taramakau River. The stopbank acts as a physical barrier between the two rivers diverting Taramakau channel flow away from the Orangipuku River. Since the strengthening of the stopbank in 1959, very few reports of the Taramakau spilling into the Orangipuku River have been recorded (WCRC, 2010). The stopbank has potentially minimised the threat of Taramakau flood flows entering the Grey valley through Lake Brunner via the Orangipuku River. An AFE, however, is very likely to damage or destroy this stopbank, allowing flood flows to reoccupy the extensive paleo channels recognised in Figure 5.11a.

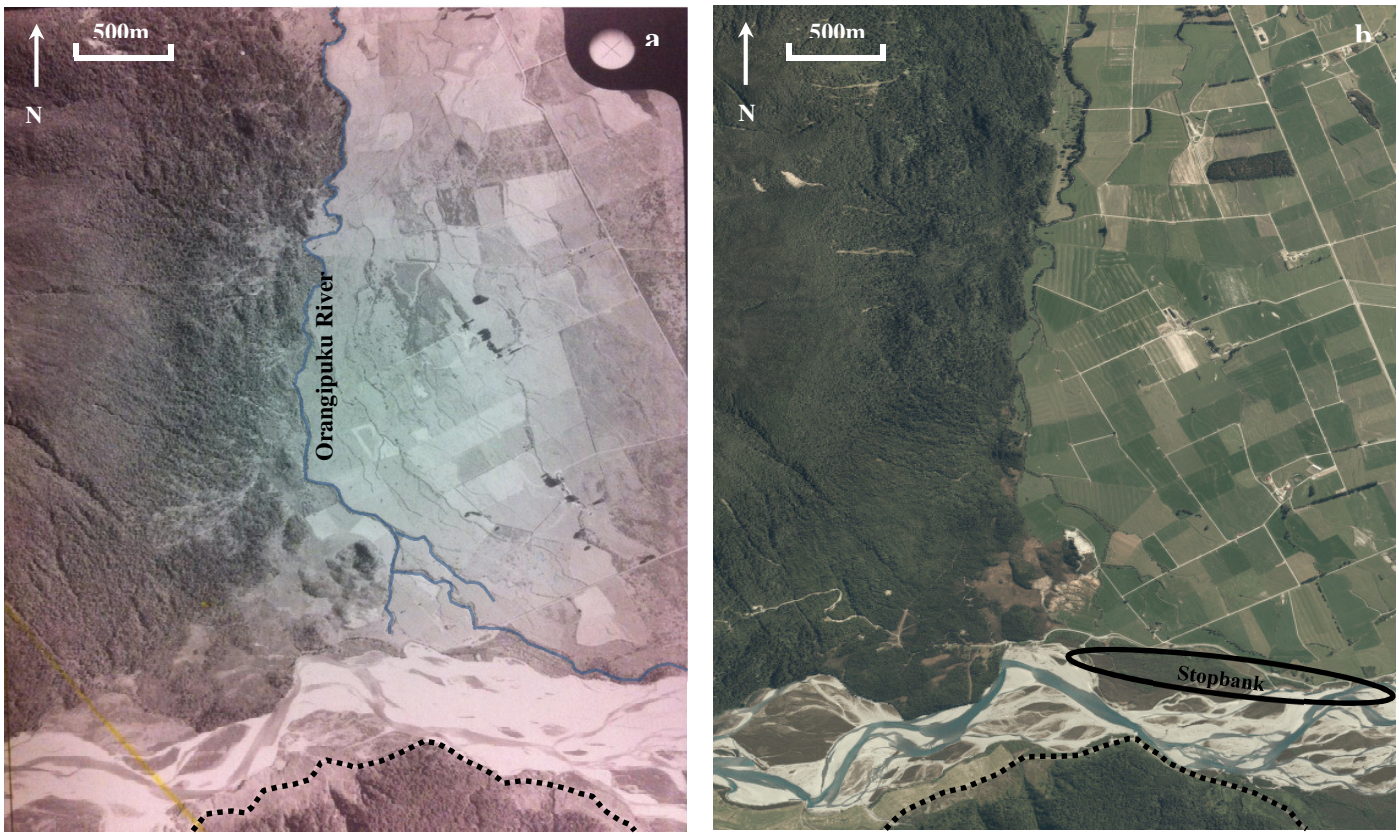

Figure 5.11 a) Aerial photograph of the Orangipuku River, north of the Taramakau River, flight path 2741/1 taken in 1959, paleo channels are seen across the land east of the Orangipuku River b) 2014 LINZ image of the Orangipuku River which has since retreated north due to the strengthening of the stopbank in 1959. Dotted line indicates State Highway 73 in both photographs.

5.3 Summary

An aerial photography analysis has highlighted Taramakau River channel avulsions within the study area. From the aerial photographs, since 1943 the trend of movement in the Taramakau River channels has been to the north. Within a time frame of 71 years (1943 - 2014) the actively moving Taramakau River has avulsed northward away from State Highway 73 in the south by as much as 500 m. The rail and road near Inchbonnie have become increasingly threatened by the northward migration of the Taramakau channels since 1943. The northward moving channel shifts continue to be recognised east of the Stanley Gooseman and Midland Railway Bridges since 1960. This north trending avulsion is also indicated by an eroded alluvial fan on the true right of the Taramakau River. In the wake of an AFE, the unstable fan front may collapse providing approximately 10^5 m^3 of sediment directly into the Taramakau, immediately enhancing the effects of aggradation, avulsion and flooding within the area.

The Taipo River has moved considerably across its floodplain since 1943. Aerial photographs in 1943, 1959 and 2014 show three different channel positions. The land that the Taipo River avulses across is at high risk of becoming inundated during periods of high flow. After an AFE, both the Taramakau and Taipo Rivers will be disturbed, potentially resulting in major channel avulsions across the adjacent low lying farmland.

In 1959 the Orangipuku River flowed parallel to the Taramakau River and the threat of hydraulic connection between these two rivers was relatively high. A stopbank was built and the Orangipuku River has since retreated and no longer flows parallel to the Taramakau River, reducing the risk of Taramakau flood flows entering the Grey valley. An AFE is likely to destroy the stopbank allowing the reconnection of the Taramakau and Orangipuku Rivers.

Chapter 6 – Micro-Scale Modelling

6.1 Introduction

Chapter 6 presents the findings of the micro-scale modelling tests, the aim of which was to indicate how the Taramakau River may respond to coseismic river offsets and sediment additions. The micro-scale model is shown in Figure 6.1. It was divided into an upstream block and a downstream block, separated by a modelled dextral strike-slip fault trace (Figure 6.1). The design of the stream board was based on studies conducted by Ouchi (1983) and Holbrook and Schumm (1999). Three experiments were performed in an effort to understand the implications of dextral strike-slip displacement perpendicular to flow in fluvial channels, together with the effects of a sudden increase in sediment input. The findings are presented here.

Each experiment was designed to replicate an AFE rupture across a braided fluvial system. Experiment I simulated a complete rupture along the modelled dextral strike-slip fault, followed by instant and complete upstream sediment addition, replicating AFE-derived landsliding. Experiment II replicated complete rupture along the fault trace coupled with multiple delayed sediment additions and Experiment III modelled incremental rupture along the fault trace with incremental sediment additions indicative of potential smaller scale aftershocks. The three separate experiments cover a range of potential AFE scenarios and indicate how the fluvial system may respond.

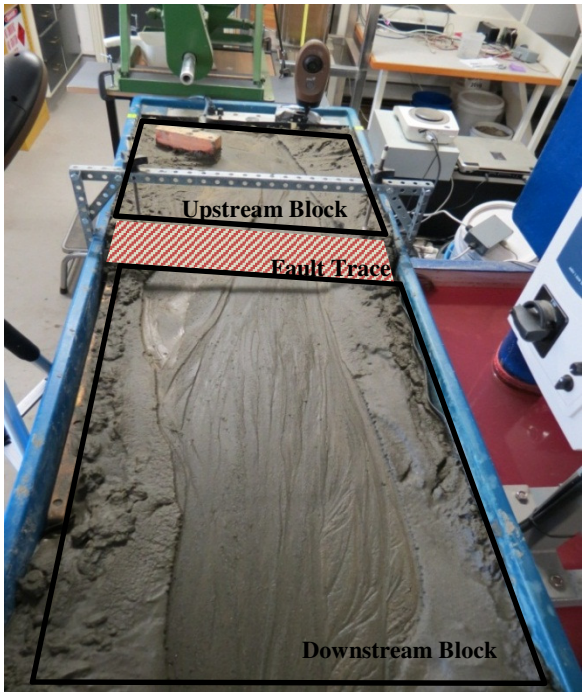

Figure 6.1 Stream board design. Upstream and downstream blocks are divided by a modelled fault trace.

Each experiment was divided into three phases, monitored closely through observations and photography. Each experiment began with the development of a braided river system on the 25 mm depth of 750 µm sieved sediment that covered the stream board. A braided river developed from constant water and sediment additions to the upstream block (Figure 6.1). Water was added at a rate of 0.4 L/min and sediment was added from a vibrating sediment feeder at a rate of 0.05 g/s. Once a braided river had developed in the first phase, the system was disturbed by lateral and vertical movement representing a displacement phase. Displacement took place by physically winding the upstream block upwards by the frame attached to the stream board; this uplift tilted the upstream block decreasing the channel slope of this section (Figure 6.2a). Vertical uplift ceased when fault traces began to develop (approximately after 25 mm of vertical uplift). The vertical component of uplift was immediately followed by lateral displacement. Right lateral displacement was modelled by physically pulling the downstream block to the true right of the river by 50 mm (Figure 6.2b). The displacement phase also included an increase in upstream sediment supply, replicating sediment addition from coseismic landsliding. The final phase of the three experiments involved monitoring how the system adjusted to the displacements and sediment addition, observing how the river began to re-establish equilibrium within the modelled environment. Fluctuations in the river systems were monitored closely and photography was used when the stream board was not physically attended.

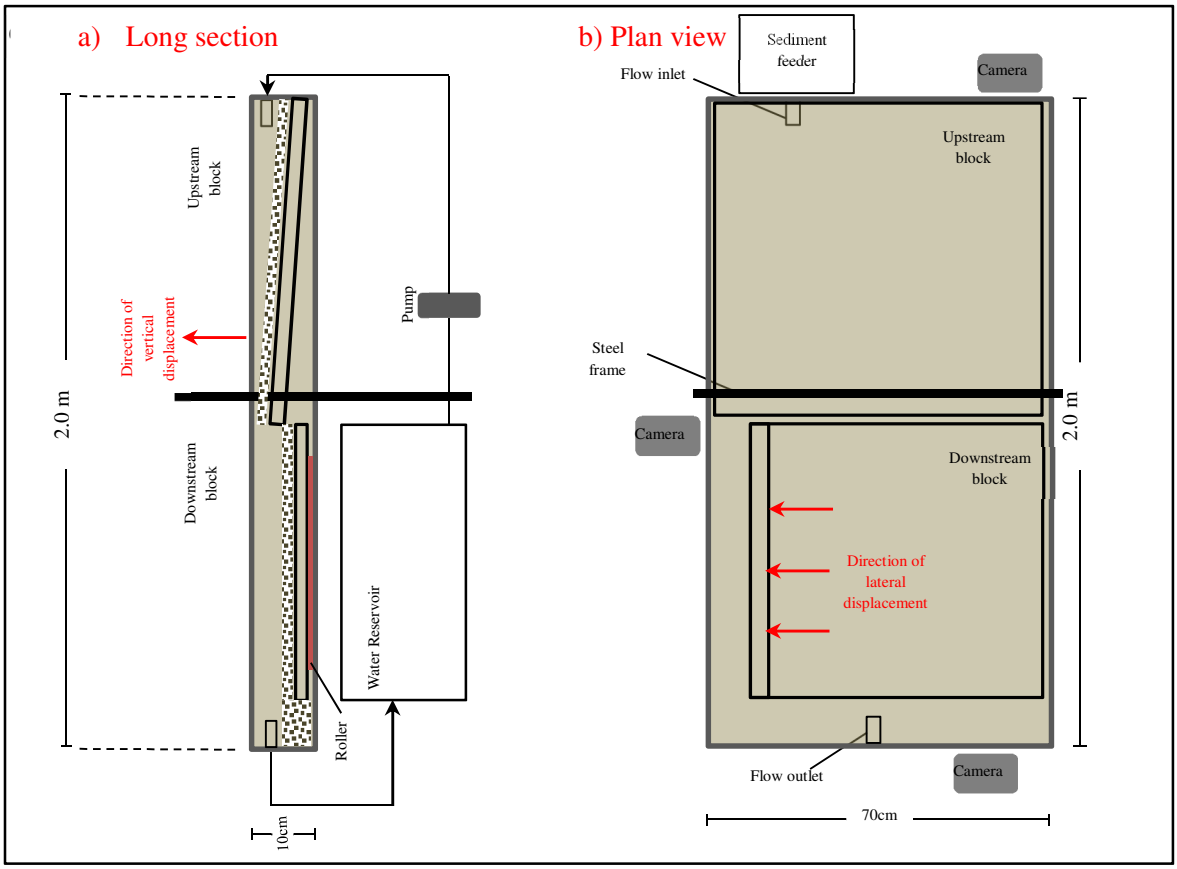

Figure 6.2 stream board during displacement a) long section of the stream board highlighting vertical uplift, the upstream block is wound upwards by ~25 mm b) Plan view of the stream board showing lateral displacement, the downstream block is narrower than the upstream block allowing for lateral displacement by 50 mm.

6.2 Experiments

Each experiment was conducted on a stream board in the Geomorphology Laboratory at the University of Canterbury. Table 6 summarises the timing of the three experiments. Experiments I and II modelled one complete displacement, whereas Experiment III replicated four separate smaller scale displacements representing potential aftershocks from an AFE.

Table 6 Summary of the micro-scale model experiments.

Experiment	Modelled	Duration of water flow before first displacement (h)	Interval of Displacement (h)	Displacement values (mm)	Total period of water flow (h)	Sediment Addition (g)
Experiment One	Complete instant rupture, instantaneous total sediment addition	4	0	25 vertical 50 lateral	9	100
Experiment Two	Complete instant rupture, multiple delayed sediment additions	4	0	25 vertical 50 lateral	10	4 x 25
Experiment Three	Incremental displacement with incremental sediment additions	4.5	1.5	4 x 6 vertical 4 x 12 lateral	9.5	4 x 25

6.2.1 Experiment I

Within four hours of water flow, a braided fluvial system developed on the stream board in Experiment I (Figure 6.3). The braided fluvial system was characterised by the formation of multiple bars and channels that flowed around them. Braids were predominantly observed in the downstream reach of the stream board at this time. Flow was confined to a meander upstream and bars existed attached to the banks of the river in this section. Once the braided system was identified, a phase of displacement followed.

Figure 6.3 Looking upstream of the micro-model four hours since flow commenced in Experiment I; a braided river formed, identified by the array of braids and multiple channels in the downstream block. The dashed lines indicate main channel flows.

Displacement immediately resulted in the formation of stepped fault scarps dissected by multiple channels (Figure 6.4a, b). Flow velocity increased in these channels due to a localised increase in channel slope. Degradation and bank-cutting became a dominant process over the fault trace. Degradation migrated upstream to a certain point where flow was no longer affected by a localised increase in channel slope. Additional sediment added at the same time as the rupture was rapidly flushed through the system by the increased stream power over the fault trace.

Vertical uplift at the fault decreased the overall slope of the upstream block inducing a brief period of back flow and flooding (Figure 6.4c). This was almost immediately followed by increased flow and the production of multiple channels over the fault trace. These channels produced mid channel bars perpendicular to the fault scarps as they incised into the fault trace (Figure 6.4a).

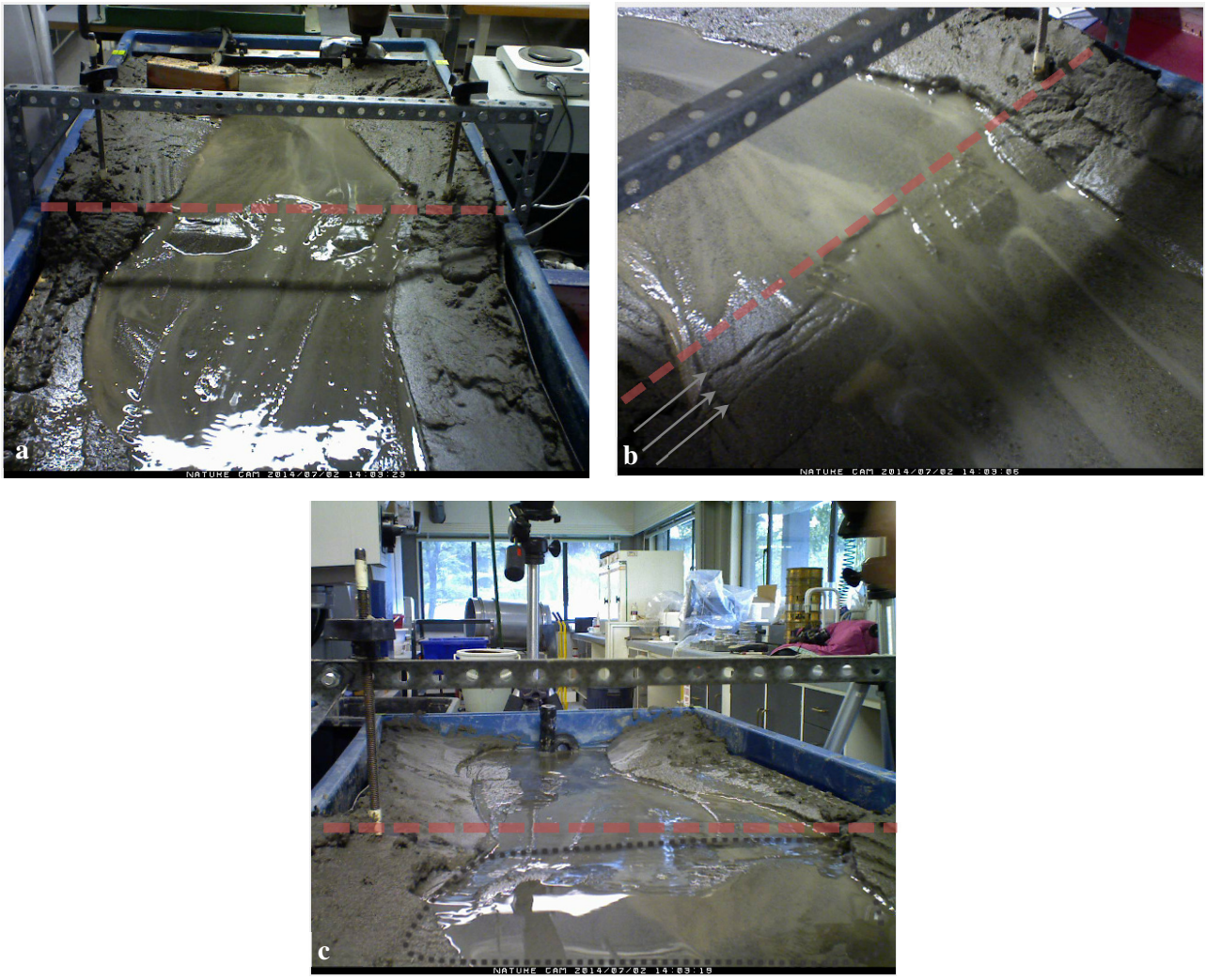

Figure 6.4 Micro-scale model during displacement in Experiment I a) looking upstream, fault scarps form and are rapidly incised by increased channel flow b) plan view of fault trace; formation of stepped fault scarps c) looking downstream; brief period of back pooling widening the upstream floodplain, red dashed lines marks the fault trace, black dashed line highlights the extent of upstream flooding.

Soon after the displacement a dominant channel developed towards the centre of the system as the previous multiple channels lost flow (Figure 6.5a). The dominant channel was relatively straight and flow began to slow over the fault, returning to normal flow rates (0.4 L/min). Incision rate decreased as the channel gradient began to slowly readjust through downstream aggradation. Some aggradation was evident upstream from the brief period of back flooding seen through the development of braids (Figure 6.5b). Up and downstream aggradation was divided by a zone of degradation over the fault trace seen by the development of elongate mid channel bars (Figure 6.5c).

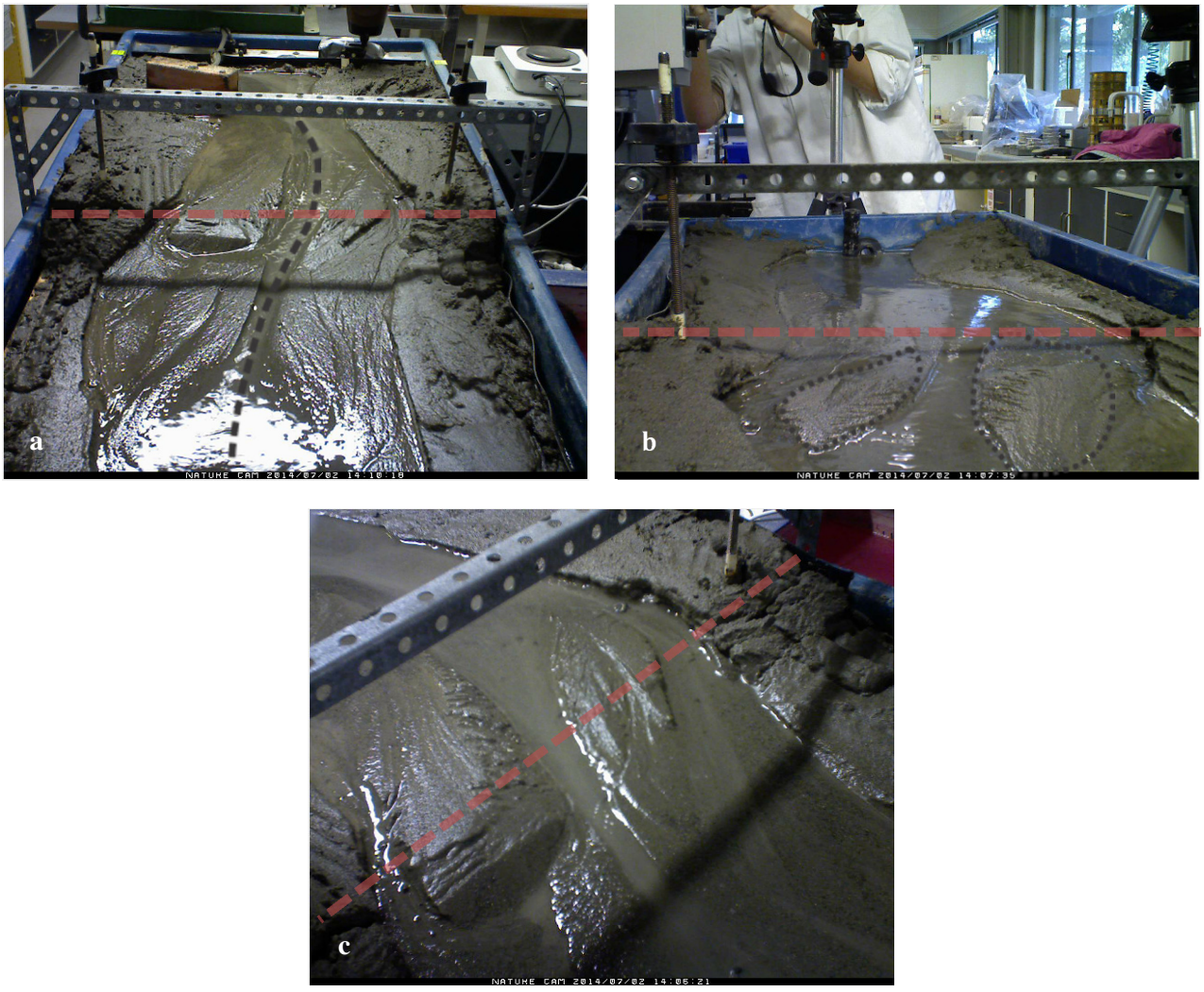

Figure 6.5 Micro-scale model 11 minutes after displacement in Experiment I. a) looking upstream; one dominant straight thalweg forms, highlighted by dashed line b) looking downstream; development of braids upstream from sediment deposition, outlined by the dashed line c) plan view of fault trace; the development of elongate mid channel bars over the fault. Red dashed line indicates fault trace.

Minor lateral shifts in the modelled channels resulted from the lateral fault displacement. The lateral channel shifts that were identified diverted flow towards the true right of the river downstream (Figure 6.6). If these lateral shifts were to occur in the Taramakau River after an AFE, flow would increase towards the true right of the river expanding the rivers active channel bed near Inchbonnie, threatening the effectiveness of the stopbank situated on the right bank of the river.

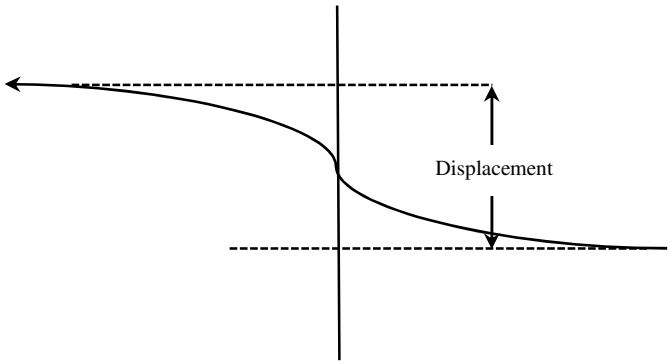

Figure 6.6 Right lateral displacement observed in some of the channels over the fault trace during displacement. Modified from Ouchi et al (2004).

The additional sediment from the modelled coseismic landsliding that did not deposit in the upstream block was reworked through the system, the effects of which were seen one and a half hours after the displacement event. This sediment was identified by the development of additional braided complexes in the downstream reach (Figure 6.7). Flow was diverted around these structures re-occupying multiple channels and enhancing the development of a braided system subsequently widening the rivers active channel bed.

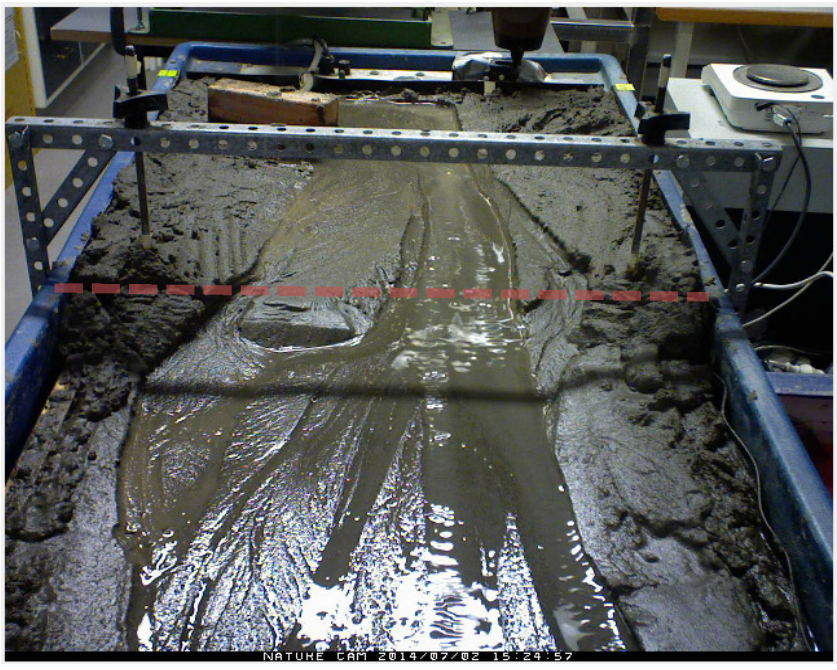

Figure 6.7 Micro-scale model 1.5 hours after displacement in Experiment I, looking upstream. Downstream aggradation is favoured, and multiple channels have reformed. Scars from faulting are recognised by prominent elongate mid channel bars over the fault trace. Red dashed line marks the fault trace.

The overall findings of Experiment I are summarised in Table 7. The lateral response of the channels was less significant than the response to vertical uplift. The system adjusted to accommodate the change in channel slope through aggradation and degradation. Upstream of the fault some aggradation was observed recognised by the development of bars. The bars in this section were irregular in shape and attached to the bank of the modelled river. During the displacement phase, a period of back flooding was observed over the upstream block resulting from a decrease in channel slope. The back flooding subsequently widened the floodplain of the upstream block. A zone of localised degradation was prominent over the fault trace after displacement, identified by the production of banks and mid channel bars. The mid channel bars formed as the channels rapidly incised over the fault trace. Clear aggradation was observed in the downstream block of the stream board following displacement, recognised by the chaotic arrangement of multiple mid channel bars as well as bars attached to the banks of the river. Multiple channels flowed around the mid channel bars creating a braided pattern. Aggradation in the downstream block was a result of sediment addition from the eroded fault scarp and the reworking of modelled coseismic landslide material downstream.

Table 7 Summarised results of Experiment I.

Position	**Upstream**	**Above Fault axis**	**Downstream**
Vertical Change	Some aggradation	Degradation	Aggradation
Channel Pattern	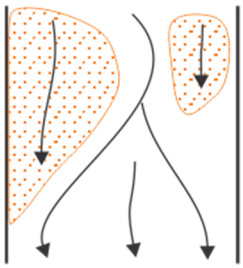	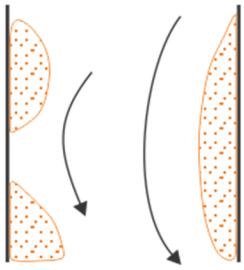	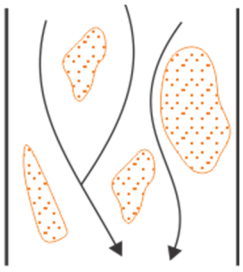
Channel Change	Widening of the floodplain, back flooding, minor braid development, meandering thalweg	Terrace formation, channel incision, straight channels	Downstream bar movement, widening of floodplain, formation of multiple channels. Bar braided system
Bar Characteristics	Inundated, irregular shape mostly attached to the bank. Submerged bars at times	Narrow and armoured with coarse grained sediment, aligned parallel to flow	Chaotic arrangement of braids and development of mid channel bars. Irregular shape
Surficial Deformation	Decrease in channel slope	Direct rupture, laterally and vertically. Fault scarp formation	Entire block was shifted true right corresponding to dextral strike-slip movement.

Figure 6.8 illustrates the pattern change of the braided channels from start to finish in Experiment I. The system began as a meandering river (Figure 6.8a), gradually developing into a braided system, as sediment began to deposit and multiple channels began to form (Figure 6.8b). Prior to the displacement phase, two prominent channels existed, interconnected by smaller secondary channels (Figure 6.8c). The dextral strike-slip displacement with uplift produced fault scarps that were rapidly incised by accelerated channel flow (Figure 6.8d). A zone of degradation was produced over the fault trace, which migrated upstream producing elongate mid channel bars that extended upstream from the fault trace (Figure 6.8e). The end of Experiment I was marked by the development of chaotic braids and multiple channels downstream with dominant meandering flow upstream (Figure 6.8f).

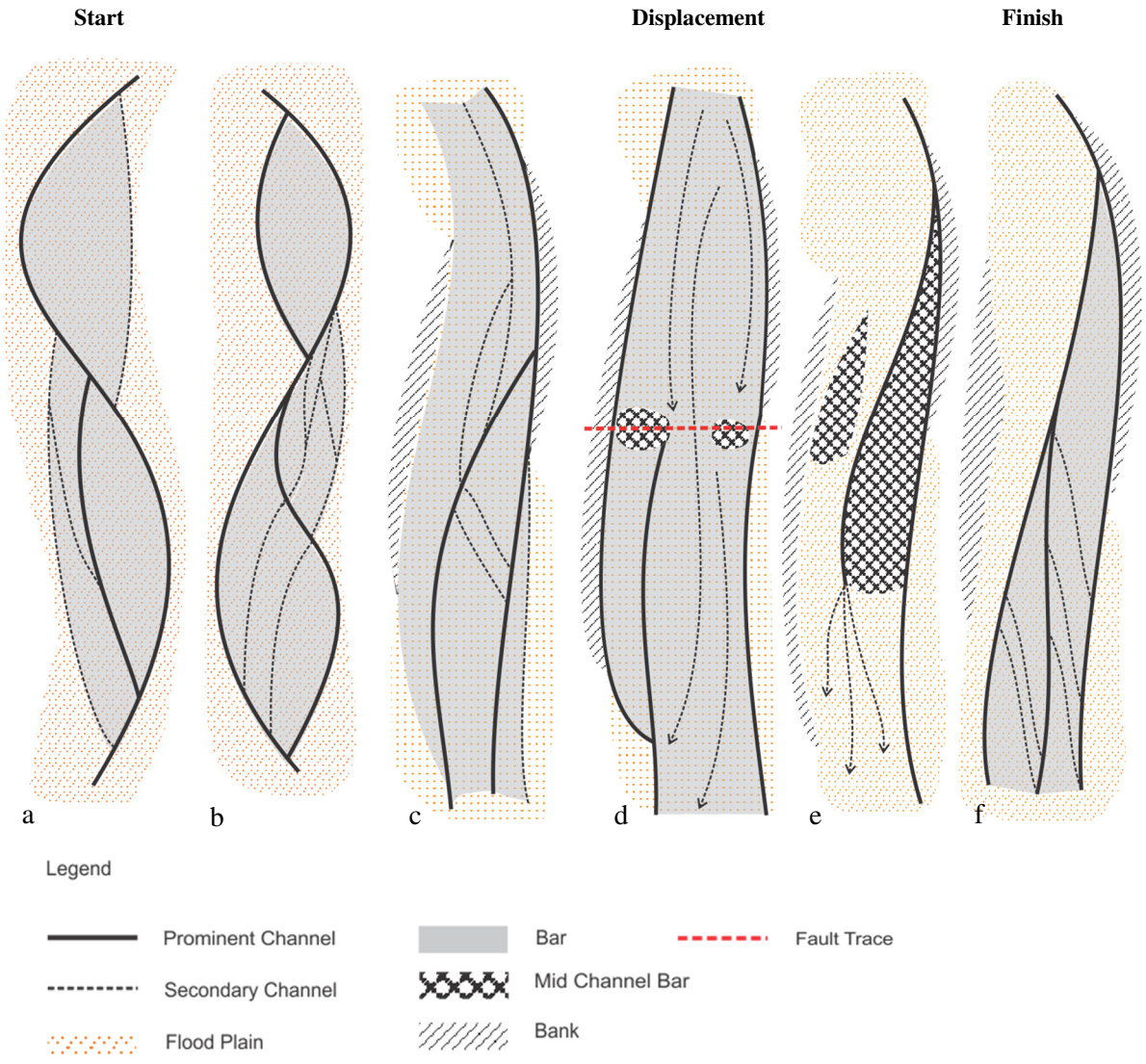

Figure 6.8 Pattern change of the experimental braided channel during vertical and lateral displacement in Experiment I.

6.2.2 Experiment II

Experiment II simulated a complete dextral strike-slip displacement, followed by episodic delivery of sediment sourced from upstream landsliding. Water flowed over the stream board at a rate of 0.4 L/min and sediment was constantly supplied upstream at a rate of 0.05 g/s. A braided fluvial system developed within four hours of water flowing over the stream board (Figure 6.9a). A clear meander was evident in the upstream block. This meander channelised flow eroding into the banks of this section (Figure 6.9b). Flow became more braided downstream, as sediment had dropped out of the system forming mid channel bars prior to displacement.

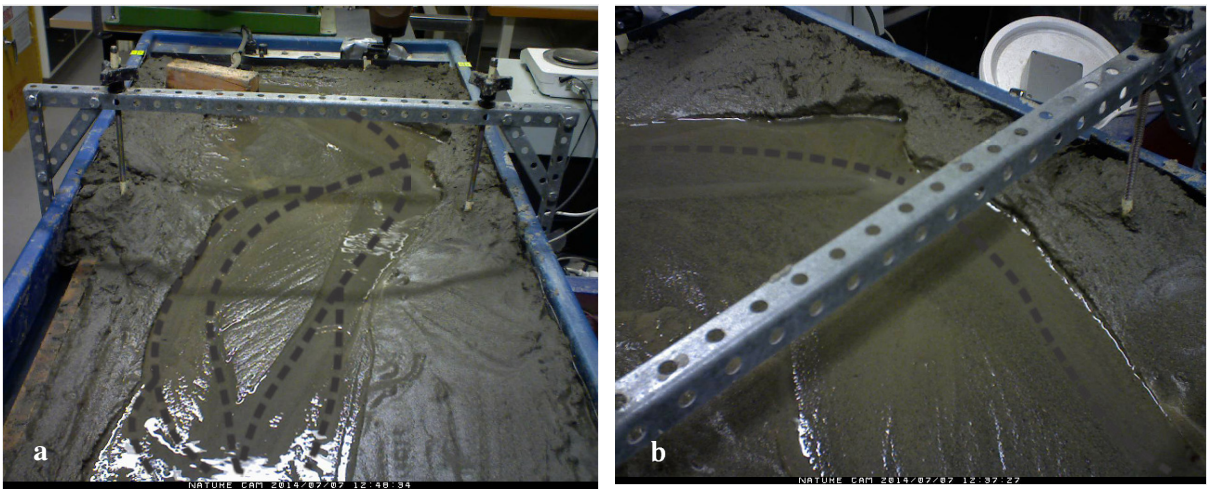

Figure 6.9 Micro-scale model after four hours of water flow in Experiment II. a) looking upstream; braided system developing downstream as mid channel bars form, b) plan view of fault trace; meandering flow upstream eroding into the true left bank. Dashed line indicates main channel flows.

The phase of displacement in Experiment II was identical to that in Experiment I. Displacement immediately resulted in the formation of stepped fault scarps and the development of two prominent channels (Figure 6.10a, b). The channels immediately incised into the fault scarp developing a natural grade at which to flow. More obvious in this experiment was a brief phase of pooling associated with the tilting of the upstream block. This induced upstream flooding, widening the floodplain of the upstream block (Figure 6.10c). Slight lateral shifts in the channels were observed corresponding to the right lateral displacement of the downstream block.

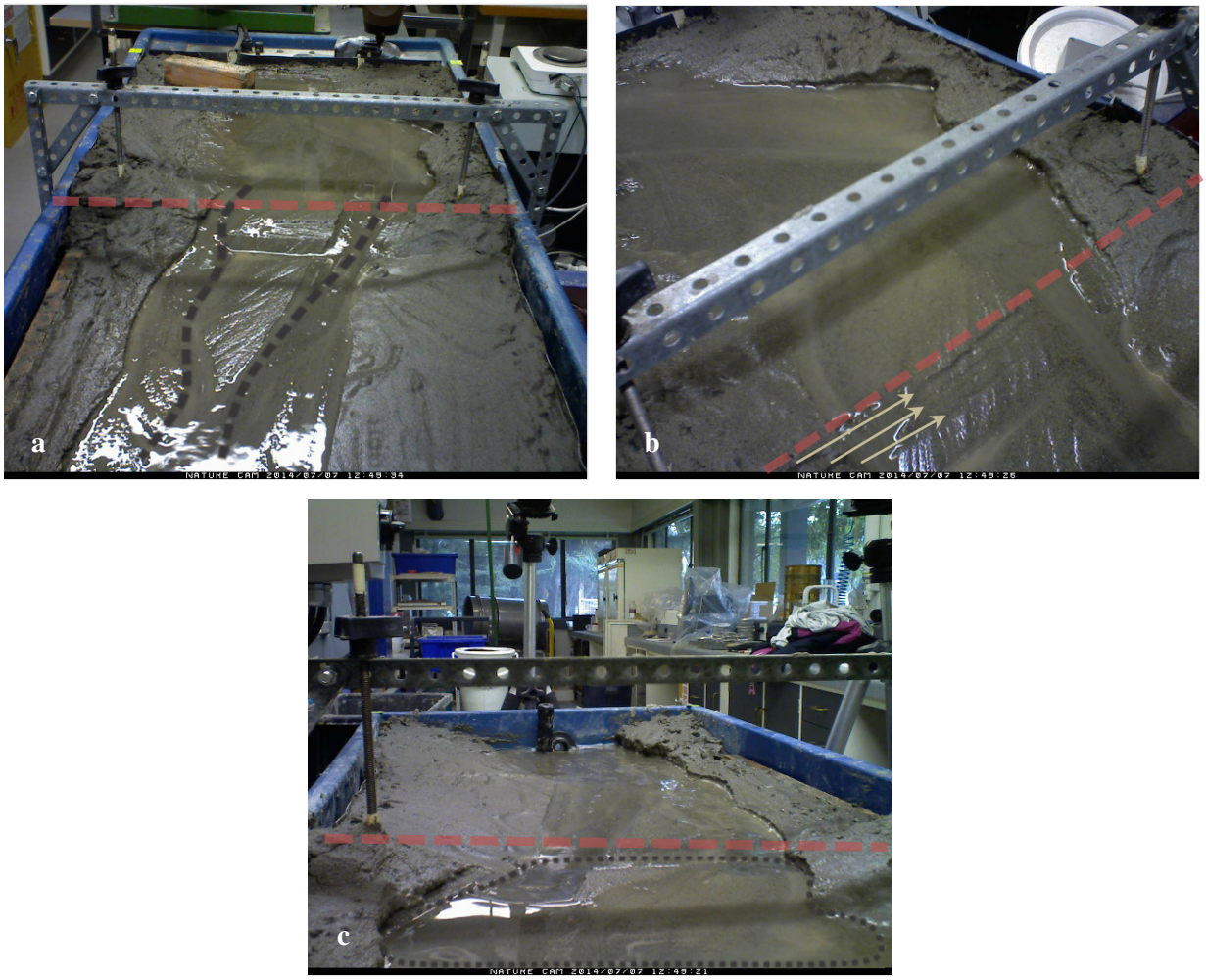

Figure 6.10 Micro-scale model during displacement in Experiment II. a) looking upstream, two prominent channels develop, highlighted by dashed line b) plan view of fault trace, multiple fault scarps form stepping downstream c) looking downstream, dashed line outlines the extent of back flooding in the upstream block. Red dashed line marks the fault trace.

Experiment II differed from Experiment I, as the addition of coseismic landslide sediment following displacement was episodic and not immediate. No additional sediment was added to the system until half an hour after displacement in Experiment II. The delayed 'landslide'

sediment addition represented smaller volumes of sediment movement through the fluvial system, as seen in Poerua (see Chapters 2 and 4). Due to the lack of immediate sediment addition, 20 minutes after displacement aggradation and degradation were less prominent. Downstream of the fault, flooding was observed with minor braid development (Figure 6.11). With no immediate additional supply of sediment following displacement, braided complexes did not form and aggradation was not obvious at this time. The lack of braided complexes downstream made it difficult to identify individual channels in the downstream reach. At this time no prominent channel had formed and the downstream block was undergoing a phase of flooding, recognised by the extent of water spread across the floodplain (Figure 6.11).

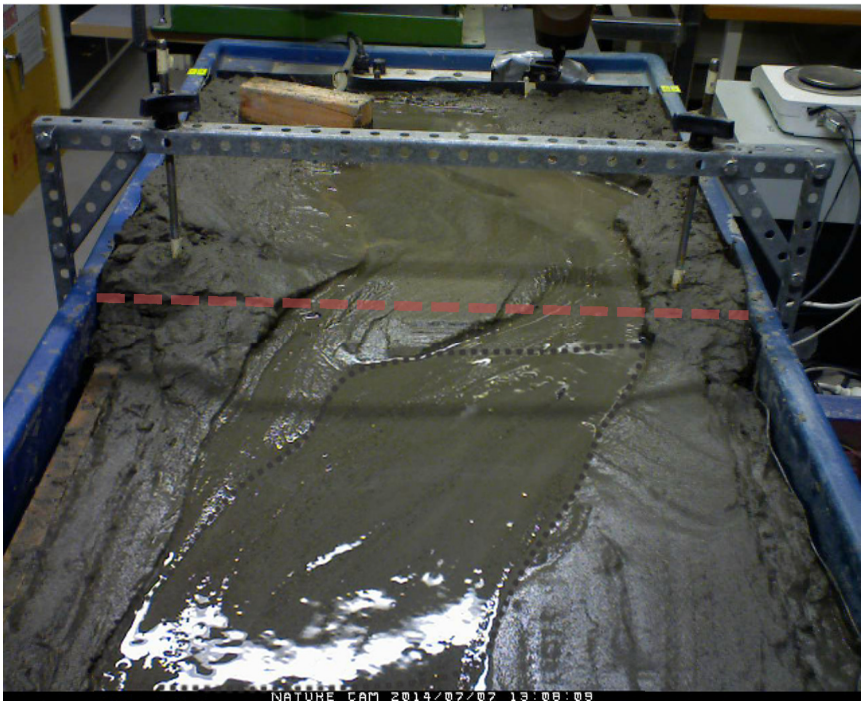

Figure 6.11 Micro-scale model, looking upstream 20 minutes after displacement in Experiment II. Flooding observed downstream with no obvious channelised flow. Upstream flow is confined to a meander incising into the true left of the river. Red dashed line marks the fault trace.

Additional 'landslide' sediment was supplied to the fluvial system, as it gradually readjusted to the displacement. 'Landslide' sediment was added approximately 30 minutes after displacement in Experiment II and subsequently three times every half an hour for the next one and a half hours. These sediment inputs initially induced aggradation in the upstream section. The sediment moved through this section much slower than it did in Experiment I, because flow had already adjusted to the change in channel slope and was no longer flowing at a rapid pace. Upstream bank erosion continued throughout the experiment further increasing the sediment load delivered downstream.

The effects of the delayed ‘landslide’ sediment addition were recorded three and a half hours after the initial displacement (Figure 6.12). The sediment was dispersed gradually and evenly across the downstream floodplain and did not accumulate as large braids because of the episodic delivery of the material. As the sediment gradually deposited, the overall slope of this block decreased, reducing the stream power and bankfull discharge, with consequential flooding.

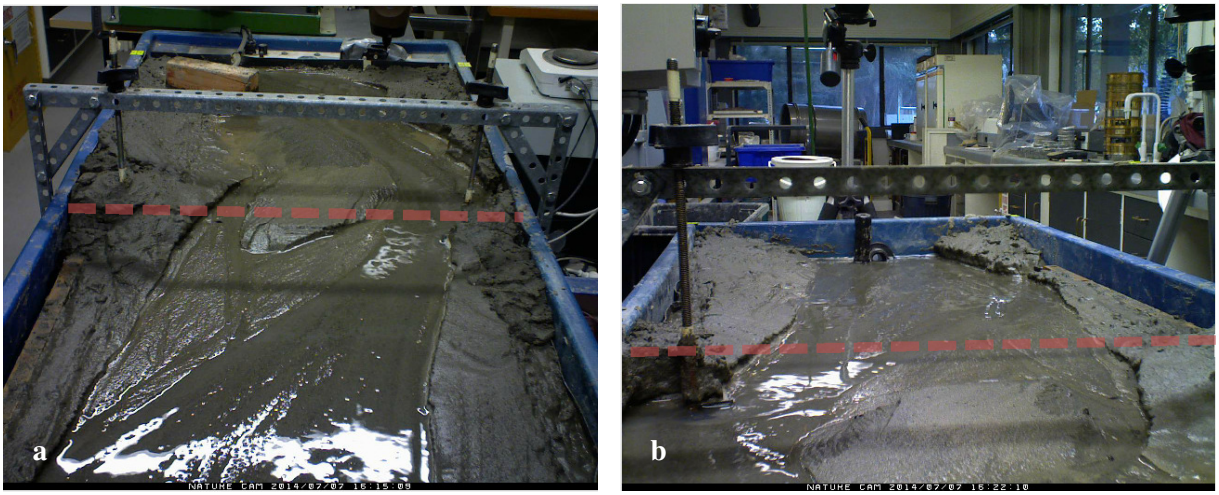

Figure 6.12 Micro-scale model 3.5 hours after displacement in Experiment II. a) looking upstream, the downstream floodplain widens as ‘landslide’ sediment is dispersed gradually and evenly across the channel bed b) looking downstream, displaying the formation of upstream bars and clear scour into the banks on the true left. Red dashed line marks the fault trace.

The overall results of the modelled dextral strike-slip displacement on the fluvial system in Experiment II are summarised in Table 8. The prominent response to dextral strike-slip displacement and delayed episodic delivery of ‘landslide’ sediment was up and downstream aggradation divided by a zone of localised degradation. Upstream of the fault, some bars developed attached to the banks of the river. Flow in this section was mainly confined to a meander incising into the true left bank of the river. The channel slope of the upstream block decreased during the phase of displacement resulting in a period of back flooding which consequently widened the floodplain of the upstream block. Degradation was prominent over the fault trace. An increase in channel gradient from vertical displacement accelerated flow over the fault trace, promoting rapid erosion. Additional ‘landslide’ sediment was not added to the system during the time of accelerated flow (during displacement) and therefore sediment deposition occurred in the upstream block as it was not rapidly flushed through the system. With each successive addition of ‘landslide’ sediment, degradation also continued to occur over the fault trace long after the initial displacement, producing highly channelised flow and elongate mid channel bars. Very few bars formed downstream, instead sediment

was dispersed across the floodplain, resulting in an overall increase in channel elevation. As the channel bed rose with successive sediment addition, flooding downstream was enhanced, if braids did exist they were inundated. If the Taramakau River responds in a similar way, widening the floodplain downstream of the Alpine Fault will occur, this may threaten surrounding agricultural land by inundation.

Table 8 Summarised results of Experiment II.

Position	**Upstream**	**Above Fault axis**	**Downstream**
Vertical Change	Aggradation	Degradation	Aggradation
Channel Pattern	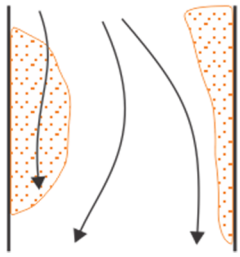	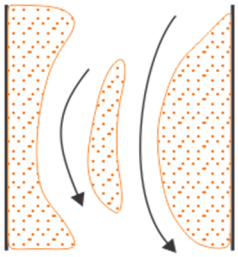	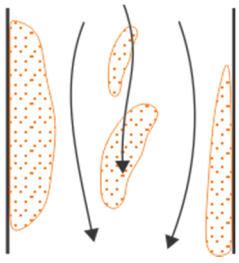
Channel Change	Brief back flooding, minor meander development	Terrace formation, bank erosion, channelised flow	No obvious thalweg, channels fill with sediment, widening of floodplain, flow spans across entire floodplain
Bar Characteristics	Inundated, irregular shape mostly attached to the bank.	Elongate extending upstream, armoured with course grained sediment.	Very few bars, those that formed were submerged
Surficial Deformation	Decrease in channel slope	Direct rupture, laterally and vertically. Fault scarp formation	Entire block was shifted true right corresponding to dextral strike-slip movement.

The progressive braided channel development from start to finish in Experiment II is represented in Figure 6.13. The fluvial system began as a simple meandering channel (Figure 6.13a), developing into a more complex braided river with time (Figure 6.13b). Prior to the rupture a dominant channel formed on the true left of the river (Figure 6.13c). This channel enhanced the formation of steep banks on this side of the river. Displacement produced fault scarps parallel to the fault trace (Figure 6.13d). The faults scarps were immediately incised by highly channelised and accelerated flow producing a mid channel bar in the centre of the stream board over the fault trace (Figure 6.13e). Flow was diverted around this mid channel bar. The mid channel bar grew in length and ‘landslide’ sediment was progressively reworked downstream. Clear braids did not develop in the downstream block nor did prominent channel flow (Figure 6.13f). Downstream, the floodplain had widened and secondary channels intertwined across it, resulting in widespread flooding of the channel bed. The

observed pattern change for Experiment II differed from Experiment I. The channel morphology in Experiment II changed from prominent channel flow prior to displacement to dispersed secondary channel flow after displacement. Flow was dispersed across the downstream block promoting downstream flooding and the subsequent widening of the floodplain within this reach. Clear braids developed in the downstream block of Experiment I and prominent channels flowed around them, this was not observed in the downstream block in Experiment II.

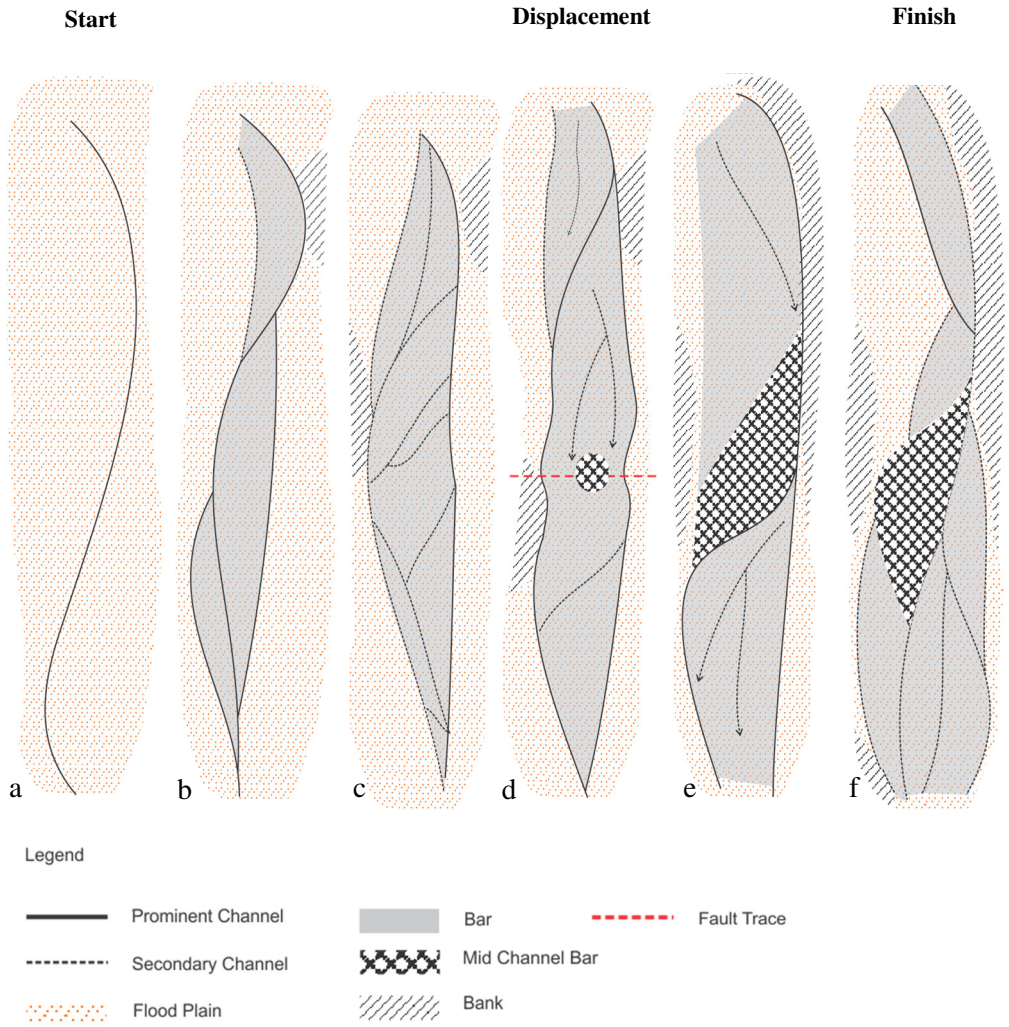

Figure 6.13 Generalised pattern change of the experimental braided channel during vertical and lateral displacement in Experiment II.

6.2.3 Experiment III

Experiment III simulated incremental fault displacement coupled with incremental sediment addition. The Experiment was designed to model the effects of potential smaller scale aftershocks following an AFE, therefore the results should be thought of as following the results of one of the previous experiments which modelled the main shock. Four smaller scale

displacements and sediment additions were applied. Similarly to the previous two experiments, water and sediment were constantly added to the stream board at a rate of 0.4 L/min and 0.05 g/s respectively. An established braided fluvial system had developed within four and a half hours of water flow over the stream board. Experiment III developed wider flood plains initially than the previous two experiments (Figure 6.14). Upstream flow meandered developing into a braided system downstream. Some of the downstream braids were submerged and others were isolated by very minor channels prior to the displacements.

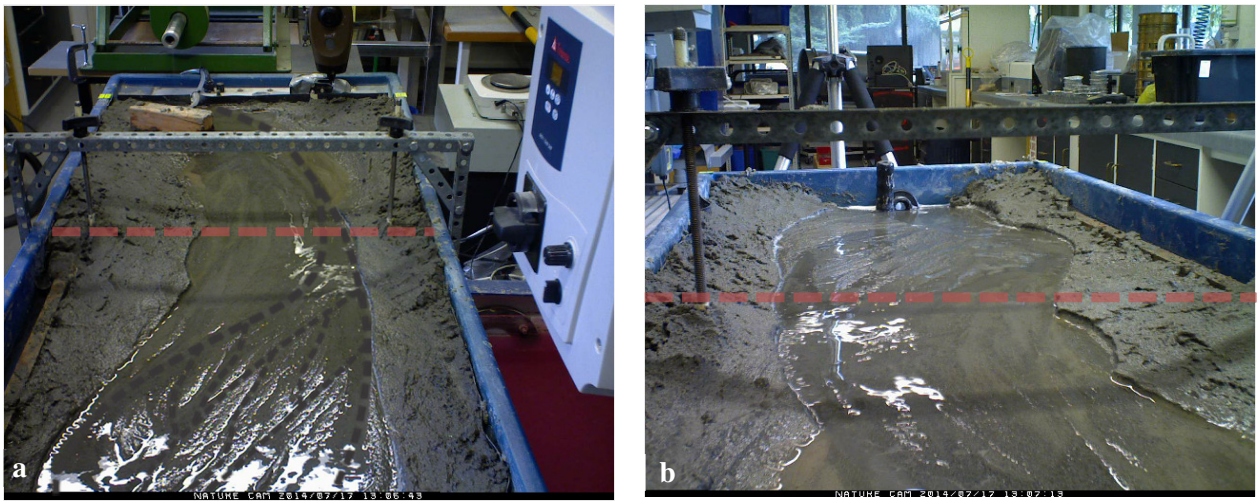

Figure 6.14 Micro-scale model after 4.5 hours of water flow in Experiment III. a) looking upstream, development of braids downstream, flow meanders across the upstream block at this time, highlighted by black dashed line b) looking downstream, wide floodplain in the downstream reach. Red dashed line marks the fault trace.

Four phases of displacement were modelled and equal volumes of additional sediment were supplied with each successive phase, representing landslide material input. Each displacement was 6 mm vertically and 12 mm laterally, thus the effects of faulting were less significant than observed in Experiments I and II which modelled complete displacement (25 mm vertical, 50 mm lateral). The first displacement took place after a braided system had developed on the stream board. Fault scarps did not develop during the first phase of displacement. Minimal incision occurred over the fault trace caused by temporary increased flow velocity. Aggradation was not observed up- or downstream of the fault during this time. Right lateral channel shifts were, however, identified as the effects of vertical uplift (incision and accelerated flow) were not prominent in the first small scale displacement. The lateral displacement resulted in a prominent channel developing on the true right of the modelled river (Figure 6.15). This increased the width of the channel bed downstream, incising into the river banks on this side prior to the second phase of displacement.

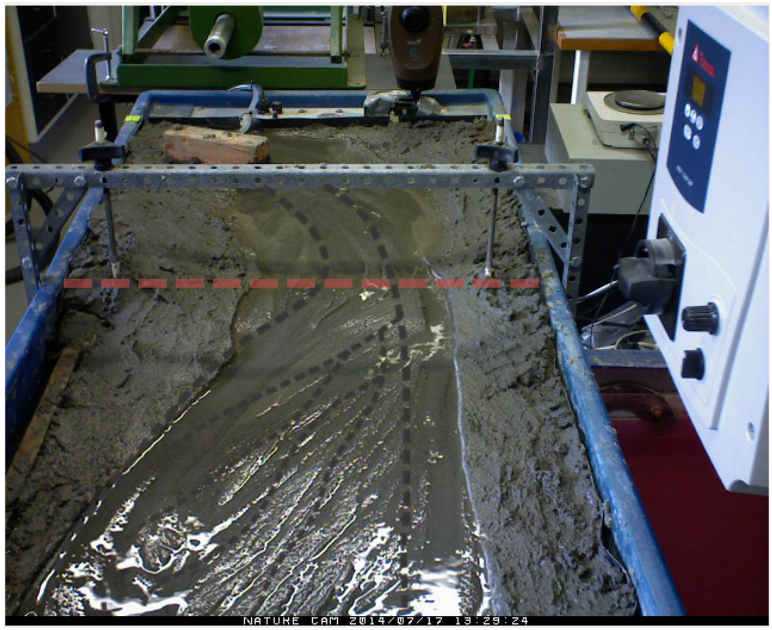

Figure 6.15 Micro-scale model looking upstream, during the first small scale displacement in Experiment III. A prominent channel formed on the true right of the river from lateral displacement. Red dashed line marks the fault trace.

The second incremental displacement took place 30 minutes after the first. An equal amount of additional sediment was supplied to the system at this time. Immediately after the second rupture a noticeable fault scarp developed, the channels immediately incised into the fault scarp as flow accelerated due to the increase in channel slope. Degradation migrated upstream, producing elongate mid channel bars over the fault trace (Figure 6.16). Three prominent channels developed flowing around the mid channel bars. Pre-existing channels were laterally displaced to the right by the dextral strike-slip movement, further widening the subsequent floodplain downstream (Figure 6.16).

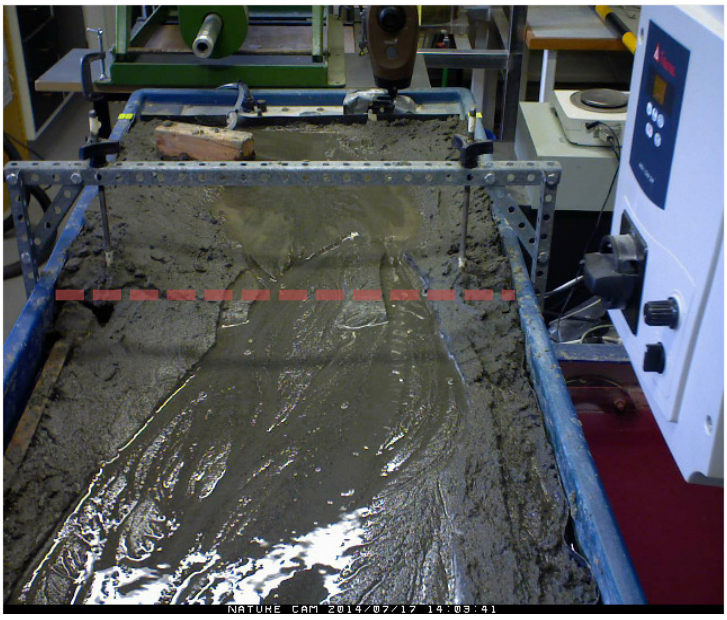

Figure 6.16 Micro-scale model looking upstream during the second small scale displacement in Experiment III; elongate mid channel bars formed over the fault as flow diverted around them. Red dashed line marks the fault trace.

Displacement number three was simulated one hour after the first displacement. The fault scarp over the fault trace increased in height subsequently cutting off some channel flow as the slope of the upstream block decreased. A mid channel bar over the fault trace widened as the upstream block was vertically displaced (Figure 6.17). Two prominent channels remained flowing over the fault scarp diverting around the widened mid channel bar. 'Landslide' and bed sediment flowed through these channels over the steepened gradient of the fault trace and then splayed out into a fan downstream. The splaying out of the sediment induced multiple channel formation downstream consequently widening the active channel bed of the modelled river (Figure 6.18). The fanning out of the sediment was most noticeable in Experiment III as channel flow was not as rapid as it was in the previous two experiments due to the smaller scale incremental displacements replicated in Experiment III.

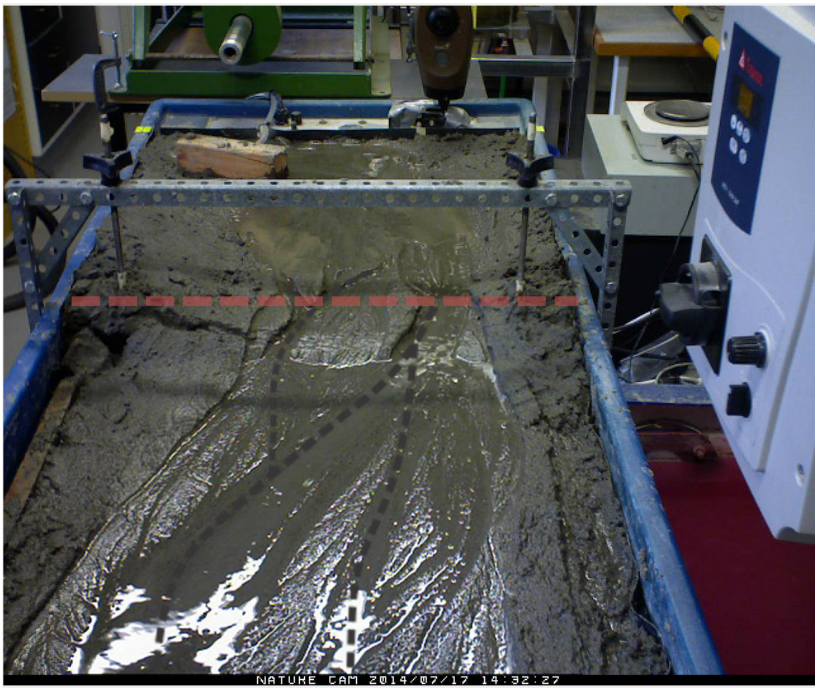

Figure 6.17 Micro-scale model, looking upstream during displacement three in Experiment III. Channels flowed around the widened mid channel bar over the fault trace. Red dashed line marks the fault trace.

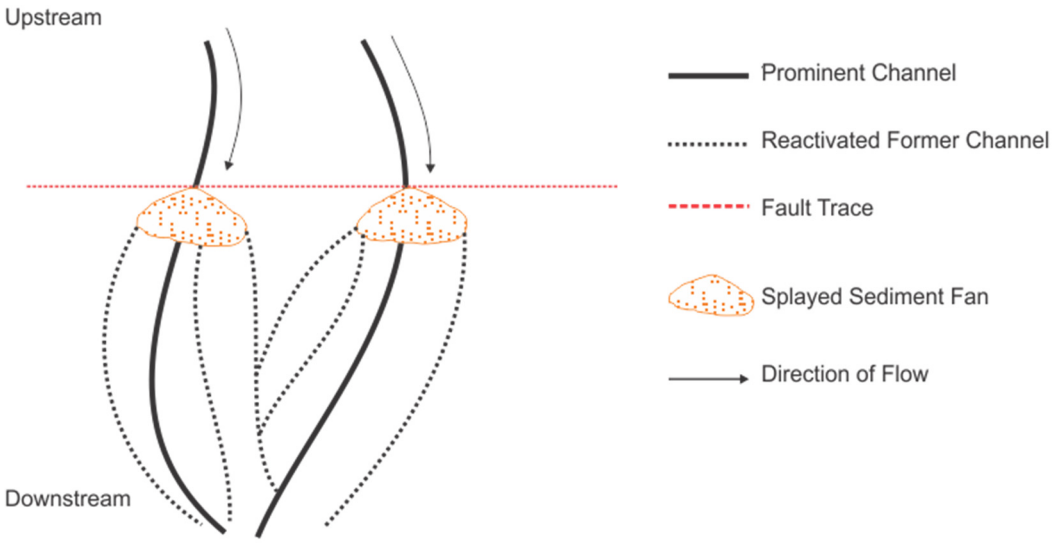

Figure 6.18 Simplified diagram of the reoccupation of former channels due to addition of sediment from degradation forming splayed out fans.

The fourth and final incremental displacement of Experiment III took place one and a half hours after the first displacement. The additional sediment from previous additions was now contributing to up- and downstream aggradation, evident by the development of braided complexes in both blocks (Figure 6.19). During displacement four, the fault scarp heightened and incision over the fault trace increased, supplying a greater load of sediment downstream enhancing aggradation. The decrease in slope of the upstream block cut off one of the remaining prominent channels flowing over the fault trace, leaving one main channel on the true left of the river flowing between the upstream and downstream block (Figure 6.19). Some secondary channels remained active on the true right of the river in the downstream block, flowing across the channel bed, creating narrow elongate mid channel bars aligned parallel to flow.

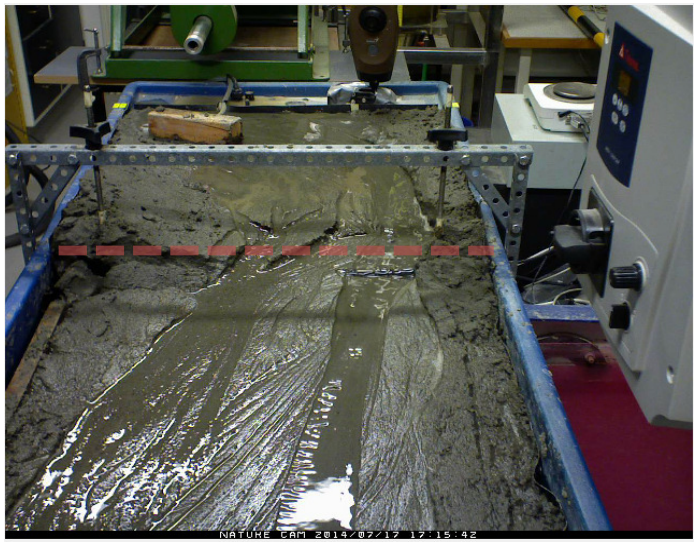

Figure 6.19 Micro-scale model, looking upstream after the final phase of incremental displacement in Experiment III. One prominent channel remains flowing on the true left of the river, some secondary channels continue to flow across to the true right of the downstream block. The secondary channels flow around parallel narrow and elongate mid channel bars. Mid channels bars protrude over the fault trace, extending into the upstream block. Red dashed line marks the fault trace.

The overall results of multiple small scale displacements modelled in Experiment III are summarised in Table 9. The prominent channel responses to the smaller scale dextral strike-slip displacements, were similar to those observed in the previous two experiments but on a smaller scale. Overall upstream and downstream aggradation resulted, divided by a zone of degradation over the fault trace. The aggradation and degradation took longer to develop than in Experiments I and II. Upstream of the fault bars developed from sediment deposition. Some of these were an extension of the mid channel bars that formed over the fault trace from accelerated flow and degradation, which had migrated upstream. At the start of Experiment III, channel flow began as a meander in the upstream block, transforming into multiple channels that flowed around the angular mid channel bars. Episodic increases in channel slope over the fault trace from incremental displacements, promoted channel incision and the development of a prominent fault scarp perpendicular to channel flow. Multiple small scale changes in channel slope occurred and therefore flow was not as highly accelerated as in Experiments I and II, but incision occurred and mid channel bars formed. The additional loads of sediment did not flow so rapidly through the system as in Experiment I. Long, narrow and elongate bars formed in the downstream block parallel to channel flow. The downstream section of the modelled river had become highly braided representing a depositional and aggradational environment. While the overall results of Experiment III were similar to those seen in Experiment I and II, the modelled system in Experiment III constantly had to adjust to change from multiple smaller scale displacements and therefore the effects were longer-lived.

Table 9 Summarised results of Experiment III.

Position	**Upstream**	**Above Fault axis**	**Downstream**
Vertical Change	Aggradation	Degradation	Aggradation
Channel Pattern	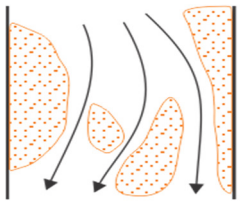	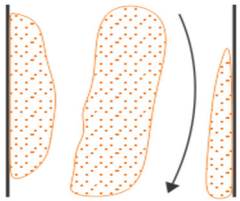	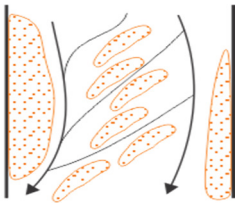
Channel Change	Initial meander, becoming braided with aggradation	Terrace formation, rapid bank erosion, highly channelised flow	Highly braided, right lateral shift.
Bar Characteristics	Angular shape, formed predominantly by migration of degradation upstream	Wide and armoured with course grained sediment. Elongate extending upstream	Long, narrow elongate bars
Surficial Deformation	Constant incremental decrease in channel slope	Incremental displacement. Gradual	Entire block gradually shifted to the true right

		fault scarp formation	corresponding to dextral strike-slip movement.

The progressive change in channel pattern for Experiment III is shown in Figure 6.20. The fluvial system began with simple meandering flow both in the upstream and downstream blocks (Figure 6.20a). Sediment was continually added at a constant rate of 0.4 L/min contributing to formation of a preliminary braided fluvial system. Prior to the first displacement multiple prominent channels and secondary channels intertwined across the stream board (Figure 6.20b). After the first displacement, the channels responded by shifting laterally towards the true right of the river, in the direction of dextral slip (Figure 6.20c). After the second displacement, a fault scarp developed which promoted accelerated channel flow enhancing degradation and the development of mid channel bars over the fault trace (Figure 6.20d). Banks formed on either side of the river as flow became channelised in the second phase of displacement. The third displacement increased the height of the fault scarp inducing further degradation and promoting the development of three major mid channel bars (Figure 6.20e). Flow became channelised between the mid channel bars. A highly braided system began to form downstream after the third displacement, at this time 'landslide' sediment was being reworked from upstream and deposited in the downstream block, similarly to Experiments I and II (Figure 6.20e). The fourth and final displacement heightened the fault scarp and shifted the channels towards the true right of the river (Figure 6.20f). Flow increased over the fault trace and degradation began to migrate upstream, extending the mid channel bars upstream. Braids remained in the downstream reach. Towards the end of Experiment III one large mid channel bar existed over the fault trace that extended into the upstream block (Figure 6.20g). Two prominent channels existed in the downstream block on the outer parts of the floodplain, connected by secondary channels flowing across the floodplain. The change in pattern development seen in Experiment III illustrates the longevity of fluvial processes induced by multiple smaller scale displacements. While the individual displacements were much smaller in Experiment III than in Experiments I and II, the fluvial response was much greater and longer lived, seen through the development of multiple mid channel bars over the fault trace extending upstream and the development of a highly complex braided system downstream.

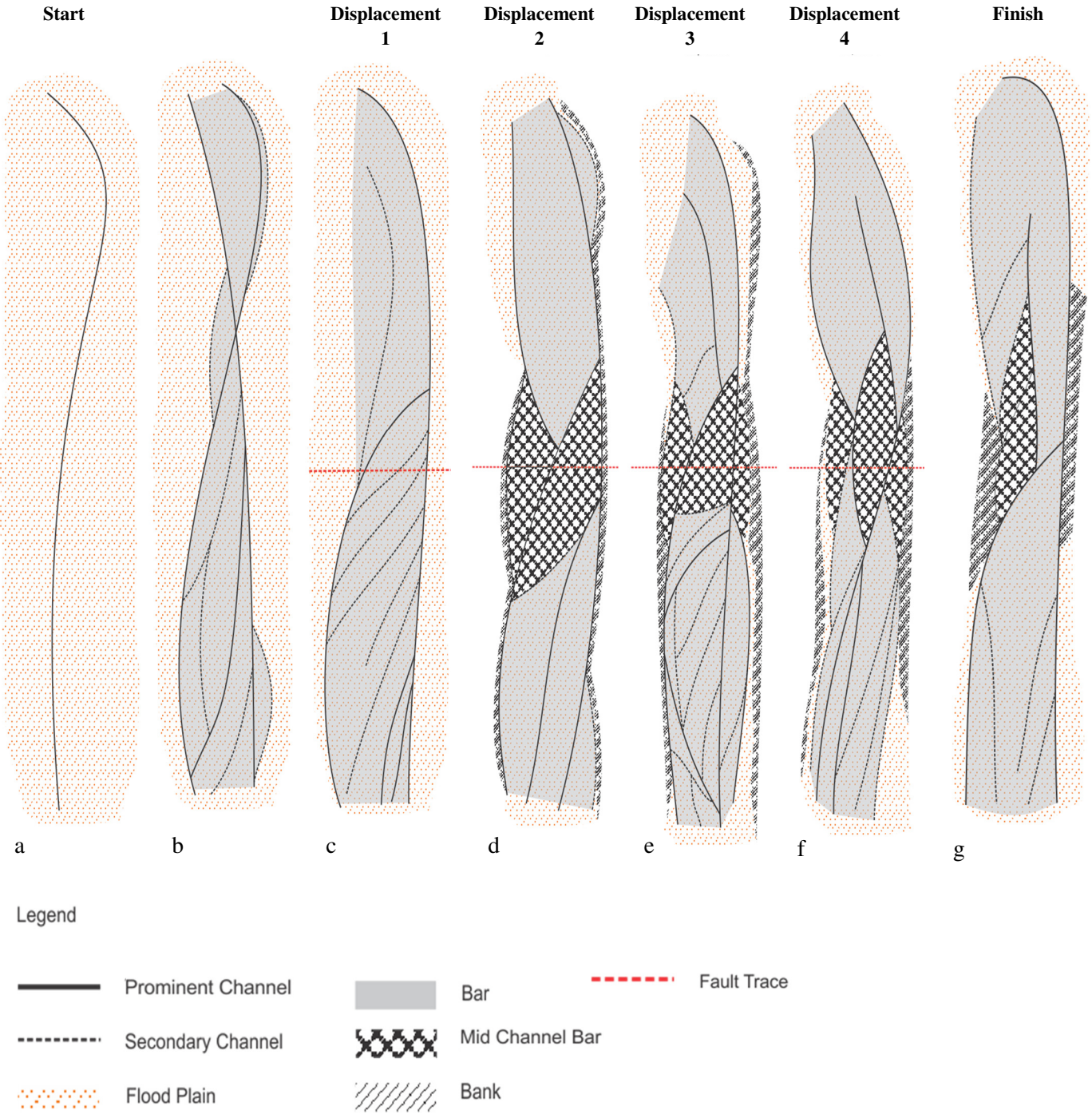

Figure 6.20 Simplified experimental pattern change for the modelled fluvial system in Experiment III.

6.3 Summary

Three micro-scale model experiments showed that the primary response to dextral strike-slip displacement and uplift on the fault was upstream and downstream aggradation divided by a zone of degradation over the fault trace. Differences in the pattern and timing of aggradation and degradation were highlighted by the three different experiments. Experiment I replicated an AFE where landslide material was immediately added to the fluvial system. Powerful incision over the fault trace, led to an increase in sediment load downstream. Both 'landslide' sediment and that eroded from the fault trace contributed to downstream aggradation. Experiment II best represented the most likely AFE scenario, with delayed sediment additions. Delaying the addition of sediment meant that it was not influenced by the temporary spike in flow velocity immediately following vertical uplift, and therefore the sediment had an opportunity to deposit upstream. The sediment was then gradually and evenly reworked downstream, inducing downstream aggradation and flooding. Experiment III was conducted to model potential AFE aftershocks. Lateral avulsions were sensitive to the smaller slope deformations, resulting in channel shifts towards the true right of the river following the direction of displacement. Consistent displacement and sediment addition resulted in deep incisions from highly channelised flow over the fault. Sediment was transported downstream contributing to aggradation. The movement of sediment and the change in channel pattern resulting from micro-modelled dextral strike-slip displacement and 'landslide' sediment additions provides an insight on how the Taramakau River as well as other braided alpine rivers may respond to an AFE.

Chapter 7 – Discussion
Hazard Implications and Management Measures

7.1 Introduction

The aim of Chapter 7 is to outline the hazards that may result from the effect of an AFE on the behaviour of the Taramakau River within the study area based on the findings presented in the previous three chapters. Chapter 4 quantified the hazards of landsliding and aggradation through hydraulic and landslide data analyses. Chapter 5 examined the study area through aerial photography recognising patterns of channel avulsion as well as highlighting potential flood-threatened areas during and after an AFE. Chapter 6 analysed the direct implications of a dextral strike-slip surface rupture along a braided fluvial system as well as replicating the effects of an increase in sediment load from modelled coseismic landslides through micro-scale model experiments.

How the topics discussed in Chapter 7 relate to one another and which research methods have been used to address such hazards is graphically represented in Figure 7.1. Chapter 7 is organised with respect to the likely chronological order of hazards that may occur within the study area following an AFE. This is: surface rupture (see section 7.2.1), coseismic landsliding (see section 7.2.2), aggradation (see section 7.2.3) and avulsion and flooding (see section 7.2.4). Finally, management measures that may be implemented to minimise the risks within the study area deriving form an AFE, are also discussed.

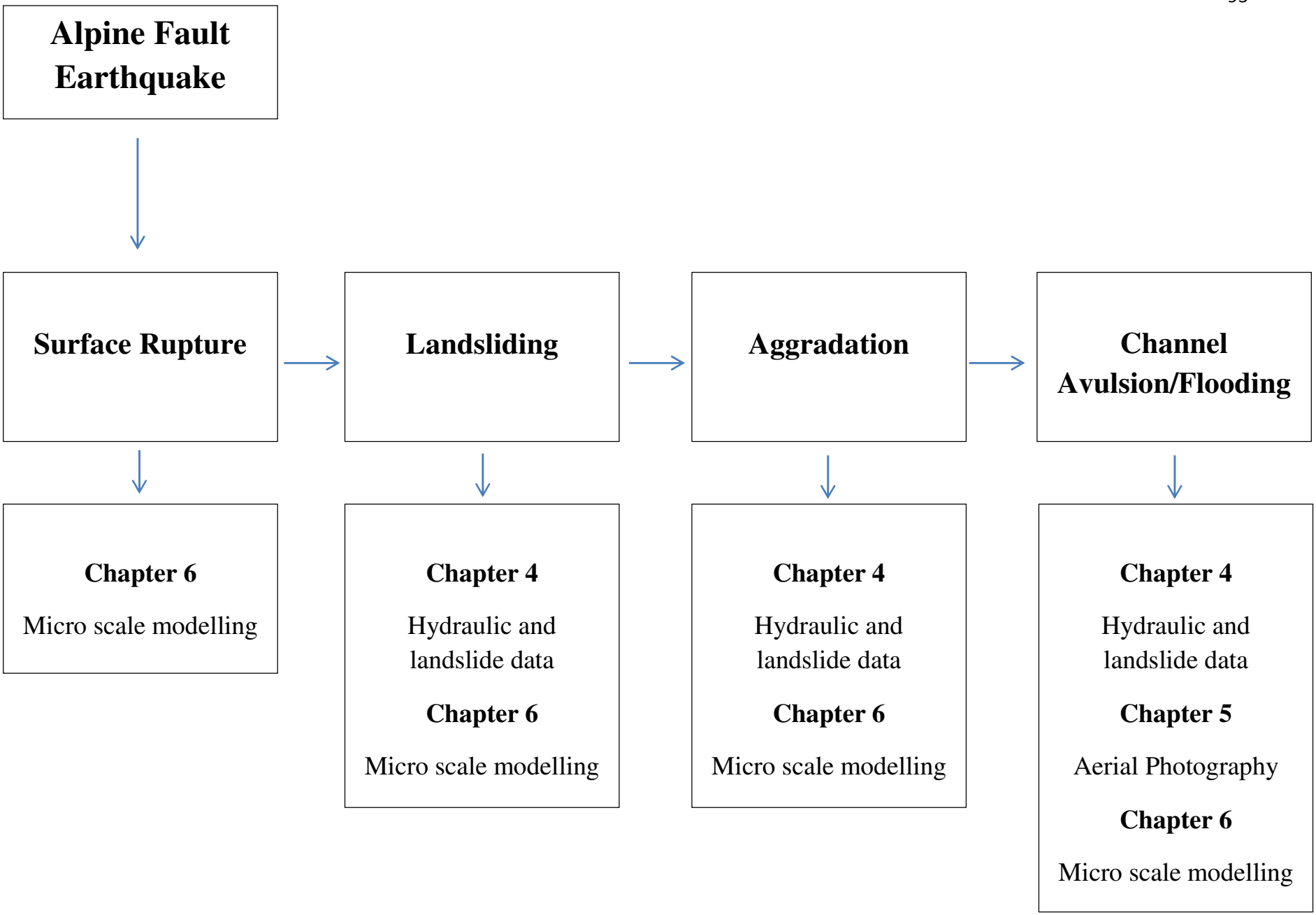

Figure 7.1 Flow diagram of how the topics discussed in Chapter 7 relate to one another, highlighting which research methods were used to address each hazard.

7.2 Hazards

The threat of AFE-related hazards in the study area is high and ranges from earthquakes to extensive flooding. The consequential risks derive from the vulnerability of critical systems such as the cross-island road and rail transportation links in the Taramakau valley. The fluvial hazards that may directly affect the adjacent road and rail transportation routes following an AFE include aggradation, avulsion, erosion and flooding. These derive from surface rupture and from the addition of sediment from upstream coseismic landsliding. The likely sequence of events following an AFE impacting the Taramakau River is: surface rupture, approximately perpendicular to channel flow, followed by upstream landsliding, supplying a significant increase in sediment load to the Taramakau River, followed by changes in river behaviour. The landslide material is likely to be reworked through the Taramakau valley, filling the river channels with sediment (aggradation) and promoting channel avulsion. As the channels increase in elevation and shift across the floodplain, previously unaffected land may be threatened by flooding and sediment deposition. The fluvial hazards induced by an AFE and coseismic landsliding may be long-lived and continue to occur throughout the Taramakau catchment for many years or decades after an AFE (Robinson & Davies, 2013).

7.2.1 Surface Rupture

The surface rupture and attendant ground shaking of an AFE will be the first hazard to cause immediate disturbance within the study area. Yetton (2000) suggests that the next AFE will have a magnitude of $M_w = 8.0$, rupturing from Haast to Inchbonnie. The likely surface lateral displacement around the Inchbonnie area will be about eight metres with approximately one metre of vertical uplift on the eastern side of the fault (Grey District Council, 2007). The effects of surface rupture within the study area were investigated through the experiments conducted on the micro-scale model discussed in Chapter 6.

The modelled vertical displacement induced a change in channel morphology. From the three micro-scale model experiments, vertical uplift caused river bed degradation over the fault trace, with up- and downstream aggradation. Incision occurred over the fault trace during vertical displacement. Mid channel bars developed over the fault trace and retreated upstream through incision, becoming less defined with time. Rapid degradation over the fault trace increased the sediment supplied downstream, inducing channel aggradation and the development of a highly braided system downstream of the fault. The observed pattern of degradation over the uplift zone coupled with downstream aggradation corresponds to models

of sedimentary response of rivers to active tectonics produced by Holbrook and Schumm (1999) (Figure 7.2).

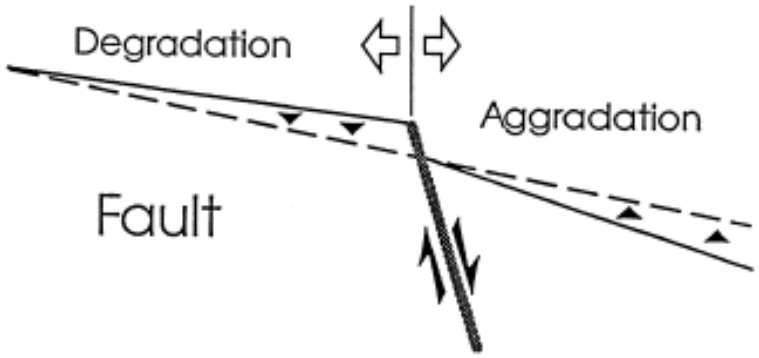

Figure 7.2 Simplified sedimentary response to faulting across channelised flow. Holbrook and Schumm (1999).

Holbrook and Schumm's (1999) model is a valid representation of how a river may respond to active faulting, however, it cannot be applied to the vertical displacement of an AFE as it does not consider the significant addition of sediment sourced from upstream landsliding. Experiment II of the micro-scale modelling was most representative of an AFE scenario. Sediment addition from landsliding was delayed, replicating gradual additions of sediment moving through the valley, based on data from Poerua (see Chapter 4). Initially, the modelled river did respond similarly to Holbrook and Schumm's (1999) model (Figure 7.2); a zone of degradation formed over the fault trace and retreated upstream, and aggradation occurred downstream. Additional 'landslide' sediment, however, was supplied to the system half an hour after displacement. Part of the 'landslide' sediment settled in the upstream block contributing to upstream aggradation, similar to observations in models by Ouchi (1983) (Figure 7.3), and differing from Holbrook and Schumm's (1999) model. Ouchi (1983) suggests that aggradation occurs upstream of an uplift axis due to a decrease in channel slope. The slope of the upstream block in the micro-scale modelling decreased with vertical uplift, the decrease in channel slope coupled with the deposition of 'landslide' delivered sediment enhanced the effects of upstream aggradation. The modelled river in all three micro-scale experiments adjusted to the vertical component of displacement, similarly to Holbrook and Schumm's (1999) model (Figure 7.2) and Ouchi's (1983) model (Figure 7.3) through degradation and aggradation.

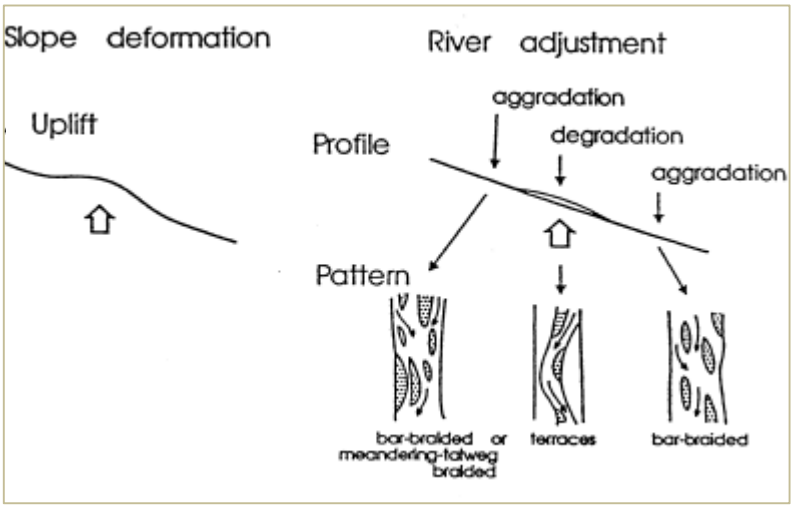

Figure 7.3 Common channel response to longitudinal profile deformation. Up and downstream aggradation result from a zone of uplift divided by a zone of degradation over the uplift zone. From Ouchi (1983).

The lateral component of displacement may affect the Taramakau River system immediately following an AFE. The modelled strike-slip displacement induced horizontal channel shifts in the micro-scale experiments. These were not as obvious as the changes in channel morphology induced by vertical uplift, but flow shifted slightly towards the true right of the river, in the direction of displacement. From horizontal displacement studies on fluvial systems, three different forms of horizontal responses have been identified in river channels (Ouchi, 2004). Assuming flow is perpendicular to the fault trace, the following deflections may be a consequence of lateral displacement; right laterally deflected (RI), left laterally deflected (LI) and undeflected channels (UI), each of which vary depending on the initial conditions (Figure 7.4). In the micro-scale experiments right laterally (RI) deflected channels were observed, slightly displacing flow towards the true right of the modelled river.

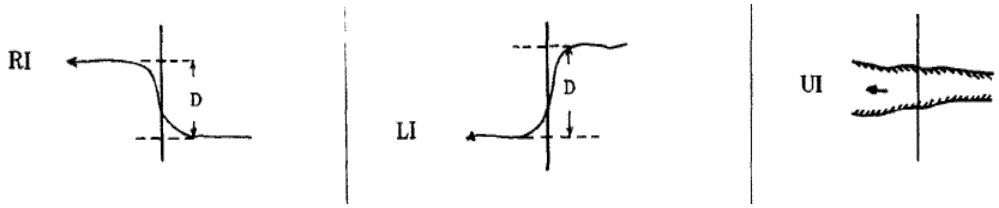

Figure 7.4 Different forms of river deflections associated with lateral displacement perpendicular to river flow. From Ouchi (2004).

Ouchi's (2004) models also replicated complete horizontal offset of river channels, consequently beheading a channel and producing a form of dam. The damming, briefly attenuated flow and the movement of sediment downstream. The beheading and subsequent

formation of dams was not observed in the micro-scale experiments and thus water flow and sediment transportation were not hindered, and sediment throughput was more or less enhanced by the subsequent addition of modelled landslide- and incision- derived sediment. If a larger lateral displacement was used some channels may have been beheaded and completely offset. Temporary beheading of Taramakau River channels less than eight metres wide may occur following an AFE which is expected to induce approximately eight metres of lateral displacement. Beheading, should it occur, will be a short-term, temporary and relatively insignificant process compared with aggradation and avulsion.

7.2.2 Landslides

Coseismic landsliding is expected to be the second major hazard affecting the Taramakau River study area following an AFE. In the wake of a M_w = 8.0 AFE, the Taramakau catchment will produce a maximum credible volume of 3.0 x 10^8 m^3 of material. This has the potential to cause direct damage through river blockage and burial of land, transportation links and other infrastructure as well as inducing an array of subsequent hazards, throughout the fluvial networks of the Southern Alps. The effects of landsliding within the study area were identified in Chapters 4 and 6, from an analysis of landslide volume data provided by Robinson (2014) and through the micro-scale model experiments. The mass of sediment added to the system may induce large scale aggradation and wide spread channel avulsion.

The volume of landslide material produced in the Taramakau catchment will determine the magnitude and extent of river-induced damage within the study area. Robinson (2014) calculated minimum and maximum credible AFE-derived landslide volumes in the Taramakau catchment as 6.8 x 10^7 m^3 and 3.0 x 10^8 m^3 respectively. The 1999 Mt Adams rock avalanche had 10 - 15 x 10^6 m^3 of landslide material (see Chapter 2 and 4). The maximum credible Taramakau landslide volume is an order of magnitude greater than that of Poerua, therefore the impacts may be significantly greater than that observed in 1999. Poerua, however, was one event, whereas the estimated landslide volumes used in this thesis account for the entire Taramakau catchment. The volume of Taramakau landslide material may be distributed throughout the catchment from a multitude of landslides and therefore the consequent hazards may not be as severe, although they may be more widespread and of longer duration.

Large-scale landsliding is unlikely to occur along the slopes that border the Taramakau valley in the study area. Strong ground motion caused by the earthquake, however, may result in the

collapse of the river banks close to the fault line. Of considerable concern is the 1100 m long, 30 m high river-cut bank of an alluvial fan on the true right of the river located immediately upstream of the Stanley Goosemen Bridge and the Midland Rail Bridge (see Chapter 5). The collapse of this bank could supply up to 10^5 m^3 of sediment to the river causing rapid channel aggradation and avulsion.

Coseismic landslide material sourced upstream of the study area will be reworked down through the Taramakau River towards the study area causing aggradation. The micro-scale model experiments showed that additional 'landslide' material caused aggradation, predominantly downstream of the fault with some evidence of aggradation upstream.

7.2.3 Aggradation

Aggradation is a common response to an increase in sediment load in fluvial systems, and will be the first fluvial hazard to result from the next AFE. As the Taramakau River channels and adjacent floodplains progressively aggrade with landslide-derived sediment, it is likely that channel avulsion will occur.

The time sequence of aggradation expected to occur within the study area was estimated by a comparison with the effects of the Mt Adams rock avalanche that fell into the Poerua valley in 1999 (see Chapter 4). Data from Poerua indicate that approximately 15% of the rock avalanche material migrated down the Poerua valley depositing on the Poerua River alluvial fan. The rest of the avalanche material remained in the lower gorges, upstream of the Poerua River alluvial fan (Korup et al., 2004, Nelson, 2012), at least in the short term (decade). The comparison indicated that not all of the Taramakau landslide material will immediately migrate through the valley towards the study area after the next AFE. Approximately 47% (Table 3) of the landslide material may be deposited and remain in the lower gorges of the Taramakau valley upstream of the study area. Within nine years of an AFE almost 15% of the maximum credible landslide volume (3.0×10^8 m^3) could be reworked through the valley onto the floodplain of the Taramakau River study area. However, sediment in the form of a landslide dam at Poerua was readily available for transportation; Taramakau landslide volumes may not be stored within landslide dams and therefore may take longer to migrate down the valley to the study area. Nevertheless, referring to the Poerua comparison, 15% of sediment input on the alluvial fan accounts for a total of 4.4×10^7 m^3 of sediment, resulting in just over 0.5 m of aggradation when averaged over the whole of the Taramakau floodplain in the study area. As the river bed rises, the free-board between the river and its banks will

reduce, increasing the frequency of overbank flows. The free-board between the water level and the Stanley Goosemen and Midland Rail Bridges that cross the Taramakau River will also be reduced (assuming that the bridges survive ground shaking, which is unlikely unless they are specifically strengthened before the AFE). An average of 0.5 m of aggradation over the whole floodplain width means that the aggradation in the present river bed, which is lower than the floodplain, will be greater than 0.5 m. Detailed topography to assess this effect is not available, but given that the river bed is incised of the order of metres below the floodplain it would be prudent to anticipate of the order of metres of aggradation beneath these bridges as a result of AFE-induced landsliding. This clearly has the potential to put the bridges (or their replacements) at risks during major rainstorms in the years following the AFE.

The micro scale model experiments revealed that aggradation occurred both up- and downstream of the modelled fault after displacement. The sediment used throughout the modelling was uniform (750 μm), whereas in reality the sediment produced from AFE landslides will be of all sizes from microscopically small to house-sized and therefore sediment deposition and thus aggradation may not be evenly distributed across the floodplain. Neither will it be confined to the study area, but the important concept is that most if not all of the landslide-derived sediment that the river reworks will at some stage pass through the study area. Aggradation will also occur downstream of the fault trace at the confluence of the Taipo River with the Taramakau River. The Taipo River is a major tributary to the Taramakau and has the potential to add a significant load of landslide sediment to the Taramakau River following an AFE. The addition of sediment from the Taipo River will cause the Taipo alluvial fan at the confluence with the Taramakau to aggrade, in turn inducing additional aggradation in the Taramakau River bed upstream. Aggradation may thus become particularly high between Inchbonnie and the Taipo River which may increase the risk of channel avulsion across low lying farmland adjacent to the Taramakau River, downstream of the Alpine Fault in the study area.

All rivers have a sediment input that varies with time, and in large alpine rivers this is often affected by large scale earthquakes. Presently the Taramakau, along with other southern alpine rivers, are receiving minimal if any landslide material derived from the last known AFE in 1717AD (Figure 7.5). Large scale earthquakes cause a spike in sediment input, the effects of which commonly result in channel aggradation; this is followed by an exponential decay as sediment input returns to normal after several years, decades or centuries (Davies &

Korup, 2007). The cyclic pattern presented in Figure 7.5 will likely occur in the Taramakau River during and after the next AFE.

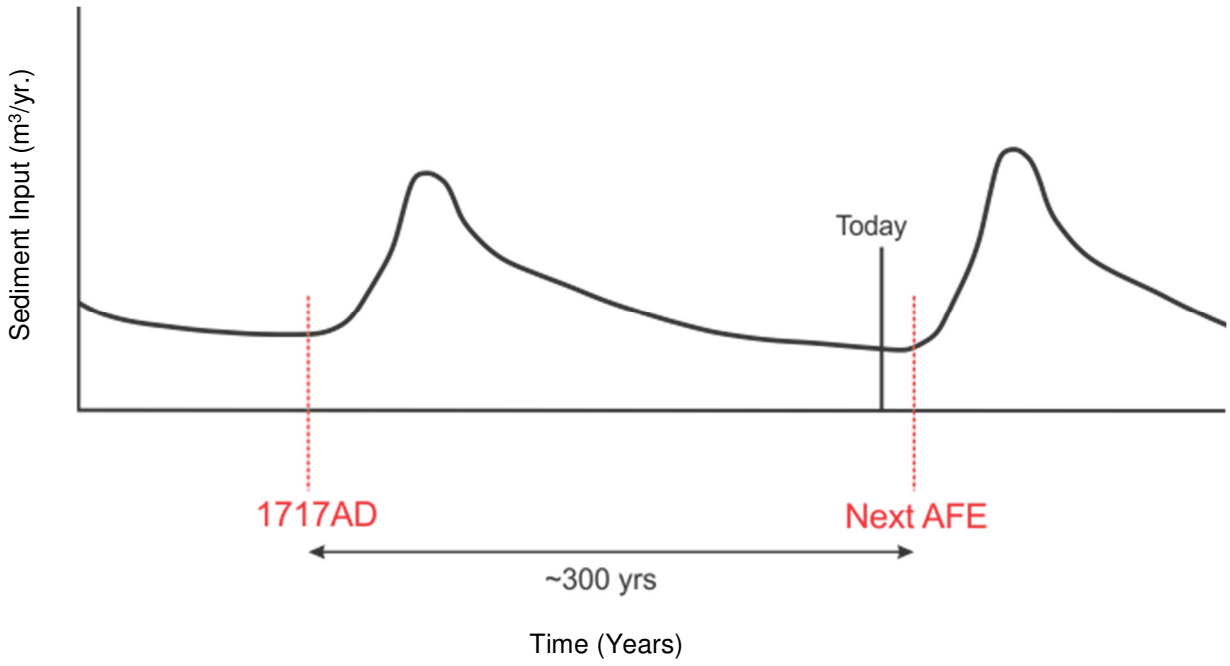

Figure 7.5 Alpine river sediment input rates, controlled by large scale earthquakes. From Davies and McSaveney (2011).

Korup et al (2004) and Davies and Korup (2007) suggest that a spike in sediment input following large scale earthquakes and landsliding is frequently succeeded by post-event incision. Incision is often the first sign of the system ceasing to aggrade (Korup et al., 2004). Part of this cycle is seen in the Poerua data and is expected to occur in the Taramakau River. Data from Nelson (2012) show that the Poerua River began to incise into the alluvial fan head approximately six years after the dam failed (Table 2). The river elevation, however, remains much higher than it was prior to the landslide. The Taramakau is likely to behave similarly, as the system gradually becomes depleted of AFE landslide material with time. Direct comparison with Poerua suggests that the Taramakau River may complete its aggradation within a decade after the next AFE; however Wells and Goff's (2007) dating of dune ridges associated temporarily with previous AFE events delivering sediment to the much larger Landsborough-Haast river system in South Westland, shows that excess sediment was delivered to the coast for several decades after each earthquake. Therefore the Taramakau fluvial system may not return to pre landslide conditions for several decades, or even longer, after the next AFE.

7.2.4 Channel Avulsion and Flooding

Channel avulsions and flooding will result from aggradation of the Taramakau River, causing extensive inundation and sedimentation of farmland as well as affecting both the road and rail bridges that cross the Taramakau River within the study area. WCRC (2002) found that flood damage and disruption occurs three times per year on average in this region, this frequency will increase dramatically as the alpine fluvial systems of the South Island respond to an AFE.

One-in-100 year flood levels were estimated to affect both road and rail transportation bridges crossing the Taramakau River within the study area. From the NIWA data provided, an estimated one-in-100 year flood for the Taramakau River study area has a flow rate of 3200m^3/s. This discharge value corresponds to a flow increase of just over seven metres. Currently, the Stanley Goosemen and Midland Rail Bridge have a free-board of seven metres. Thus any increase in the bed level due to landslide-induced aggradation increases the risk of inundation of the bridges. This is particularly serious as once the water level reaches the bridge deck, the flow is obstructed, causing both further increase in water level and slowing of the flow velocity, potentially causing further aggradation in a positive feedback. The failure of these structures would have significant consequences to the transportation links from the West to East Coasts of the South Island, New Zealand. In reality, as noted above, it is likely that both bridges will fail during the AFE, so present concepts may be more useful in designing suitable deck elevations for the replacement structures. Re-establishing the transport links will be a matter of urgency, and it is vital that the reconstructed bridges are not impacted by aggradation soon after completion.

Aggradation in the vicinity of Inchbonnie has the potential to cause flood waters to flow across low lying land towards Lake Brunner, inundating farmland. Such overbank flows carry mainly fine sediment; thus coarse sediment will then, in this situation tend to deposit in the Taramakau bed because there is less flow to carry it downstream, again a positive-feedback effect increasing aggradation in the Taramakau at the overflow point. This will tend to prograde upstream, again increasing the threat to the Stanley Gooseman Bridge and the Midland Rail Bridge, or their replacements five km upstream.

Taramakau River flood paths across farmland on the true right of the Taramakau at Inchbonnie have been recognised by hazard reports for the region and are supported by aerial photographic interpretation in this thesis. Hazard reports commissioned by Solid Energy

(2011) and Asset Management Plans (AMP) for the Inchbonnie area conducted by WCRC (2010), address the concern of AFE induced flooding within the Taramakau River. One scenario mentioned in both reports is the potential for the Taramakau River to change its course at Inchbonnie and flow north towards Lake Brunner and/or northeast through Lake Poerua, past Rotomanu also entering Lake Brunner. A concern of these flood routes, in addition to inundating extensive farmland and imperilling road and rail links, is the potentially significant increase in flood flows in the Arnold and Lower Grey Rivers, north of Lake Brunner. WCRC is well aware of this threat and maintains a stopbank to prevent this from happening. Aerial photograph interpretation recognises that the construction of this stopbank in 1959 reduced the risk of hydraulic connection between the Orangipuku and Taramakau River (see Chapter 5), minimising the risk of Taramakau induced flooding in the Grey valley. Thus far the stopbank has reduced the threat of flood waters entering Lake Brunner through the Orangipuku River. While flood waters may not flow through the Orangipuku River they may reoccupy and flow through recognised paleo channels across the land surrounding Inchbonnie.

Aerial photograph interpretation highlights extensive presently unoccupied channels across the low lying agricultural land between Inchbonnie and Lake Brunner. Langridge et al (2010) identified and dated the main paleo channels here (Figure 7.6). Langridge et al (2010) classed the most recent abandoned Taramakau paleo channel as I - 1 (Figure 7.6). Three other Taramakau paleo channels were identified extending towards Lake Brunner (I - 2a, I - 2b, I - 2c) and Taramakau greywacke cobbles were identified in the I - 4 channel extending towards Lake Poerua (Figure 7.6). The paleo channels probably correspond to former courses of the Taramakau River. Langridge et al (2010) established that the Taramakau River has migrated across the adjacent low lying land around Inchbonnie, fanning anticlockwise from the Alpine Fault to its current course during the Late Holocene. The evidence for Taramakau flow across the land towards Lake Brunner is thus strong. Following an AFE the palaeo channels identified through aerial photograph interpretation and recognised by Langridge et al (2010) may be reactivated potentially inundating the land around Inchbonnie, causing significant damage to pastures as well as threatening livestock, settlement and transportation links.

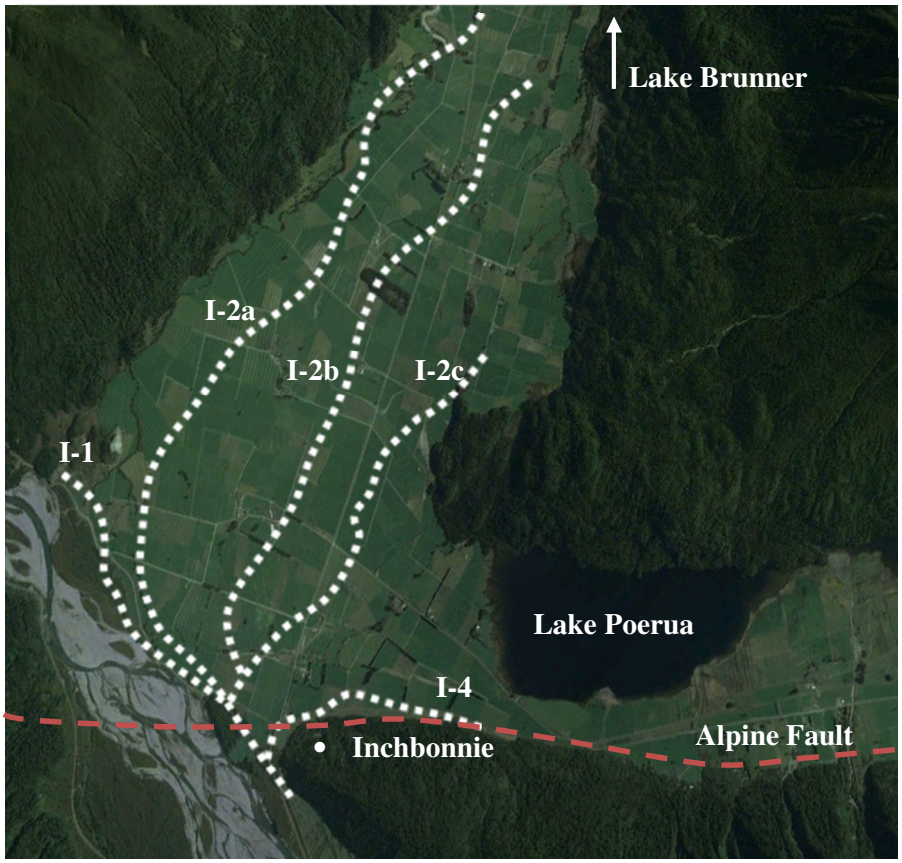

Figure 7.6 Taramakau outwash alluvial surfaces identified by Langridge et al (2010). Most recent Taramakau outwash surface recognised as I-1.

Aerial photographic interpretation coupled with the findings of the micro-scale modelling experiments highlighted areas of high flood risk upstream of the fault. Aerial photograph interpretation showed that the Taramakau River since 1943 has gradually shifted north incising into the land around Inchbonnie threatening the road and rail by bank erosion and inundation. Briefly observed in all experiments of the micro-scale modelling was a phase of back pooling following vertical uplift, subsequently widening the floodplain and inducing sediment deposition. The reduction in slope upstream of the fault decreased the velocity of the channel flow as well as elevating the river bed. In the field, an elevated river bed together with aggradation and northward shifting channels may increase the risk of flooding upstream of the Alpine Fault, breaching natural levees and laterally spreading towards the road and rail transportation links between Inchbonnie and the Stanley Goosemen and Midland Rail Bridges. The river may also undercut the road and rail transportation routes resulting in the collapse of such structures as seen in Otira in 1950 (Figure 7.7).

Figure 7.7 Railway settlement in Otira undercut by Otira River channel avulsion (1950). Source History House Greymouth, WCRC (2002)

Based on the findings of the micro-scale experiments, channel avulsion and flooding will also likely occur in the aggradational environment downstream of the fault. This is important as this locality coincides with the confluence of the Taipo River with the Taramakau. The sediment addition from the Taipo River, combined with the downstream aggradation induced by surface rupture, will increase the channel elevation of the Taramakau as it attempts to redevelop a natural grade at which to flow. The elevated Taramakau River bed is likely to become significantly wider, possibly breaching the Inchbonnie stopbank, prompting channel avulsion and flood flows down elevation towards Lake Brunner, inundating farmland. This form of flooding is depended on the amount of downstream aggradation and is unlikely to occur immediately following an AFE, being instead somewhat delayed.

The direction of fault displacement may hinder the reoccupation of paleo channels and flooding towards Lake Brunner. While paleo channels have been recognised across the low lying land between Inchbonnie and Lake Brunner, the dextral strike-slip displacement does not favour immediate flooding in this direction (Figure 7.8). Because of this, it is less likely that the Taramakau will flow towards Lake Brunner or Lake Poerua soon after an AFE. Flood waters, however, will be forced to flow towards Lake Brunner as aggradation gradually

increases downstream of the Alpine Fault trace from upstream landslide sediment addition and Taipo River sediment loads. Management measures need to be cognisant of the possible delays and time-scales of these effects.

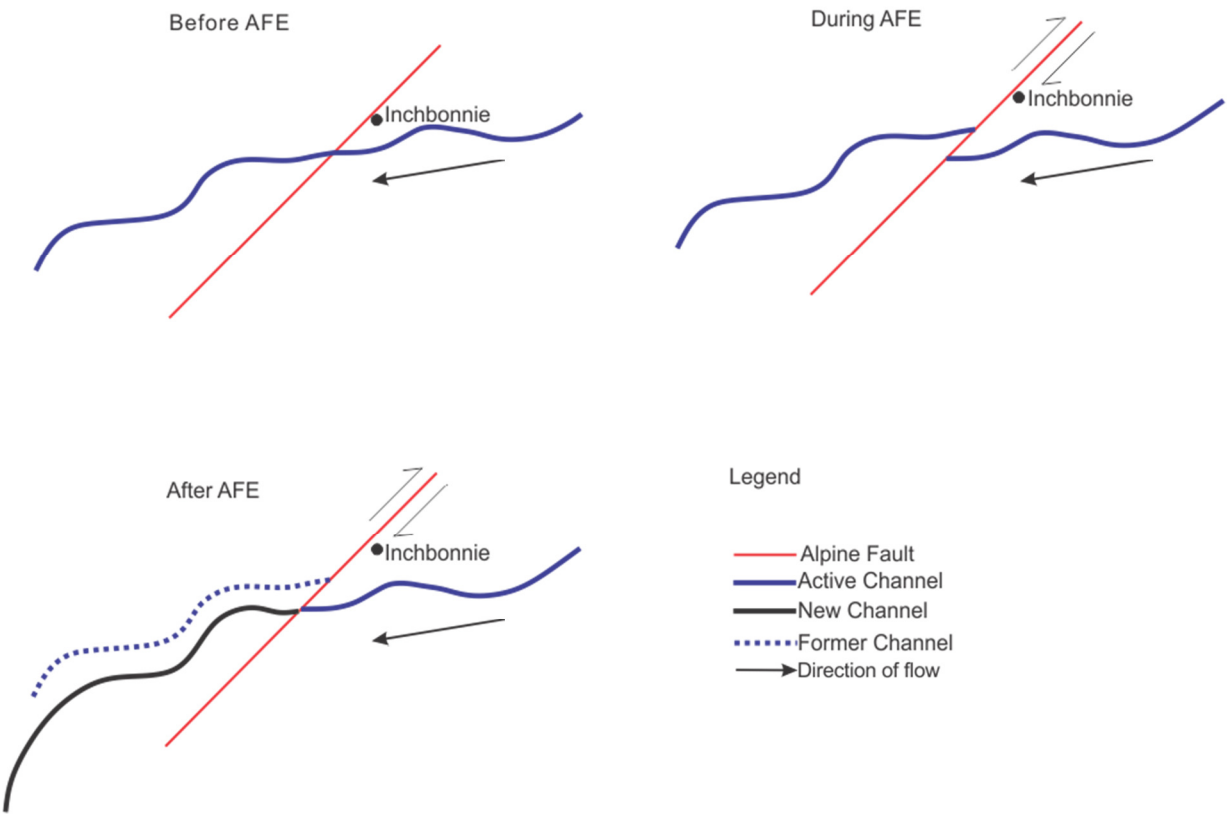

Figure 7.8 Progressive alignment of Taramakau channels following an AFE. Direction of displacement may not favour flood flows towards Lake Brunner and Lake Poerua.

7.3 Management Measures

Risk management measures include engineering solutions and/or planning solutions. Engineering solutions involve the modification and/or construction of physical structures to prevent damage during and following natural hazards such as an AFE. Planning solutions focus on minimising the impacts that natural hazards will have on people and organisations, increasing their ability to withstand the effects and recover from the hazard more effectively, by limiting development in areas identified as being particularly hazardous. Engineering solutions may include the strengthening of the Inchbonnie stopbank coupled with the construction of a secondary stopbank, should the first be damaged. To further protect the stopbanks, erosion control works may be built to absorb the energy of the river, however

unless these are deigned to be earthquake proof, they will be damaged during an AFE. Systematically increasing the elevation of the low sections of road and rail in the study area, may best resolve and minimise the risk of AFE induced hazards. Planning solutions include educating the local communities about the hazards surrounding an AFE and involving them in critical decision making. Implementing both engineering and planning solutions may reduce the damage incurred from an AFE on the Taramakau River.

Currently a 2.5 km long stopbank exists on the true right bank of the Taramakau River, near Inchbonnie, preventing the hydraulic connection between the Taramakau and the Orangipuku River to Lake Brunner (WCRC, 2010). Shearing and displacement of this stopbank will result from the dextral strike slip of an AFE, damaging and probably destroying the stopbank and allowing flood water to flow to Lake Brunner. In 2010 intense shaking from the Darfield earthquake (M_w = 7.1), in the South Island of New Zealand severely damaged the Waimakariri River stopbanks, 30 km away. The intense shaking of the Darfield earthquake resulted in widespread liquefaction and as a result the stopbank foundation soils were subject to lateral spreading and slumping (Green et al., 2011). The earthquake decreased the flood capacity of the Waimakariri stopbanks from a 450 year flooding event (4730 m^3/s) to an approximate 15 year flooding event (1500 m^3/s) (Green et al., 2011). The Inchbonnie stopbank has been built to withhold a 400 year Taramakau flooding event (WCRC, 2010). The Alpine Fault crosses the Inchbonnie stopbank and therefore during an AFE the damage to this stopbank will be far worse than the damage seen at the Waimakariri River in 2010, significantly decreasing – perhaps to zero – the flood capacity of the stopbank. Erosion control works and a secondary stopbank may be built to protect the primary stopbank from major flows, however unless these are designed to be earthquake proof they will also be damaged during an AFE. Grey District Council (GDC) and WCRC recognise the importance of the Inchbonnie stopbank and recommend that road access to Inchbonnie is given top priority following a major catastrophic event such as an AFE, enabling earthmoving equipment to come in and repair the stopbank, in order to reduce the risk of floodwaters flowing towards Lake Brunner. In reality, of course, there will be a multitude of competing demands on plant and access following an AFE and the reliance on the stopbank is questionable, therefore other management measures must be implemented prior to an AFE to minimise the disturbance of such an event in the study area.

Systematically raising the elevation of the low sections of road and rail within the study area, including the Stanley Goosemen Bridge and the Midland Rail Bridge will minimise the impacts of AFE induced flooding. The next AFE will cause an average of 0.5 m of aggradation within the study area enhancing the effects of floods. Raising the low sections of road and rail on the true right bank of the Taramakau River between Inchbonnie and the Stanley Gooseman Bridge and the Midland Rail Bridge by two metres will significantly decrease the probability of inundation during periods of high flow after an AFE. It is recommended that the elevation of the Stanley Goosemen Bridge and Midland Rail Bridge are also raised by at least two metres, increasing the free-board of these bridges allowing for flood waters to flow under the bridges, decreasing the risk of inundation and potential collapse. As previously noted, however, these bridges will likely be damaged during an AFE and therefore they should also be adequately strengthened while being raised, minimising the risk of collapse and inundation. The maintenance of the Inchbonnie stopbank does not take priority over the raising of the low sections of road and rail as well as strengthening and raising both bridges that cross the Taramakau River within the study area. The best possible way to minimise disturbance in the study area is through an increase in elevation of road and rail coupled with an increase in community awareness.

One of the best ways to reduce damage caused by natural hazards is through public awareness. An aware and involved public significantly decreases the losses caused by natural hazards, resulting from better designed measures to reduce impacts, planning and emergency evacuation routes. The risks from fluvial hazards must be outlined so that the population becomes aware of the hazards, involving them in the decision making so that they can plan to deal with such events. Due to the remoteness of the study area it is important that the community have direct involvement in the response process to the hazards following an AFE. Those living in the area have a good knowledge of the landscape and may become aware of conditions that could lead to future hazards. These people become important in transferring information to whom it should be directed and therefore become valuable emergency management resources (Becker et al., 2007). Actively involving the community may reduce several of the problems induced by an AFE and the consequent hazards. The results of this thesis aim to assist the local community by providing a better understanding of the potential effects that an AFE may have on the Taramakau River, the adjacent land and the road and rail transportation links.

7.4 Future Work

The research conducted in this thesis is a preliminary step in estimating the impacts of an AFE on the Taramakau River. There is obviously need for further research in this area as well as across other South Island fluvial networks. To further build on this thesis, the evaluation of the landslides volumes employed for calculation requires verification. More extensive aerial photograph interpretation and acquisition of missing photo sets would assist in understanding past avulsions of the Taramakau River and numerical modelling would complement the findings of the physical modelling. To further understand the implications of an AFE, in depth investigations on previous ruptures would also be beneficial:

- It is recommended that an investigation on alluvial fan vegetation should be undertaken in an attempt to recognise possible geomorphic stress, exposing information on previous large scale events, potentially hinting at previous AFE's.
- Future studies may look at the impact that an increase in sediment load transported through the fluvial networks, following an AFE, may have on the marine environment. The elevated supply of sediment delivered to the coast from large scale earthquakes may be recorded in offshore stratigraphy. This information may assist in the reconstruction of large scale earthquake recurrence intervals as well as the amount of landslide sediment produced from such events.

7.5 Summary

The likely chronological order of events following an AFE will begin with a surface rupture with severe ground shaking and damage to infrastructure, possible including channel shifting where the fault crosses the Taramakau, followed by coseismic landsliding which will induce river aggradation further enhancing channel avulsion and consequent flooding.

The impacts of surface rupture perpendicular to braided river channel flow were identified through the micro-scale model experiments. Surface rupture caused up and downstream aggradation divided by a zone of localised degradation over the fault trace. Slight right lateral channel shifts were also observed downstream of the modelled strike-slip fault. The effects of landsliding were recognised through an analysis of landslide volume data and observations made during micro-scale model experiments. Coseismic landsliding will create a spike in sediment input to alpine fluvial systems resulting in aggradation. The impacts of aggradation were identified through a data analysis coupled with the findings of the micro-scale model experiments. As the Taramakau channels and floodplain aggrade, channel avulsion and flooding will increase. The effects of channel avulsion and flooding were highlighted through a data analysis, aerial imagery and micro-scale modelling. The major concern of flooding is the inundation and sedimentation of critical road and rail transportation links as well as adjacent low lying farmland.

Recognising the hazards and the threat that they pose to adjacent infrastructure and land in the study area, it would be sensible to maintain and implement management measures to minimise the likelihood of damage in the wake of an AFE. The most economically sound way to minimise the damage induced by an AFE and the consequent hazards, is not through the maintenance of the Inchbonnie stopbank or the construction of erosion control works, but by increasing the elevation of low lying road and rail and actively involving the community. In addition, plans should be developed for the rapid reinstatement of the Stanley Goosemen and the Midland Rail Bridges at a deck level that will survive the landslide-induced aggradation. The response of the Taramakau River relative to an AFE recognised in this thesis might be worse, or less severe or significantly different in some way, nevertheless management measures must be considered to minimise the implications of surface rupture, coseismic landsliding, river aggradation and channel avulsion/flooding.

Chapter 8 - Conclusion

8.1 Research Objectives and Methods

The principal aim of this thesis was to analyse the impacts of an AFE on the transportation links in the Taramakau valley. The effects of surface rupture, landsliding, aggradation, avulsion and flooding were estimated and their implications to the transportation links within the study area were assessed. The steps taken to achieve the aim have been;

1. To conduct a hydraulic data analysis of the Taramakau River based on values supplied by NIWA.
2. To estimate aggradation levels from reworked landslide volume data compared with data from the Mt Adams rock avalanche in 1999.
3. To examine aerial photographs, identifying historic channel avulsions in the Taramakau River and areas at high risk to flooding.
4. To observe how a modelled braided fluvial system may respond to dextral strike-slip displacement with vertical uplift, coupled with an increase in sediment supply modelling landslide sediment loads.
5. To evaluate the possible fluvial hazards induced by an AFE and recommend potential management measures that may be implemented to minimise the associated risks.

8.2 Main Conclusions

A review of the literature revealed that large scale earthquakes are capable of causing a large number of landslides, the sediment of which can be transported through fluvial networks contributing to downstream river aggradation and channel avulsion. In many instances river aggradation has led to the burial of structures and has promoted channel avulsion subsequently resulting in flooding of adjacent land.

A data analysis highlighted the relationship between hydraulic parameters in the Taramakau River and provided insight on the amount of aggradation likely to be induced by AFE landsliding. Based on a comparative study with the Mt Adams rock avalanche that fell into the Poerua valley in 1999, approximately 15% of the total Taramakau catchment landslide material may be deposited on the Taramakau River floodplain, nine years after an AFE. An AFE may induce a maximum credible volume of 3.0×10^8 m^3 of landslide material, 15% of this may gradually migrate downstream depositing on the floodplain of the river contributing an average of 0.5 m of aggradation over the whole floodplain. Substantially greater

aggradation in river channels will enhance the effects of all floods, increasing the river bed and water surface elevations and threatening both the Stanley Gooseman and Midland Railway Bridges that cross the Taramakau River within the study area (or their replacements, if they are destroyed in the AFE, as seems likely). Given that the river bed is incised approximately metres below the floodplain it would be sensible to expect of the order of metres of aggradation beneath these bridges putting them at risk during periods of high flow.

Aerial photograph interpretation showed that the Taramakau River has generally been shifting north since 1943. The river has in places moved northward away from State Highway 73 in the study area by approximately 500 m, shifting closer to the road and rail that run between Inchbonnie and the Stanley Gooseman and Midland Railway Bridges on the true right bank of the river. The northward migrating channels have incised into a large alluvial fan east of the road and rail bridges, producing an approximate 30 m high vertical wall. During an AFE this wall may fail due to intense shaking, supplying an immediate and direct load (10^5 m^3) of sediment into the Taramakau River. This may result in channel avulsion and flooding extremely close to the transportation links that cross the river within the study reach. The Taipo River, a major tributary to the Taramakau, has an active alluvial fan at its confluence with the Taramakau. Three different channel positions were identified since 1943. In the wake of an AFE the Taipo River will supply additional sediment to the Taramakau contributing to channel aggradation at its confluence. Aerial photograph interpretation also recognised Taramakau River paleo channels across the low lying land between Inchbonnie and Lake Brunner.

Micro-scale modelling showed how a braided river may respond to dextral strike-slip displacement and an increase in sediment load. Three experiments modelled three different AFE rupture scenarios. For all three experiments it was found that up- and downstream aggradation will likely occur following the lateral and vertical displacement of a dextral strike-slip fault and landslide sediment input. Degradation occurred over the uplifted fault trace due to a localised increase in channel slope. Slight right lateral channel shifts were recognised corresponding to the direction of displacement. Overall the active channel bed of the downstream reach widened following displacement. A widened channel bed may increase the risk of flooding and erosion downstream of the Alpine Fault.

Based on the findings of this thesis, it would be sensible to implement management measures designed to minimise the associated risks of fluvial hazards induced by an AFE. The

stopbank at Inchbonnie will be sheared and potentially destroyed by the surface rupture of an AFE. A secondary stopbank and erosion control works may be built, to protect the primary stopbank, but unless these are designed to be earthquake proof, they too, will be destroyed by an AFE. The most practical way to minimise the damage induced by an AFE and the consequent hazards, is not through the maintenance of the Inchbonnie stopbank or the construction of erosion control works, but by increasing the elevation of low lying road and rail links by approximately two metres and planning to replace and/or adequately strengthen the Stanley Gooseman and the Midland Rail Bridges at a higher elevation. It is critical that the gaps in hazard knowledge and information are minimised to prevent loss associated with natural hazards. The results from this thesis contribute to a greater understanding of how the Taramakau may respond, when potentially disturbed by an AFE.

The fluvial hazards of aggradation, avulsion and flooding may be felt across all alpine rivers in the South Island following an AFE. The hazards discussed in this thesis as well as other coseismic hazards may reflect throughout the landscape of New Zealand following the next AFE.

References

Becker, J.S., Johnston, D.M., Paton, D., Hancox, G.T., Davies, T.R., McSaveney, M.J., & Manville, V.R. (2007). Response to Landlise Dam Failure Emergenices: Issues Resulting from the October 1999 Mount Adams Landslide and Dam-Break Flood in the Poerua River, Westland, New Zealand. *Natural Hazards Review,* 8(2), 35-42.

Berryman, K., Cooper, A., Norris, R., Villamor, P., Sutherland, R., Wright, T., Schermer, E., Langridge, R., & Biasi, G. (2012). Late Holocene rupture history of the alpine fault in South Westland, New Zealand. *Bulletin of the Seismological Society of America*, 102(2), 620-638.

Brunetti, M. T., Guzzetti, F., & Rossi, M. (2009). Probability distributions of landslide volumes. *Nonlinear Processes In Geophysics*, 16(2), 179-188.

Cave, M. P. (1987). *Geology of Arthur's Pass National Park* (Vol. no.7). Wellington, New Zealand. Department of Conservation.

Chamberlain, C. G. (1996). *Seismic hazard from cross-faulting in North Canterbury: broader implications from the Arthur's Pass earthquake sequence of 18 June 1994*. Unpublished master's thesis, Univesity of Cantebrury, Christchurch, New Zealand.

Chen, T.C., Lin, M.L., & Hung, J.J. (2004). Pseudostatic analysis of Tsao-Ling rockslide caused by Chi-Chi earthquake. *Engineering Geology,* 71(1), 31-47.

Cheng, G., He, X., Chen, G., & Tao, H. (2010). Change in sediment load of the Yangtze River after Wenchuan earthquake. *Journal of Mountain Science*, 7(1), 100-104.

Collins, P. (2014). *The Taramakau River Bridge – Figure*. Canterbury Recreational Aircraft Club. Retrieved from http://www.recwings.com/newsletters/2013/mar13/index.html

Costa, J. E & Schuster, R. L. (1988). The formation and failure of natural dams. *Geological Society of America Bulletin*, 100(7), 1054-1068.

Dai, F. C., Xu, C., Yao, X., Xu, L., Tu, X. B., & Gong, Q. M. (2011). Spatial distribution of landslides triggered by the 2008 Mw 8.0 Wenchuan earthquake, China. *Journal of Asian Earth Sciences*, 40(4), 883-895.

Davies, T. R. H., Campbell, B., Hall, B., & Gomez, C. (2013) Recent behaviour and sustainable future management of the Waiho River, Westland, New Zealand. *Journal of Hydrology New Zealand,* 52(1), 41-56.

Davies, T. R. H., & Korup, O. (2007). Persistent alluvial fanhead trenching resulting from large, infrequent sediment inputs. *Earth Surface Processes and Landforms*, 32(5), 725-742.

Davies, T. R. H., Manville, V., Kunz, M., & Donadini, L. (2007). Modeling Landslide Dambreak Flood Magnitudes: Case Study. *Journal of Hydraulic Engineering*, 133(7), 713-720.

Davies, T. R. H., & McSaveney, M. J. (2006). Geomorphic constraints on the management of bedload-dominated rivers. *Journal of Hydrology New Zealand*, 45(2), 111-130.

Davies, T. R. H., & McSaveney, M. J. (2011). Bedload sediment flux and flood risk management in New Zealand. *Journal of Hydrology New Zealand*, 50(1), 181-190.

Davies, T. R. H., McSaveney, M. J., & Doscher, C. (2005). *Monitoring and Effects of Landslide- Induced Aggradation in the Poerua Valley, Westland, final report, Project 03/499. Earthquake Commission:* Wellington, New Zealand. Earthquake Commission

De Pascale, G. P., Quigley, M. C., & Davies, T. R. H. (2014). Lidar reveals uniform Alpine fault offsets and bimodal plate boundary rupture behavior, New Zealand. *Geology*, 42(5), 411-414.

Dundas, K. (2008). *An all-hazards vulnerability assessment of Arthur's Pass township, South Island, New Zealand*: Unpublished master's thesis, University of Canterbury, New Zealand.

Earthquake Museum of Taiwan. n.d. *Pifeng Bridge - Figure*. 921 Earthquake Museum. Retrieved from http://www.geologie.geowissenschaften.unimuenchen.de/archiv/taiwan_/index.html

Freund, R. (1971). *The Hope Fault, a strike slip fault in New Zealand* (Vol. n. s. no. 86). Wellington, New Zealand. Department of Scentific and Industrial Research.

Green, R.A., Allen, J., Wotherspoon, L., Cubrinovski, M., Bradley, B., Bradshaw, A., Cox, B., & Algie, T. (2011). Performance of Levees (Stopbanks) during the 4 September 2011 M_w 7.1 Darfield and 22 February M_w 6.2 Christchurch, New Zealand, Earthquakes. *Seismological Research Letters*, 82(6), 939-949.

Grey District Council. (2007) *Grey District Lifelines Plan- Communities and Council*. Retreieved from http://www.wcrc.govt.nz/Documents/Natural Hazard Reports/GDC Lifelines Study Dec 2007.pdf

Hancox, G. T., McSaveney, M. J., Manville, V. R., & Davies, T. R. H. (2005). The October 1999 Mt Adams rock avalanche and subsequent landslide dam-break flood and effects in Poerua River, Westland, New Zealand. *New Zealand Journal of Geology and Geophysics,* 48(4), 683-705.

Harp, E. L., & Jibson, R. W. (1996). Landslides triggered by the 1994 Northridge, California, earthquake. *Bulletin of the Seismological Society of America*, 86(1B), 319-332.

Hessell, J. W. D. (1982). *The climate and weather of Westland* (Vol. 115 (10)). Wellington, New Zealand. Ministry of Transport New Zealand Meteorological Service

Hewitt, K. (1998). Catastrophic landslides and their effects on the Upper Indus streams, Karakoram Himalaya, northern Pakistan. *Geomorphology*, 26(1–3), 47-80.

Hicks, M. D. (2014), personal communication.

Hicks, M. D., Shankar, U., McKerchar, A. I., Basher, L., Lynn, I., Page, M., & Jessen, M. (2011). Suspended Sediment Yields from New Zealand Rivers. *Journal of Hydrology New Zealand*, 50(1), 81-142.

Holbrook, J., & Schumm, S. A. (1999). Geomorphic and sedimentary response of rivers to tectonic deformation: a brief review and critique of a tool for recognizing subtle epeirogenic deformation in modern and ancient settings. *Tectonophysics*, 305(1–3), 287-306.

Huang, R., & Li, W. (2014). Post-earthquake landsliding and long term impacts in the Wenchuan earthquake area, China. *Engineering Geology*.

Jones, L. S., & Schumm, SA. (2009). Causes of avulsion: an overview. *Fluvial sedimentology VI,* 171-178.

Keefer, D. K. (1984). Landslides caused by earthquakes. *GSA Bulletin*, 95(4), 406-421.

Keefer, D. K. (1994). The importance of earthquake-induced landslides to long-term slope erosion and slope-failure hazards in seismically active regions. *Geomorphology*, 10(1–4), 265-284.

Keefer, D. K. (1999). Earthquake-induced landslides and their effects on alluvial fans. *Journal of Sedimentary Research*, 69(1), 84-104.

Korup, O. (2002). Recent research on landslide dams - a literature review with special attention to New Zealand. *Progress in Physical Geography*, 26(2), 206-235.

Korup, O. (2004a). Geomorphic implications of fault zone weakening: Slope instability along the Alpine Fault, South Westland to Fiordland. *New Zealand Journal of Geology and Geophysics*, 47(2), 257-267.

Korup, O. (2004b). Geomorphometric characteristics of New Zealand landslide dams. *Engineering Geology*, 73(1–2), 13-35.

Korup, O. (2004c). Landslide-induced river channel avulsions in mountain catchments of southwest New Zealand. *Geomorphology*, 63(1–2), 57-80.

Korup, O. (2005a). Geomorphic hazard assessment of landslide dams in South Westland, New Zealand: fundamental problems and approaches. *Geomorphology*, 66(1–4), 167-188.

Korup, O. (2005b). Geomorphic imprint of landslides on alpine river systems, southwest New Zealand. *Earth Surface Processes and Landforms*, 30(7), 783-800.

Korup, O. (2005c). Large landslides and their effect on sediment flux in South Westland, New Zealand. *Earth Surface Processes and Landforms*, 30(3), 305-323.

Korup, O. (2006). Rock-slope failure and the river long profile. *Geology*, 34(1), 45-48.

Korup, O., McSaveney, M. J., & Davies, T. R. H. (2004). Sediment generation and delivery from large historic landslides in the Southern Alps, New Zealand. *Geomorphology*, 61(1-2), 189-207.

Korup, O., Strom, A. L., & Weidinger, J. T. (2006). Fluvial response to large rock-slope failures: Examples from the Himalayas, the Tien Shan, and the Southern Alps in New Zealand. *Geomorphology*, 78(1–2), 3-21.

Langridge, R. M., Villamor, P., Basili, R., Almond, P., Martinez-Diaz, J. J., & Canora, C. (2010). Revised slip rates for the Alpine fault at Inchbonnie: Implications for plate boundary kinematics of South Island, New Zealand. *Lithosphere*, 2(3), 139-152.

McSaveney, E. R. (1982). *Recent geomorphic changes in the Bealey, Otira, Mingha and Deception Valleys: Arthur's Pass National Park : a report to the National Parks Authority of New Zealand, Department of Lands and Survey*. Christchurch, New Zealand. University of Canterbury

Nathan, S., Rattenbury, M. S., & Suggate, R.P. (2002) *Geology of the Greymouth Area*¸ 1:250,000, Map 12. Lower Hutt, New Zealand. Institute of Geological and Nuclear Sciences, Ltd.

National institute of Water and Atmospheric Research (2003). *Overview of New Zealand Climate - figure*. Wellington, New Zealand: National Institute of Water and Atmospheric Science (NIWA). Retrieved from https://www.niwa.co.nz/education-and training/schools/resources/climate/overview

Nelson, M. C. (2012). *The impact of landslides on sediment yield, South Westland, New Zealand*. Unpublished master's thesis, Simon Fraser University, British Columbia, Canada.

Norris, R. J., & Cooper, A.F. (2001). Late Quaternary slip rates and slip partitioning on the Alpine Fault, New Zealand. *Journal of Structural Geology*, 23(2), 507-520.

Ouchi, S. (1983) *Response of alluvial rivers to active tectonics*. Unpublished doctoral dissertation, Colorado State University, Fort Collins, Colorado, United States of America.

Ouchi, S. (2004). Flume experiments on the horizontal stream offset by strike-slip faults. *Earth Surface Processes and Landforms*, 29(2), 161-173.

Paterson, B. R. (1996). Slope instability along State Highway 73 through Arthur's Pass, South Island, New Zealand. *New Zealand Journal of Geology and Geophysics*, 39(3), 339-351.

Rhoades, D. A., &Van Dissen, R. (2003). Estimates of the time-varying hazard of rupture of the Alpine Fault, New Zealand, allowing for uncertainties, *New Zealand Journal of Geology and Geophysics*. 46(4), 479–488.

Robertson, N. G. (1963). *The frequency of high intensity rainfalls in New Zealand*. Wellington, New Zealand. New Zealand Meteorological Service

Robinson, T. R. (*in prep* 2014). *Assessment of coseismic landsliding from an Alpine fault earthquake scenario, New Zealand.* Unpublished doctoral thesis, University of Canterbury, Christchurch, New Zealand

Robinson, T. R., & Davies, T. R. H. (2013). Review Article: Potential geomorphic consequences of a future great (Mw = 8.0+) Alpine Fault earthquake, South Island, New Zealand. *Natural Hazards and Earth System Sciences*, 13(9), 2279-2299.

Schumm, S. A, Dumont, J. F., & Holbrook, J. M. (2000). *Active tectonics and alluvial rivers*. Cambridge, United Kingdom. Cambridge University Press.

Slingerland, R., & Smith, N. D. (2004). River avulsions and their deposits. *Annual Review of Earth and Planetary Sciences*, 32, 257-285.

Smith, E. (2004). *Mass movement hazard to infrastructure, Arthur's Pass to Greymouth* Unpublished masters thesis, University of Canterbury, Christchurch, New Zealand

Solid Energy New Zealand. McCahon, I., Elms, D., & Dewhirst, R. (2011) Transalpine Rail Link: Vulnerability to Natural Hazards. Unpublished Report

Tang, C., Zhu, J., Ding, J., Cui, X., Chen, L., & Zhang, J. (2011). Catastrophic debris flows triggered by a 14 August 2010 rainfall at the epicenter of the Wenchuan earthquake. *Landslides,* 8(4), 485-497.

Wang, W, N., Chigira, M., & Furuya., T. (2003). Geological and geomorphological precursors of the Chiu-fen-erh-shan landslide triggered by the Chi-chi earthquake in central Taiwan. *Engineering Geology*, 69(1–2), 1-13.

Wang, Z., Cui, P., & Wang, R. (2009). Mass movements triggered by the Wenchuan earthquake and management strategies of quake lakes. *International Journal of River Basin Managemen*t, 7(4), 391-402.

Wells, A., & Goff, J. (2007) Coastal dunes in Westland, New Zealand, provide a record of paleoseismic activity on the Alpine Fault. *Geology,* 35(8), 731-734.

Wells, A., Yetton, M. D., Duncan, R. P., & Stewart, G. H. (1999). Prehistoric dates of the most recent Alpine fault earthquakes, New Zealand. *Geology*, 27(11), 995-998.

West Coast Regional Council: Natural Hazards Review. (2002). DTec Consulting Ltd., Christchurch

West Coast Regional Council. (2010) *Inchbonnie rating district Asset Management Plan*. Retrieved from http://www.wcrc.govt.nz/our-council/asset-management-plans/Pages/Inchbonnie.aspx

Whitehouse, I. E., & McSaveney, M. J. (1992). Assessment of geomorphic hazards along an alpine highway. *New Zealand Geographer*, 48(1), 27-32.

Xu, X., Wen, X., Yu, G., Chen, G., Klinger, Y., Hubbard, J., & Shaw, J. (2009). Coseismic reverse- and oblique-slip surface faulting generated by the 2008 Mw 7.9 Wenchuan earthquake, China. *Geology*, 37(6), 515-518.

Yanites, B. J., Tucker, G. E., Mueller, K. J., & Chen, Y. G. (2010). How rivers react to large earthquakes: Evidence from central Taiwan. *Geology*, 38(7), 639-642.

Yetton, M. D. (2000). *The probability and consequences of the next alpine fault earthquake, South Island, New Zealand*. Unpublished doctoral dissertation, University of Canterbury, Christchurch, New Zealand.